South Dakota State University

[Electronic Theses and Dissertations](https://openprairie.sdstate.edu/etd2)

2023

Livestock Wastewater and Air Quality Management Using Microalgae, Capacitive Deionization, and Biofilters

Augustina Kwesie Osabutey
South Dakota State University, osabuteya@gmail.com

Follow this and additional works at: https://openprairie.sdstate.edu/etd2

Part of the [Bioresource and Agricultural Engineering Commons](#), and the [Environmental Engineering Commons](#)

Recommended Citation

LIVESTOCK WASTEWATER AND AIR QUALITY MANAGEMENT USING

MICROALGAE, CAPACITIVE DEIONIZATION, AND BIOFILTERS

BY

AUGUSTINA KWESIE OSABUTEY

A dissertation submitted in partial fulfillment of the requirements for the

Doctor of Philosophy

Major in Agriculture, Biosystems & Mechanical Engineering

South Dakota State University

2023

DISSERTATION ACCEPTANCE PAGE

Augustina Kwesie Osabutey

This dissertation is approved as a creditable and independent investigation by a candidate for the Doctor of Philosophy degree and is acceptable for meeting the dissertation requirements for this degree. Acceptance of this does not imply that the conclusions reached by the candidate are necessarily the conclusions of the major department.

Xufei Yang

Advisor   Date

Kasiviswanathan Muthukumarappan

Department Head   Date

Nicole Lounsbery, PhD

Director, Graduate School   Date

This dissertation is dedicated to my parents (Mr. Peter Osabutey and Mrs. Catherine Osabutey), my husband (Mr. Christopher Montgomery), my unborn baby, my siblings (John Paul Osabutey, Adelaide Osabutey, and Richard Osabutey), and my late grandmother (Mrs. Drucillia Arthur). My family has been the greatest support system I could have asked for. I would not have been able to get this far without all your support. Thank you very much for the relentless encouragement, support, and prayers.

ACKNOWLEDGEMENTS

Words cannot be enough to express my appreciation to all key individuals and institutions for their support in making this journey possible. To my advisor, Dr. Xufei Yang, thank you for granting me the opportunity to work with you in pursuit of my doctorate. I am grateful for your guidance, patience, love, understanding, criticisms, and relentless support in both my academic and personal development. You never hesitated to correct me when I went wrong or lagged behind. For that, I truly appreciate and will forever be grateful.

Thank you to Dr. Gary Anderson who was always available to listen to me, advise, and guide me in both my personal and academic life. You have been very instrumental in my Ph.D. journey. I am equally grateful to Dr. Min Kyungnan for constantly working with me in the laboratory on my research, introducing me to wastewater treatment techniques, and thoroughly reviewing and discussing my results, writeups, and PowerPoint presentation slides. Thank you to Dr. John McMaine and Dr. Hua, Guanghui for their excellent mentorship and guidance throughout my Ph.D. journey. I sincerely appreciate you all and the marvelous support I have and continue to receive from you.

I am grateful to the Agriculture & Biosystems Engineering department of South Dakota State University for funding my Ph.D. studies and to the staff (Mrs. Brenda Pratt and Mrs. Cindy Shea) for their friendship and support. Many thanks to Mr. Brian Langum for always assisting me in my experimental setups and repairing defective laboratory instruments when needed. To Karlee Albert, thank you very much for all your support working with me in the laboratory, especially in data collection.

TABLE OF CONTENTS

ABBREVIATIONS

AEM	Anion exchange membrane
ANOVA	Analysis of variance
ASAR	Average salt adsorption rate
ATP	Adenosine triphosphate
Ave	average
BBM	bold basal medium
BF	biofilter
BOD	Biochemical oxygen demand
CAFOs	Concentrated animal feeding operations
CDI	Capacitive deionization
CEM	Cation exchange membrane
COD	Chemical oxygen demand
CV	coefficient of variance
DAB	dry algal biomass
DC	Direct current
DNA	Deoxyribonucleic acid
DU	distribution uniformity
EBPR	Enhanced biological phosphorus removal
EDL	Electrical double layer
EPA	Environmental protection agency
eqSAC	Equilibrium salt adsorption capacity
FCDI	Flow-electrode capacitive deionization
HAPs	Hazardous algal blooms
HCL	Hydrochloric acid

IEM	Ion exchange membrane
LPM	liter per minute
MCDI	Membrane capacitive deionization
mSAC	Maximum salt adsorption capacity
OD	optical density
PAM	Polyacrylamide
PAOs	Polyphosphate-accumulating organisms
PBRs	photobioreactors
PHAs	Polyhydroxyalkanoates
RNA	Ribonucleic acid
SAC	Salt adsorption capacity
SCC	Short-circuit closed-cycle
SD	standard deviation
SDSU	South Dakota State University
SW	Swine wastewater
TKN	Total Kjeldahl nitrogen
TN	Total Nitrogen
TP	Total phosphorus
TSS	Total suspended solids
UTEX	University of Texas

LIST OF FIGURES

CHAPTER 4 FIGURES

APPENDIX B FIGURES

APPENDIX C FIGURES

LIST OF TABLES

ABSTRACT

LIVESTOCK WASTEWATER AND AIR QUALITY MANAGEMENT UTILIZING

MICROALGAE, CAPACITIVE DEIONIZATION, AND BIOFILTERS

AUGUSTINA KWESIE OSABUTEY

2022

Environmental protection and resource reuse have gained attention in various industries recently. The agriculture industry, which is significant to humanity, is no exception. The provision of food for humanity is the core responsibility of the agriculture industry. However, its activities are also likely to create a nuisance to the environment. While the agriculture industry has a high resource management and reuse performance, it also creates environmental problems. Pollution from odor in fertilizer application on crop fields and livestock facilities, nutrient runoff from agricultural fields, which leads to eutrophication, and bacteria and pathogens pollution from manure applications or mismanagement are some environmental problems. This study's overarching goal was to explore various techniques for finding solutions to some environmental issues (odor, nutrients, associated with the livestock industry.

We first reviewed phosphorus (a limiting but environmentally nuisance nutrient) removal or recovery from wastewater utilizing the capacitive deionization (CDI) technology (**chapter 1**). The capacitive deionization technology was earlier used for water desalination. However, its ability to remove ions from water attracted the attention of researchers to use it in wastewater treatment and for phosphorus recovery or removal. The review describes the capacitive deionization technology and its architectures. It focuses on

using the technology for phosphorus removal from wastewater by summarizing studies conducted and discussing our perspectives. This review informs researchers on the work done on phosphorus recovery or removal and the relevance of CDI application.

In addition, several technologies have been developed for odor mitigation in livestock facilities. The horizontal bed biofilter is often used compared to other technologies. Although less expensive in construction and easy to manage for odor mitigation in the livestock industry, it requires larger space for installation. Another challenge encountered is the non-uniform distribution of airflow and moisture across the biofilter. **Chapter 2** of this study focused on providing an alternative solution for the limited space for biofilter construction in livestock facilities for odor mitigation and studied the cause of uneven airflow and moisture distribution across the biofilter. Two vertical bed biofilters were constructed at the university swine facility and monitored for two months. A vertical biofilter that required small square footage was installed, monitored, data collected (27 sample points from both biofilters), and analyzed to address the research gap or challenges. Results indicated an uneven airflow and moisture content distribution, and recommendations were given to address these challenges.

On the other hand, microalgae provide valuable benefits such as wastewater treatment, fertilizer, and livestock feed to the livestock industry. However, water management in microalgae cultivation is significant. Makeup water in microalgae cultivation and its effects on algal growth has received little or no attention. Microalgae cultivation is susceptible to water loss; thus, makeup water addition cannot be ignored. **Chapter 3** of this study explores the effects of makeup water addition during microalgae cultivation in two-time intervals (every day and every four days). *Scenesdesmus dimorphus*

microalgae seed was obtained from the University of Texas culture laboratory and cultivated with a Bold basal medium before the makeup water addition study. Data collected and analyzed include cell count, dry biomass, and optical density for the makeup water effects on algal growth. The results revealed everyday water makeup sustained algal growth compared to every four days of makeup water addition. This research provides information on improving water management in PBR and open pond algal cultivation.

Chapter 4 of this study further focused on microalgae growth in raw versus pretreated swine wastewater. As stated earlier, wastewater treatment is a benefit in microalgae cultivation. *Scenesdesmus dimorphus* microalgae were cultivated in raw and pretreated (via solid separation) swine wastewater, and its ability to grow and reduce nutrients were studied. Pretreatment of the swine wastewater improved algal growth compared to raw swine wastewater and reduced phosphorus concentrations in swine wastewater. The results also indicated nitrogen concentration reduction as algae absorbed it. This study provides insights into microalgae-based swine wastewater treatment processes.

CHAPTER 1: Phosphorus Recovery From Wastewater Via Capacitive Deionization:

Existing Knowledge And Perspectives

Abstract

Wastewaters play a significant role in the negative impact of phosphorus on the environment, such as eutrophication. However, phosphorus is a limiting nutrient essential for life which has gained global attention on productive technologies for phosphorus recovery. Several technologies have been developed for phosphorus removal and recovery from wastewater to help alleviate phosphorus loss to the environment. Capacitive deionization technology, which was earlier developed for water desalination and ion removal, is actively being explored for its ability to remove phosphorus from wastewater. This review describes capacitive deionization technology (CDI) and its various types. Significant attention is given to the use of CDI technology for phosphorus/phosphate removal and recovery from wastewater. Some studies on phosphorus removal or recovery by CDI are summarized. This review also discusses our perspective on the CDI technology for phosphorus removal from wastewater. This paper informs researchers of the work done on using CDI for phosphorus removal from wastewater and the need for more studies in the application of CDI and phosphorus removal.

Keywords: capacitive deionization, phosphorus ion removal, wastewater, phosphorus recovery

1. Introduction

Phosphorus (hereafter P) is vital for all known life forms on Earth. Phosphate and sugar constitute the backbone of deoxyribonucleic acid (DNA) and ribonucleic acid (RNA) that carry genetic information. P is a constituent of adenosine triphosphate (ATP) that

serves as an energy currency in living organisms. In human bodies, P can be found as calcium phosphate in bones. As stated by Isaac Asimov, a biochemist and science writer, "We may be able to substitute nuclear power for coal, and plastics for wood, and yeast for meat, and friendliness for isolation—but for phosphorus there is neither substitute nor replacement" (Asimov, 1974).

By nature, all P in biosphere originates from P-containing minerals, predominantly phosphorite. It is a non-renewable and finite resource. Only a handful of countries in the world (e.g., Morocco, China, Algeria, Russia, Australia, and the U.S.) can boast of having phosphorite reserves or deposits. Limited access to phosphorite creates economic stress and political issues, particularly to developing countries that heavily depend on P for agricultural production. The agricultural industry in developed countries also rely on phosphorite for production of fertilizers, animal feeds and food additives. With an ever-growing global population, P fertilizers are being sought after at an unprecedented pace. This however results in depletion of phosphorite, especially high-grade ores (Desmidt et al., 2015; Mayer et al., 2016). According to a United States Geological Survey (USGS) 2012 report, phosphorite reserves would be completely depleted in 372 years at current mining rates (Desmidt et al., 2015).

On the other hand, excessive amounts of P can cause numerous environmental complications upon reaching water bodies, including eutrophication, hazardous algal blooms (HAPs), hypoxia, and fish kills. The associated economic impact is enormous. For example, HAPs were estimated to result in a loss of $1 billion per year for the U.S. fishing and boating industry (US EPA, 2013b). Municipal wastewater and agricultural runoff are the two major sources of P discharge into the aquatic environment (Bradford-Hartke et al.,

2015; Desmidt et al., 2015; Mayer et al., 2016; US EPA, 2013; Venkatesan et al., 2016). P recovery from wastewater is beneficial from both resource conservation and environmental protection perspectives (Mayer et al., 2016; US EPA, 2013).

For years, P recovery has received a great interest from the government, academia, and industry. In the U.S., P recovery is considered as a critical tool to mitigate the nation's reliance on P reserves and to reduce the occurrence of eutrophication and HAPs that jeopardize public health and well-beings (Tonini et al., 2019). In the 1950s, the Swedish government established a strategic goal to recover at least 40% of phosphorus from municipal wastewater treatment plants (Wu et al., 2016). This early action and alike have stimulated the development and implementation of P-recovery technologies at laboratory and/or industrial scales.

More than 30 technologies for P recovery have been developed (Li et al., 2019) and they can be grouped into three categories (Bunce et al., 2018; Mohan et al., 2016; Wang et al., 2006): (1) physical methods, including electrodialysis, reverse osmosis, and ion exchange (Yeoman et al., 1988); (2) chemical methods, including chemical precipitation in forms of struvite and vivianite (Le Corre et al., 2009; Wilfert et al., 2018); and (3) biological methods, including enhanced biological phosphorus removal and microalgal systems (Mehta et al., 2015, 2016; Ahmed et al., 2015). Many of these technologies stay in the laboratory stage and have yet to be widely adopted by the industry. A major reason is that P recovery often requires additional treatment steps or reactors, which means a high capital or operating cost. As a result, the industry and academia continue to pursue new technologies.

A recent player entering the arena is capacitive deionization (CDI). CDI, also known as electrosorption, is an energy-efficiency technology for brackish water treatment (Anderson et al., 2010; Gabelich et al., 2002b), wastewater reclamation (Lee et al., 2006), and sea water desalination/softening (Forrestal et al., 2012; Huang et al., 2016; Jeon et al., 2013; Suss et al., 2015). A basic CDI cell consists of two porous carbon electrodes and a flow channel in-between (P. M. Biesheuvel et al., 2017; Suss et al., 2015). The operation of a CDI involves two stages: adsorption and desorption. Adsorption occurs when a direct current (DC) voltage is applied across the electrodes. Driven by the electric field, salt ions in the flow channel migrate towards their counter-electrode (i.e., the electrode carrying opposite charges) and become adsorbed on the electrode surface. During desorption, the two electrodes are shorted-circuited or reversed with polarity and salt ions are released and collected as brines. In theory, any soluble ions and charged particles can be separated from wastewater with CDI, including heavy metals, viruses, bacteria, and organic molecules (Salari et al., 2022). Recently, CDI has found applications in nutrient recovery and removal from wastewater (Huang et al., 2013; Porada et al., 2013; Rittmann et al., 2011; Wimalasiri et al., 2015; Zhang et al., 2013). (2019)

Although most existing CDI studies focus on water desalination, increasing attention has been paid to nutrient separation and recovery. To our knowledge, no review of CDI-assisted P recovery has been available. This review is expected to fill this gap. It consists of four parts: (1) a brief summary of CDI technologies; (2) P in wastewater and conventional P recovery methods; (3) existing studies of CDI-assisted P recovery from wastewater; and (4) a discussion on challenges and perspectives. The purpose of Parts 1

and 2 is to provide readers with essential background information; while Parts 3 and 4 constitute the focus of this review effort.

2. Capacitive deionization (CDI): Principles, construction and operation

The purpose of this section is to allow readers without prior knowledge of CDI to develop a basic understanding about the technology, preparing them for later discussions on CDI involved P recovery. The section covers two subjects: (1) the working principle of CDI, and (2) the types of CDI cells and their operations. For in-depth discussions on the CDI technology, interested readers may refer to Oren (2008), Porada et al. (2013) and Suss et al. (2015).

2.1. Working principle of CDI

The whole idea of CDI is centered around electrical double layer (EDL), the boundary structure that forms on liquid-solid interfaces. In a CDI cell, the liquid can be sea water, brackish water, or any aqueous solutions that carry ions or charged particles; while the solid is often a porous electrode. The CDI cell utilizes the EDLs on the electrode surface to store ions or charged particles removed from an aqueous solution. The EDLs can be strengthened (polarized) or weakened (relaxed) by manipulating the voltage on the electrodes.

As aforementioned, the operation of a CDI cell typically consists of two stages: adsorption (also known as charging) and desorption (also known as discharging).

- During adsorption, a DC voltage [of typically 1-1.4 V (Qu et al., 2016)] is applied and the electric field that it creates drives ions and charged particles to migrate towards the electrodes of opposite charges (Suss et al., 2015). This phenomenon is dubbed "electromigration" (for ions) or "electrophoresis" (for charged particles).

When the ions or charged particles approach the electrode, they are held in and, in turn, further the development (polarization) of the EDL (P. M. Biesheuvel et al., 2009; Ying et al., 2002). Adsorption ends when the EDLs' polarization potentials on the two electrodes balance out the applied DC voltage. By removing ions or charged particles, the feed stream (e.g., brackish water) can, thus, be desalinated. A CDI cell can be charged in a constant voltage or a constant current mode. While the former is more commonly used, the latter (constant current) mode was reported by some to deliver an improved desalination performance (Jande & Kim, 2013; Zhao et al., 2012).

- During desorption, the CDI cell is short-circuited, leading to relaxation of the developed EDLs. As a result, ions or charged particles are released from the EDLs back to the bulk liquid. The liquid containing concentrated ions or charged particles, known as a brine stream or concentrate, can be collected for disposal or further processing, including nutrient recovery. Desorption can also be realized by reversing the polarity of the applied voltage. This forces the EDLs to reverse their polarities and undergo a relaxation-repolarization process, and repulses the ions or charged particles desorbed from one electrode to migrate towards the other electrode. A benefit of polarity reversal is its greater desorption rate than that of short circuiting. However, short circuiting is more energy efficient because it consumes no power. Furthermore, the charge flowing out of a CDI cell during short-circuiting may be leveraged for energy recovery (Suss et al., 2015).

According to the classic Gouy-Chapman-Stern model, an EDL formed on a charged electrode surface can be divided into two regions. Adjacent to the electrode surface is a

compact layer, also known as a Stern layer, where ion distribution is dense and rigid and is driven by the space charge carried by the solid electrode. Farther from the electrode surface is a diffuse layer where ion distribution is loose and governed by both the space charge and Brownian diffusion. The space charge can be regulated with the control of electrode potentials, e.g., by changing the applied voltage over a CDI (Bazant et al., 2004); and when the CDI reaches an equilibrium, the same amount of opposite charges (as the surface charge), in forms of adsorbed ions, will be accumulated in the EDL including the compact and diffuse layers. Differential capacitance (C_d), which characterizes the amount of charge accumulation in the EDL per unit of electric potential, is a serial combination of the capacitance in the compact layer (C_C) and that in the diffuse layer (C_D). A CDI cell, thus, can be regarded as a capacitive device (which partly explains the origin of its name).

It is noteworthy that the Gouy-Chapman-Stern model has several limitations. For example, it fails to consider the polarization and adsorption of dipole molecules (e.g., water) and it does not apply to porous electrodes with micropores smaller than the thickness of diffuse layers. To address these limitations, revised EDL models, such as the Grahman model and the Bockris-Devanathan-Muller model, were developed. Specifically for CDI, numerous efforts have been made in recent years to model the thermodynamics and kinetics of CDI processes. A summary of the recent advances in CDI theory is lacking. However, it is beyond the scope of this review effort.

2.2. Types of CDI cells

This section summarizes the common CDI cell types in the literature. It is noteworthy that the summary is not exhaustive as new CDI designs continue to surface. As aforementioned, a basic CDI cell is comprised of a pair of electrodes and a flow channel.

CDI electrodes are typically made from porous carbon materials (e.g., granular activated carbon, carbon felt, graphene, and carbon aerogels) with large surface areas and superior chemical stability. The flow channel is constructed by cutting a void space through a spacer that separates the CDI electrodes. Differences in the arrangement of electrodes and spacers, flow directions, and accessory components lead to various types of CDI cells.

2.2.1 Flow-by CDI

A flow-by CDI cell (Figure 1-1a) is the most classic type but still widely used. It was first built by Blair and Murphy (1960) and extensively studied by Dr. Yoram Oren and his colleagues in the 1970s and 1980s (Oren, 1978; Oren & Soffer, 1983). In a flow-by CDI cell, two electrodes are placed in parallel, and a channel in the midst takes the feed stream in during adsorption and discharges the concentrate out during desorption (Suss et al., 2015; Tang et al., 2019). This cell type is named for its flow direction – the feed stream flows *by* and in parallel to the two electrodes. As a result, the flow direction is perpendicular to the electric field. Mass transport across the flow channel is likely to be diffusion limited because of the lack of bulk or turbulent flows along the electric field lines (Bouhadana et al., 2010; Porada et al., 2013; Remillard et al., 2018; Suss et al., 2015).
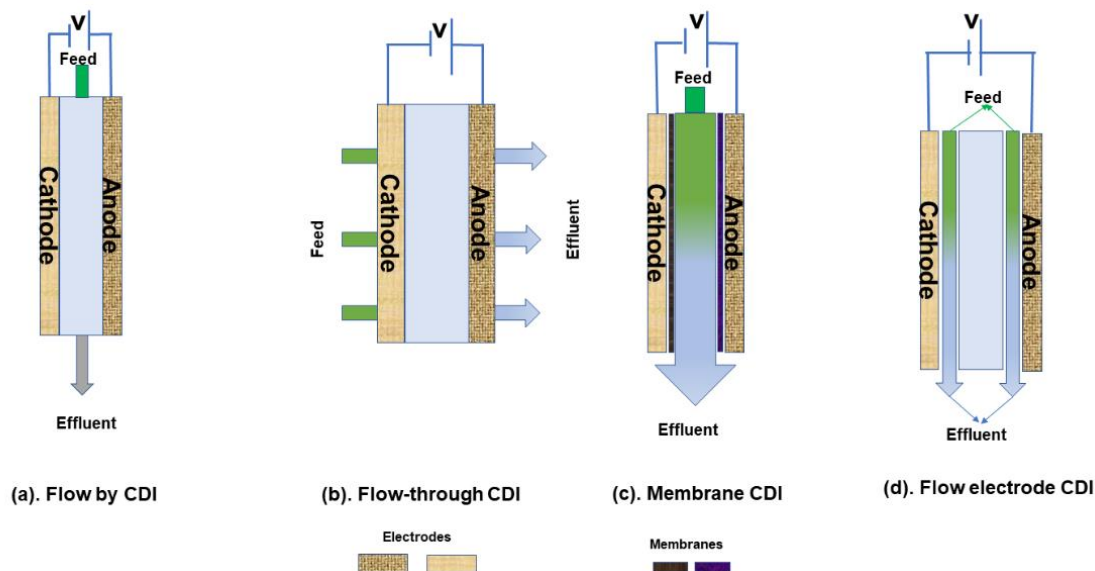
Figure 1-1. The Four main types of CDI cells (a) Flow by CDI (b) Flow-through CDI (c) Membrane CDI (d) Flow electrode CDI.

2.2.2   *Flow-through CDI*

To overcome the mass transport limitation, Johnson et al. (1970) proposed the design of flow-through CDI cells. In a flow-through cell, the feed stream flows *through* the electrodes in a direction parallel to the electric field (Figure 1-1b). With enhanced ion transport, a deionization throughput ~4-10 times greater than that of a similarly-sized flow-by CDI cell can be achieved. Another advantage of flow-through cells is their faster charging (adsorption) rate than flow-by cells when consuming a similar level of energy (Avraham et al., 2009, 2011; Oren & Soffer, 1983). A simple transmission line model was developed to describe the ion and charge transfer in flow-through CDI cells (Qu et al., 2016).

2.2.3   *Membrane CDI*

Membrane CDI (MCDI) was first reported by Lee et al (2006). In an MCDI cell, an anion-exchange membrane is inserted between the cathode and the flow channel and a

cation-exchange membrane between the flow channel and the anode (Figure 1-1c). With that, only the counter-ions (i.e., ions carrying charges opposite to an electrode) are permitted to pass through the membrane. During adsorption when a DC voltage is applied, an electrode attracts its counter-ions from the feed stream and repulses its co-ions (i.e., ions carrying the same charges) from the electrode surface. The latter process consumes current but makes little contribution to desalination. Ion-exchange membranes block down the process, thereby improving the CDI's charge efficiency (Biesheuvel et al., 2011). Compared to conventional flow-by CDI cells, MCDI cells have an increased salt removal rate, decreased energy consumption, and a stable desalinated stream (Biesheuvel and Wal, 2010; Lee et al., 2006; Lee et al., 2011).

2.2.4   *Flow-electrode CDI*

Instead of using fixed electrodes (e.g., carbon rods or cloth), a flow-electrode CDI (FCDI) uses flow electrodes, also known as fluidized bed electrodes, that are made of fluidized carbon granules or powders (Figure 1-1d). These carbon granules or powders are recirculated between electrode chambers – where ion adsorption occurs – and an external neutralization vessel – where desorption occurs and the carbon electrodes are regenerated. This unique design allows the FCDI cell to work continuously in the charging (adsorption) mode, thereby simplifying the operation. Another advantage of FCDI is its greater desalination capacity. The desalination capacity of conventional CDI cells is limited by the amount of adsorbents (electrode materials); while in FCDI cells, extra carbon adsorbents are available in the recirculation loop.

3. Phosphorus in wastewater and its removal

Phosphorus (P) exists in various forms in wastewater, including organic P and inorganic P. Both usually occur as phosphate. Organic P (e.g., ATP and DNA) comes from biological sources such as human sewage, animal waste, and food residues. Organic P generally accounts for a small portion of total P as it can be converted into inorganic P by microbes through a process known as mineralization. However, microbes may also produce organic P from inorganic P in a biological treatment process. Inorganic P can be further classified into orthophosphate (with one P atom) and condensed phosphate (pyro-, meta- and polyphosphate; with multiple P atoms) based on the number of P atoms per molecule. They are also named as reactive phosphorus and acid hydrolysable phosphate, respectively, after their analysis methods. Orthophosphate can easily bond with various cations (e.g., Al, Fe, Ca) or chemicals and could constitute up to 60% to 70% of total P in a wastewater stream (Melcer, 2003).(Water Environment Research Foundation, Alexandria, VA). It is also the most prevalent ingredient in commercial P fertilizers. When poorly managed, these fertilizers will end up in surface waters, causing eutrophication. Condensed phosphate is produced from the condensation of multiple orthophosphate molecules via P-O-P linkages. The calcium, sodium, and potassium salts of condensed phosphate are commonly used as food additives (Dabkowski, 2015; Hach, 2013; Melcer, 2003). Condensed phosphate salts are also used in water distribution systems to prevent corrosion. Both inorganic and organic phosphates can be water soluble or insoluble. However, their overall solubility can be generalized as: orthophosphate > condensed phosphate > organic phosphate. Accordingly, solid separation is normally effective in the removal and recovery of organic phosphate (organic P).

Numerous methods have been developed to remove and/or recover P from municipal and agricultural wastewater. Based on their working principles, they can be classified into physical, chemical, and biological methods/processes.

- Physical methods include ion exchange, adsorption, and membrane separation (Chrispim et al., 2019). They can work over a wide temperature range and are typically used for wastewaters with relatively low P concentrations (Carrillo et al., 2020). Johir et al. (2011) used anion exchange resins to further remove P from the effluent of a membrane bioreactor and reported a removal efficiency up to 95-98%. A similar finding was made by Chrispim et al. (2019) for P removal from the secondary effluent of wastewater treatment plants. Adsorbents such as zeolites and biochar were also tested for P removal and recovery from wastewater (Bian et al., 2016; Yin et al., 2019). However, many of them had a limited adsorption capacity for P (Carrillo et al., 2020). The regeneration of ion exchangers or adsorbents required additional reaction beds/vessels, resulting in high operating costs (Miladinovic & Weatherley, 2008; Puchongkawarin et al., 2015). Another challenge is that the effluents from these systems could contain P concentrations up to 1-4 mg P/L (Johir et al., 2011; Vera et al., 2014), which were greater than wastewater discharge standards in certain countries/regions such as China (0.05 mg P/L) and Europe (1–2 mg P/L) (Committee Report, 1970; Zou & Wang, 2016). The membrane separation method is highly efficient (Koh et al., 2020). However, its energy consumption is intensive and fouling could occur because of contaminant and salt accumulation on membrane surfaces (Mehta et al., 2015).

- Chemical methods convert dissolved P into solid forms, a process known as crystallization (Mehta et al. 2015). Phosphate precipitates can be obtained by adding the soluble salts of Al, Fe, Mg, or Ca to a wastewater (Melia et al. 2017). By doing this, P can be recovered as struvite, hydroxyapatite, vivianite, or other P-containing minerals (Muster et al. 2013; Peng et al. 2018). Struvite is usually preferred rather than hydroxyapatite and vivianite. Because of its great bioavailability (94%) and high purity (97-99%), struvite is considered as a high-quality slow-release fertilizer (Kataki et al., 2016; Talboys et al., 2016); and the formation of struvite removes ammonia concurrently from wastewater (Muster et al. 2013; Melia et al. 2017). The precipitation of struvite is affected by numerous factors, such as pH (typically 7.0-11.5) and Mg concentrations (Münch and Barr, 2001; Moss et al., 2013). Muster et al. (2013) acquired struvite with >98% purity when [Mg]:[Ca] > 4:1 and pH > 7.9 and found an optimal pH range of 8.0-9.5 for effective precipitation. Ye et al. (2017) reported that chemical precipitation at pH = 7.0-7.5 resulted in struvite of 99.7% purity. Certain limitations are associated with the chemical methods. First, system setup is challenging because of struvite deposition and clogging. Secondly, it requires chemicals including magnesium salts and pH adjusters. Thirdly, struvite may co-precipitate with toxic ions (e.g., arsenic and fluoride), organic contaminants, pathogens or viruses (Melia et al. 2017; Perera et al. 2019).

- Biological methods involve the assimilation of P by organisms, especially microorganisms (Carrillo et al., 2020; Xuan et al., 2019). They are more economically feasible and produce less sludge than physical or chemical methods

(Banu et al., 2008). A group of bacteria, polyphosphate-accumulating organisms (PAOs), can store excess P and live in both anaerobic and aerobic environments and, thus, are utilized to remove soluble P from wastewater. Example of PAOs include *Acinetobacter, Rhodocyclus*, *Pseudomonas, Aerobacter, Moraxella, Escherichia coli, Mycobacterium, Corynebacterium*, and certain coccus-shaped bacteria (Bond et al., 1995; Wong et al., 2005). They can amass P up to 5-12% of cell weight (Rajesh Banu et al., 2009). With PAOs, various biological treatment technologies have been developed for P removal/recovery from wastewater, the vast majority of which feature alternated anaerobic and aerobic phases. Among them, enhanced biological phosphorus removal (EBPR) is most commonly used. An EBPR process consists of three steps. First, under anaerobic conditions, the energy released from polyphosphate hydrolysis and organic matter degradation is used by PAOs to produce polyhydroxyalkanoates (PHAs), a group of energy-rich substances. The produced PHAs are stored in the PAOs' volutin granules. Next, under aerobic conditions, PAOs consume the stored PHAs to support cell growth. Meanwhile, the cells' polyphosphate reserves are reloaded with P absorbed from the environment. During this step PAOs absorb more P than required into their cells – known as "luxury uptake". The final step involves the removal of P-enriched PAOs as sludge (Machnicka et al., 2008; Ong et al., 2016). When properly designed and operated, an EBPR process can remove or recover ~60% P from wastewater (Baeza et al. 2017; Guisasola et al., 2019). Numerous factors can affect the efficiency, including temperature, pH, cations, dissolved oxygen levels, carbon sources, COD/P ratios, and solid retention time (Schönborn et al., 2001a).Further

information can be found in (Oehmen et al., 2007; S. Raj et al., 2012; S. E. Raj et al., 2013; Schönborn et al., 2001b) .

4. **CDI for phosphorus recovery**

Only a few CDI studies were dedicated to P removal or recovery from wastewater (Table 1-1). However, P removal can occur concurrently with other salts or nutrient ions and be a side outcome of CDI experiments. CDI could particularly be useful for P (and salinity) removal from the secondary effluent of municipal wastewater treatment plants (Liang et al., 2013; Stevens et al., 2003). The effluent has relatively low ion concentrations (and low electrical conductivities accordingly). As a result, it requires only a small current for the electrosorptive P removal process to proceed (Ge et al., 2018).

Table 1-1. List of studies using CDI for P removal or recovery.

Reference	Wastewater type	CDI type	Applied voltage	pH	Initial P concentration	Efficiency / Concentration
Huang et al. (2013)	Synthetic (KH_2PO_4)	Commercial CDI; n/a	1.5 V	5~6	50 mg/L	80% P
Huang et al. (2017)	Synthetic (Na_2HPO_4, NaH_2PO_4 and NaCl)	MCDI	Constant voltage (CV) mode: 1.2 V Constant current (CC) mode: 1 A	5~9	_	$H_2PO_4^-$ at pH < 7 HPO_4^{-2} at PH > 7 % P not specified
Bian et al. (2019)	Synthetic (Na_2HPO_4, NaH_2PO_4)	FCDI	1.2 V	_	18.1 ± 1 mg/L	49−91%
Ge et al. (2018)	Synthetic (Na_2HPO_4, NaH_2PO_4)	Regular CDI	1.2-3.0 V	7	18.1 ± 1 mg/L	46.4-80.7% after 12 hours
Jiang et al. (2019)	Synthetic domestic wastewater	MCDI	< 1.23	7-8	5-15 mg/L	_
Bian et al. (2020)	Synthetic	FCDI	CV: 1.2 V CC: 12 mA	4 ~ 9	500 mg P/L	_

Chen et al. (2020)	Synthetic (KH_2PO_4)	CDI	_	_	2 mg/L	_
Hong et al. (2020)	Real water matrix (Han River, Seoul, Korea	CDI	1.5 V	7	0.4 mg/L	98%
Zhang et al. (2020)	Synthetic (NaH_2PO_4)	FCDI	0-1.2 V	5.0	50 mg/L; 100 mg/L; 150 mg/L	97.72% at 1.2 V 97.23% at 1.2 V 95.79% at 1.2 V
Miao et al. (2021)	Ternary solution (NaH_2PO_4)	CDI	1.2 V	_	0.8 mM	72.12%
Xu et al. (2021)	Synthetic urine	FCDI	1.5 - 2.1 V	4.8 ~ 11.3 Optimum: 2	~1200 mg/L NaCl and ~720 mg/L $Na_2HPO_4 \cdot 12H_2O$	164 mg/L per cycle % not specified
Zhang et al. (2021a)	Synthetic anaerobic digest supernatant	FCDI	~2.0 V	7	200 mg/L P	63%
Zhang et al. (2021b)	Synthetic	FCDI	_	_	8 mg/L P	61.9%
Gao et al. (2022)	Phosphate solution	CDI	1.2 V	4 ~ 9	_	23–30 mg PO_4^{3-}
He et al. (2022)	Synthetic (150 mg/L P)	FCDI	1.2 V	4.8	150 mg/L P	Vivianite with P content of 12.4 %.
Zhang et al. (2022)	NaH_2PO_4 and Na_2HPO_4	CDI	1.2 V	3~ 10	2- 10 mg/L	95%

Selectively removing or recovering P from wastewater with CDI technology has been proven by researchers to result in a higher percentage of P removal/recovery (Gao et al., 2022; Zhang et al., 2021a; Zhang et al., 2022). The process, however, suffers from the effects of CDI operation parameters such as the pH of the wastewater, hydraulic retention time, current density, electrode type, and competition with co-existing ions. We discuss in sections 4.1.1, 4.1.2, 4.1.3, and 4.1.4 the few research works done on the above-mentioned operational parameters effects on phosphorus/phosphate recovery from wastewater with CDI technology.

4.1. Effects of pH

pH of the solution or wastewater plays a significant role in phosphate ions speciation and transport during CDI operation (sorption and desorption). The ideal pH of wastewater ranges between 6 to 8.5 and is mainly dominated by dihydrogen phosphate ion ($H_2PO_4^-$) and hydrogen phosphate ion (HPO_4^{2-}) of the P species (Jiang et al., 2019; Morgens, 2008). An increase in the pH of wastewater can compromise phosphate removal or recovery because of modification in dominant P species with their corresponding charges (X. Huang et al., 2017). This P speciation and its reversible reactions are shown in Figure 1-2 and Equations 1-3 (Bian et al., 2020).
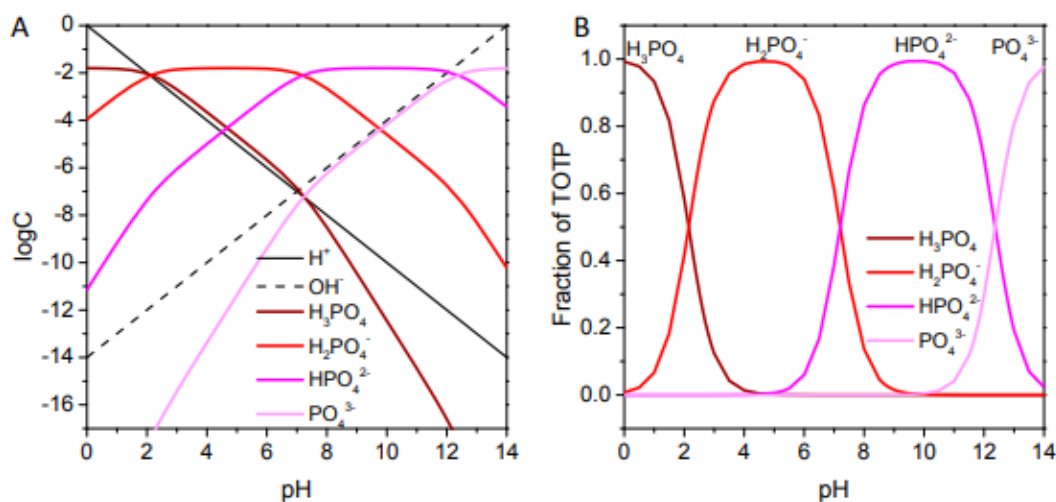
Figure 1-2. Speciation diagram of P species from pH 0 to pH 14 (initial TOTP=16 mmol). Log C-pH diagram (B) Fraction of P species. (Bian et al., 2020)

$$H_3PO_4 \leftrightarrows H^+ + H_2PO_4^- \quad pK_{a1} = 2.148 \quad (1)$$

$$H_2PO_4^- \leftrightarrows H^+ + HPO_4^{2-} \quad pK_{a2} = 7.198 \quad (2)$$

$$HPO_4^{2-} \leftrightarrows H^+ + PO_4^{3-} \quad pK_{a3} = 12.375 \quad (3)$$
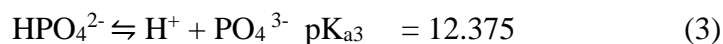
In the study by Bian et al. (2020), the pH dependence of phosphate speciation and transport in a flow electrode capacitive deionization was investigated while comparing the constant current and constant voltage charging modes. It was concluded that the pH of the initial feed or electrolyte immensely impacts the P recovery and removal. The results showed P removal rate increased from 20.8 to 38.3 mg/min for constant current at pH 9, whereas an increase from 16.8 to 34.3 mg/min P removal rate for constant voltage mode at pH 5. Following the comparison between the charging modes, the constant current charging mode was in conjunction with the Nernst-Planck equation further used to study the pH effect on P ions speciation and transport in wastewater for P removal and recovery. Under constant voltage and constant current, Huang et al., (2017) also investigated the pH dependence of phosphate removal from wastewaters utilizing MCDI. The results demonstrated that "the optimal P adsorption capacity occurred at a lower range of initial pH," especially with $H_2PO_4^-$ having a minimum radius making it preferable for adsorption. In addition, Xu et al., (2021) demonstrated the selective separation of P from synthetic urine using the FCDI technology coupled with adjusting the charging and discharging operation modes. The research resulted in a P recovery efficiency of 164 mg/L per cycle under optimal conditions of 5 wt % carbon; charging and discharging current densities of 10 and -15 Am^{-2}, respectively; charging and discharging current times of 120 and 30 min, respectively; and low electric energy consumption of 27.8 kWh/kg. The results from Xu et al., (2021) also stated that Faradaic reactions and the solution or electrolyte pH (<2), which led to converting P ions into uncharged H_3PO_4, aided in P selectivity by trapping it into the anode chamber during the discharging process.

Furthermore, to selectively recover phosphorus from wastewater, Gao et al., (2022) prepared a ferrocene polyaniline-functionalized carbon nanotube (Fc-PANI/CNT) electrode (anode) for the CDI operation. The results demonstrated that Fc-PANI/CNT has a high capacity for the adsorption of phosphate ions (35 mg PO_4^{3-} g^-) in the presence of competing ions (Cl^-, SO_4^{2-}, and NO_3^-) from complex synthetic wastewater. The above studies have proven that the pH of the wastewater contributes significantly to the speciation and transport of P ions for recovery/removal with the CDI technology.

4.2. Hydraulic retention time (HRT)

Hydraulic retention time in CDI technology refers to the time the solution or electrolyte is held in the CDI channel for ions adsorption or desorption. It is calculated by dividing the cell volume by the flow rate of the solution (Folaranmi et al., 2020). As part of investigating operational parameters to optimize the FCDI system for P recovery, Zhang et al. (2021a) researched the HRT effects on the FCDI process. The results show that a maximum P removal was attained at an HRT of 1.96 min with other optimum operational parameters (current density: 11.8 Am^{-1} and voltage: 2.0 V). A highlighted finding in this study relating to the HRT is that the FCDI operation is prone to unwanted reactions with longer HRT, although more salt removal can be achieved. Also, the higher cell voltage is utilized with longer HRT, which can increase the cost of the CDI operation, countering the merit of CDI technology's low energy usage. Zhang et al. (2021b) recovered 61.9% of P at HRT of 2.45 mins with other optimal operating parameters in the quest of selectively recovering P in an FCDI. The recovered P was done with electrode modified with a magnetic iron oxide-impregnated carbon. The results of this study also demonstrated that, with an increase in HRT, the removal efficiency of P and Cl increases. He et al. (2022) also

used an HRT of 58 s in a four-chamber FCDI to selectively extract P from wastewater as vivianite to achieve a P of 71% in the first 12 hours of the FCDI operation. Furthermore, Xu et al., (2021), in a study on selective P recovery from synthetic urine, applied an HRT of 2 min coupled with other operational parameters to recover 164 mg/L P efficiency. Hydraulic retention time is prevalent in most CDI studies. However, little research has been conducted focusing on HRT in the selective removal/recovery of P from wastewater.

4.3. Current density

The current density with the unit amperes per square meter is an essential parameter in the operation of the CDI system. In a study by Zhang et al., (2021), the current density was explored for its influence on the FCDI operation for the recovery of phosphate. Here, a current density ranging from 3.4 – 8.0 Am^{-2} was applied to determine the optimum for FCDI performance. It was observed in this study that an optimal current density of 6.14 Am^{-2} yielded 69.1% P with other optimal operational parameters. Another observation by Zhang et al., (2021) in this study showed that lower current densities made P susceptible to removal. Xu et al., (2021) also utilized current densities of 10 and -15 Am^{-2} for the charging and discharging operation of the FCDI, respectively, to recover P of 164 mg/L per cycle efficiency. The objective of this study was to separate P from synthetic urine selectively.

4.4. Electrode type

Several electrodes of different characteristics have been utilized in the CDI operation (Le et al., 2016; D.-J. Lee & Park, 2014; Nakayama et al., 2021). The electrodes aid in ion adsorption and thus should constitute properties such as high surface area, good electrical conductivity, and appropriate pore size. Carbon-type electrodes such as activated

carbon (Nakayama et al., 2021), carbon aerogels (Le et al., 2016), and mesoporous carbons (D.-J. Lee & Park, 2014) were initially mostly used in the CDI technology. Nanomaterial-based electrodes were later introduced to enhance the CDI system (Bharath et al., 2017). To selectively recover or remove P from wastewater, there has been modifications of the electrodes (Gao et al., 2022; Gao et al., 2022; Zhang et al., 2022) because most carbon materials, for example, have a deficit in ion storage capacity and selectivity (Gao, Shi, et al., 2022). In a study by Zhang et al., (2022), the anode of the CDI was constructed with a terephthalic acid intercalated carbon nanotube composite material (ZnZr-COOH/CNT) for phosphate removal. The study's objective was to investigate the selective removal of phosphate by the anode-modified electrode. It was reported that ZnZr-COOH/CNT performed significantly in the adsorption of phosphate ions (reduced 10 mg/L P to 0.5 mg/L P) due to the composite relationship of Zn and Zr with phosphate in the electrode and establishment of hydrogen bonds between the hydroxyl group of phosphate and carboxyl group of terephthalic acid. Zhang et al., (2021) reported on a 60% P removal or recovery with an FCDI with its electrode modified with magnetic iron oxide. It was observed that magnetic carbon demonstrated a close attraction with P which aided in selective adsorption of P. In addition, Hong et al., (2020) investigated the selective removal of phosphate with a CDI electrode fabricated in the form of layered double hydroxide/reduced graphene oxide (LDH/rGO). The LDH/rGO electrode performed well in selecting P ions and overriding the excess coexisting ions (Cl-) in the solution which normally competes with P ions in CDI operation. Furthermore, Gao et al., (2022) successfully achieved a P adsorption capacity of 23-30 mg PO_4^{3-} g^{-1} with a CDI anode

modified with a guanidinium-functionalized polyelectrolyte (Gu-PAH/CNT) in the presence of competing coexisting ions such as Cl^-, SO_4^{2-}, NO^{3-}.

5. Summary and Perspective

Selective removal of P ions has been identified in the studies conducted on CDI technology application in wastewater for removal for P as significant in higher recovery efficiency. The application of CDI in P removal will not only provide a solution to the global depletion of P at a low operational cost and energy-efficient way but will also facilitate the prevention of environmental damage (eutrophication) by P loss to the environment. It was observed from this review that few research work has been conducted on P removal from wastewater with the CDI technology, and thus, there is a need for more research on this topic focusing on operational parameters optimization for efficient P removal and cost effectiveness in CDI system construction and operation. This review reported on the studies that have utilized CDI for P removal or recovery, focusing on the removal efficiency and the various operational parameters effects on the CDI operation.

Operational parameters were optimized to achieve efficient P selectivity and removal. An example is the voltage range of 1.2 – 1.5 V, used mostly in the studies listed in this review as the optimized voltage to enhance P removal or selectivity. In addition, in most of the studies in this paper, low-strength or low-concentration P wastewater are utilized in the use of CDI technology for P removal or recovery from wastewater. In practice, wastewater like swine wastewater from the agriculture industry, for example, rarely constitutes P concentrations below 600 mg/L. We suggest future studies of CDI for P recovery or removal use wastewaters with higher concentrations of P to complement its application in the field. Most of the studies conducted in this review are laboratory scale

for P removal and showed satisfactory removal performance. The focus on laboratory scale experiments neglecting industrial application of the CDI technology can be attributed to challenges such as (1) membrane fouling and electrode scaling which can reduce the lifespan of the system and (2) excessive concentration of total dissolved solids (TDS) in wastewater. A pilot scale or practical application of CDI technology for P removal exploration should be encouraged considering (1) A focus on exploring ways of targeting P ions during CDI operation by optimizing the various operational parameters, (2) Improvement on electrode modification and cell architectures to recover P from wastewater selectively (3) Membrane fouling and electrode scaling reduction and (4) Reduction in cost for the CDI system construction and operation.

Comparing the CDI technology for P removal to other existing technologies (Reverse Osmosis and Enhanced Biological Phosphorus Removal), there are no standardized testing procedures for laboratory experiments and fieldwork. It was observed that the studies listed in this review on CDI for P removal did not follow a standardized protocol. We believe this can affect the CDI performance or operation for P removal. A well-laid-out standard test protocol will encourage the use of the CDI technology in practice and increase the recovery efficiency of P from wastewater. Developing a standard protocol for the CDI operation is also essential because reactions such as Faradaic effects, electrolysis, and competition with existing co-ions can be reduced or averted.

Materials used in constructing the CDI cells should also be considered for further research to enhance their performance in P removal or recovery. We observed studies cited in this review modifying electrode surfaces to aid in more P selectivity and removal. So far, reports from these studies have been positive in increasing P removal or recovery

efficiency. In future studies, significant attention should be given to the electrode pore size, pore size distribution, adsorption capacity, and P selectivity.

The economic value of CDI for P removal is highly dependent on less electrical energy, which makes it most advantageous over other P removal technologies. Benefits such as lower operational cost, higher P removal efficiency, system portability, and less or no water softness chemical demand of CDI for P removal simultaneously complement the CDI technology's economic value. It is, therefore, imperative to encourage future studies in CDI for P removal or recovery. In conclusion, CDI for P removal and recovery is an emerging technology that is both challenging and significant in the wastewater industry. Encouraging more studies in this field will create opportunities for pilot scale and field applications.

CHAPTER 2: Distribution Of Airflow And Media Moisture Content Across Two

Vertical Bed Biofilters

Authors: Augustina Osabutey, Brady Cromer, Alexander Davids, Logan Prouty, Noor Haleem, Robert Thaler, Richard Nicolai, and Xufei Yang

Abstract

For its small square footage, a vertical bed biofilter was developed for odor emission mitigation for livestock facilities with limited area available for biofilter installation. However, a concern about the design is that airflow and moisture may be poorly distributed across the biofilter due to the effects of gravity. Relevant data are sporadic in the literature. To fill the knowledge gap, two vertical bed biofilters were constructed at a university swine facility and monitored for two months. The monitoring was taken at 27 grid points on each biofilter per field visit. Results revealed that both the airflow and medium moisture content were unevenly distributed. The sun-facing side of the biofilters had significantly lower medium moisture content (p<0.01) due to solar-induced water evaporation. The side directly facing the barn exhaust had the highest airflow. Airflows varied along the height of the biofilters, but no significant difference was noted. The uniformity of airflow and moisture content, characterized by coefficient of variance (CV) and distribution uniformity (DU), respectively, were examined over the monitoring campaign. Possible reasons for uneven distribution were explored, and recommendations are made to address the uniformity issue. The findings from the study

are expected to further the development and implementation of biofiltration technology for livestock odor control.

Keywords:

Biofilter, airflow distribution, moisture content, uniformity, swine barn

1. Introduction

Odor is a top air quality challenge for pork production (Wing et al., 2008). Various odorants, such as ammonia, hydrogen sulfide, and indole, have been identified in the air of swine barns (Ni et al., 2012). Many of them are produced from the microbial decomposition of pig feces or undigested feed (Mackie et al., 1998). After being discharged into the atmosphere, those odorants can disperse to neighboring communities, causing odor nuisance. The occurrence of odor nuisance can undermine the public relations efforts of pork producers and, in certain scenarios, result in odor complaints and even lawsuits (Huang and Miller, 2006). In many counties of the U.S., rules are becoming increasingly stringent regarding the construction of new or the expansion of existing swine facilities. This is primarily driven by public concerns about odors. To promote the sustainable development of the pork industry, a simple, low-maintenance, cost-effective odor mitigation method is needed.

Biofilters are considered by many as a promising technology for odor mitigation (Nicolai and Lefers, 2006; Chen and Hoff, 2009). Compared to technologies such as wet scrubbers, activated carbon adsorption, and ozonation, biofilters are less expensive to construct and offer decent odor reduction performance when properly operated (Wang et al., 2021). In a biofilter, microorganisms are grown on a filtration medium to form biofilms. When the exhaust air passes through the medium, air contaminants are sorbed into the

biofilms and degraded by the microorganisms with the presence of oxygen and water (Cooper and Alley, 2010). Biofilters have been extensively used to treat volatile organic compounds (VOCs) emission in the chemical and petroleum industry (Iranpour et al., 2005; Barbusinski et al., 2017). The use of biofilters for livestock odor control was first reported by Dr. Zeisig in the 1970s (Noren, 1986). Since then, numerous research efforts have been made to develop cost-effective biofiltration technologies. Cost is a key factor in the success of any farm-related environmental technology. For swine barns, a biofilter can be made from lumbers, poultry wires, and organic packings (e.g., woodchips, straws, and compost), most of which are readily accessible to average farmers.

Based on the layout of filtration media, biofilters can be classified into two types: horizontal and vertical. In a horizontal bed biofilter (also known as a vertical airflow biofilter), the filtration medium is placed into a horizontal layer and the exhaust air goes vertically in the medium. Horizontal bed biofilters have been the most studied in the literature and extensively adopted for field demonstration (Chen and Hoff, 2009). However, a downside of horizontal bed biofilters is the large square footage they take. In certain scenarios, the construction is prohibited by the lack of enough area near exhaust fans. To address this limitation, an alternative design named vertical bed biofilters (also known as horizontal airflow biofilters) was proposed (Mann and Garlinski, 2002; Nicolai et al., 2005; Nicolai and Thaler, 2007). In a vertical bed biofilter, filtration media are caged or netted into vertical filtration walls. The exhaust air first reaches an inner air plenum (usually at the center of the biofilter) and then passes through the filtration walls horizontally to get treated. Because of its filtration wall design, a vertical bed biofilter takes a considerably

smaller area than a horizontal counterpart possessing the same treatment capacity (Mann and Garlinski, 2002).

For vertical bed biofilters, a challenge is how to ensure the uniform distribution of airflow and moisture content over a filtration wall (Lefers, 2006). Along the height of the filtration wall, the gravitational settling of filtration media is expected to result in a decrease in porosity from top to bottom. Thus, air friction per unit of medium thickness reaches the maximum near the bottom (Devinny et al., 2017). When the filtration wall is of uniform thickness, the airflow that passes through it is expected to increase from bottom to top. Non-uniform airflows would lead to decreased odor mitigation performance (Choi et al., 2003). Moisture is another key parameter for biofilter operation. Optimal moisture levels varied with filtration media. For compost-based media, a recommended moisture range was 50-55% (Goldstein, 1999). For a mixture of compost and woodchips, the range was 35-65% (Nicolai and Lefers, 2006). For woodchips, it was 40-60% (Chen et al., 2008). For simplicity, a watering system is typically installed at the top of a vertical bed biofilter. But because of the non-uniformity in medium porosity, airflows, and water flows along the height of the biofilter, it is difficult to predict the distribution of medium moisture contents. A rule of thumb is to make a biofilter as wet as possible but without causing spillover flooding (Lefers, 2006).

A potential solution to non-uniform airflows is to use a tapered filtration wall design, with a greater medium thickness at the top and a smaller thickness at the bottom (Nicolai et al., 2005). A taper angle of 9.6° was reported to offer the most uniform airflow distribution (Lefers, 2006). However, the construction of tapered walls is more complicated than non-tapered ones. For pork producers, this means that additional expertise, time, or

money is required. Furthermore, no long-term field experiment has been done to track the distribution of airflows and medium moisture contents in vertical filters (with either tapered or non-tapered walls), making it hard to decide between the two designs.

As part of the effort to resolve the above question, two vertical bed biofilters with uniform filtration medium thickness (i.e., non-tapered walls) were built and monitored for over two months. The overarching goal of this study is to develop biofilter design guidance for pork producers, thereby promoting the implementation of this technology. The research objectives are to (1) measure the air velocities and medium moisture contents at different spots of the biofilters, (2) conduct statistical data analysis to assess the uniformity of airflow or moisture content distribution, and (3) make recommendations for future vertical bed biofilter design and operation.

2. Material and methods

2.1. Biofilters

Two vertical bed biofilters were built at the Swine Education & Research Facility of South Dakota State University (Figure 2-1). The larger one, measured at 4.88 m (L) $\times$ 2.44 m (W) $\times$ 2.44 m (H), was installed immediately after a pit fan of the facility's gestation barn. The smaller one, with dimensions of 3.66 m (L) $\times$ 2.44 m (W) $\times$ 2.44 m (H), was ducted to a pit fan of the facility's wean-to-finish barn. A cubic inner plenum was sized in each biofilter to enable 0.6 m-thick filtration walls. Both biofilters were framed with ground-contact treated wood, netted with vinyl coated poultry wires with 19 mm mesh, and filled with 25-40 mm cedar woodchips as filtration media. Soaker hoses buried ~0.1 m under the top surface of woodchips were used to water the biofilters, and the watering was controlled with a digital watering timer. Each biofilter was watered twice per day, and the watering

system was adjusted to ensure (1) a uniform watering rate throughout the top of a biofilter and (2) that the entire biofilter became wet but with no flooded ground (caused by excess water). The adjustment was done before the experiment. No further adjustment was done unless otherwise stated.

(**a**)   (**b**)
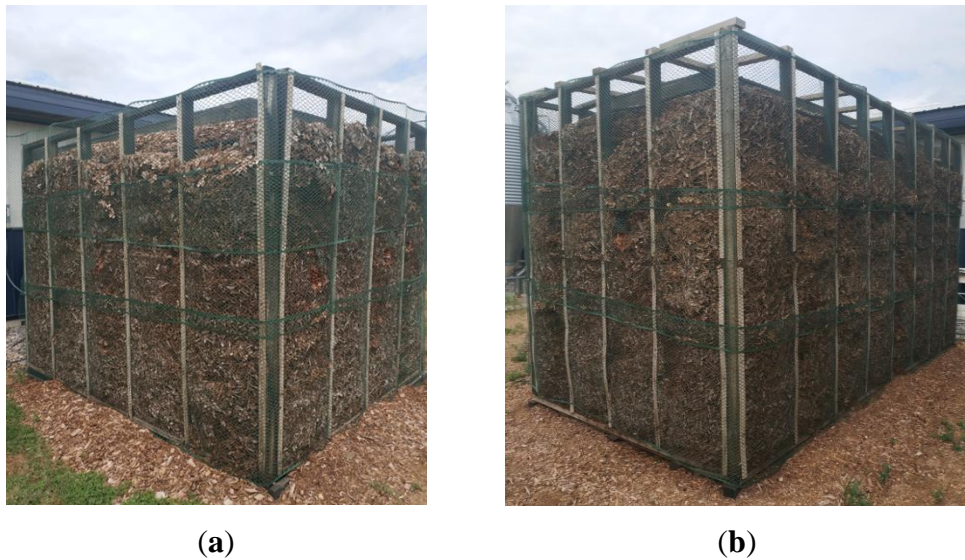
Figure 2-1. Photos of (a) the smaller biofilter (BF#1) outside of a wean-to-finish barn; and (b) the larger bio-filter (BF#2) outside of a gestation barn.

2.2. Air velocity measurement

With the current design, each biofilter had three gas outlet sides (Figure 2-2). To study the spatial distribution of effluent airflow, each side was further divided into nine sections. Thus, for each biofilter, a total of 27 sampling points were selected. The air velocity was measured with an ADM-860C AIRDATA multimeter (Shortridge Instruments, Inc., Scottsdale, AZ). The meter consisted of a digital manometer and a pitot-tube probe. To improve the measurement representativeness, a cross-shaped probe with multiple pitot tubes and a fabric duct was used for its capability of measuring the average air velocity of a 0.3 m × 0.3 m area. The meter was also equipped with temperature,

humidity, and barometric pressure sensors for air density correction (required for accurate air velocity measurement).

(**a**)   (**b**)
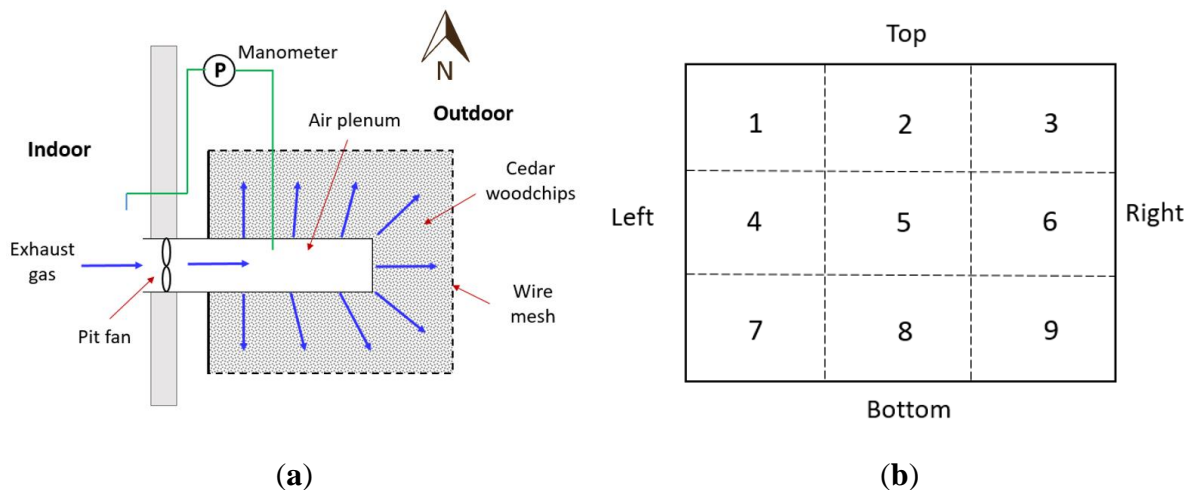
Figure 2-2. (a) Cross-section (top view) of each biofilter; and (b) side view of each biofilter. Both biofilters had the same orientation, each with three air outlet sides facing south, east, and north, respectively. Each side was divided into nine sections for measurement.

2.3. Moisture content measurement

The measurement used the same set of sampling points as aforementioned. Two methods were employed: (1) a handheld probe to measure the air humidity of effluent airflow, and (2) a gravimetric method to determine moisture content in the filtration medium (woodchips). For air humidity measurement, a Kestrel 5500 weather meter (Kestrel Instrument Inc., Boothwyn, PA) was held at the center of each section and three readings were taken to calculate the average humidity level. For woodchip moisture content measurement, a ~50-100 g woodchip sample was collected at the center of each section and kept in a Ziploc bag. To enable woodchip sampling, a 10 cm × 10 cm opening was cut near the center of each section and sealed with zip ties after each sampling. Upon return to the lab, the woodchip sample was transferred to a pre-weighed empty aluminum baking

cup, weighed at an analytical balance (for wet weight), and then dried in a lab oven at 110 ℃ for 24 hours. After drying, the cup was weighed again (for dry weight); and the moisture content (on a wet basis) was calculated as:

$$\text{Moisture } (\%) = \frac{\text{wet weight (g)} - \text{dry weight (g)}}{\text{wet weight (g)} - \text{empty cup weight(g)}} \tag{1}$$

2.4. Field monitoring and data analysis

The field monitoring was done from September 26, 2019 to December 5, 2019, with totaling nine weeks of data collected. Each biofilter was visited once or twice per week when weather and farm conditions permitted. Rainy or snowy days were avoided because of their large influence on moisture content measurement. Extremely windy days were also avoided as they could bias air velocity measurement. The pressure difference (ΔP) between the barn and the air plenum was also measured during the monitoring campaign using a manometer (Figure 2-2); however, the data were discarded because of an improper installation of manometer tubing's.

The acquired measurement data were summarized over the entire field monitoring period for each biofilter, air outlet side, or section. A Shapiro-Wilk normality test revealed that the data did not follow a normal distribution. Accordingly, non-parametric ANOVA (Kruskal-Wallis followed by Mann-Whitney post-hoc analysis) was conducted to compare air velocity or moisture between different sides or rows (of sections). For each biofilter, the uniformity of moisture content distribution was assessed with distribution uniformity (DU). DU is a measure of the spatial uniformity of watering for irrigation systems (Warrick, 1985) and it is defined as:

$$DU = \frac{Avg_{LQ}}{Avg_T} \tag{2}$$

where, Avg_T is the moisture content averaged from the 27 outlet sections of a biofilter, and Avg_{LQ} is that averaged from the lowest quartile, in this case, the lowest 7 measurements ($27/4 \approx 7$). The uniformity of air velocity distribution was assessed with coefficient of variance (CV):

$$CV = \frac{SD}{Ave} \tag{3}$$

where, Ave is the average air velocity of the 27 biofilter outlet sections, and SD is the standard deviation of air velocity. All the statistical tests were done with PAST, an open-source software program (Hammer et al., 2001). A significant level of $\alpha = 0.05$ was used for all the tests.

3. Results and discussion

3.1. Summary of field monitoring results

The gestation barn was shut down for two weeks in mid-October, during which no measurement was done for BF#2. For BF#1, a malfunction was found with the watering system; for a data quality consideration, only the moisture content measurement results after October 24, 2019 were included in data analysis.

An uneven distribution of airflows was seen for both biofilters along horizontal and vertical directions (Table 2-1). The average air velocity was 0.141 ($\pm$0.067) m/s for BF#1 and 0.143 ($\pm$0.058) m/s for BF#2, corresponding to a treated airflow rate of 3.36 m^3/s for BF#1 and 4.26 m^3/s for BF#2. An empty bed contact time (EBCT) was estimated to be ~3.7 sec for BF#1 and ~3.8 sec for BF#2. In comparison, an EBCT of typically 3-5 sec was recommended for biofilter design (Chen and Hoff, 2009). The maximum air velocity was

0.381 m/s for BF#1 and 0.517 m/s for BF#2, suggesting the occurrence of air leak (short airflow). Air leak is undesired for it compromises the odor reduction effectiveness of biofilters.

Table 2-1. Average air velocity (m/s) of each section over the entire monitoring period.

BF#1								
South side			East side			North side		
0.16±0.11	0.11±0.02	0.12±0.02	0.12±0.04	0.18±0.07	0.17±0.06	0.17±0.09	0.14±0.07	0.13±0.07
0.10±0.00	0.12±0.04	0.18±0.11	0.17±0.14	0.15±0.06	0.18±0.10	0.14±0.05	0.12±0.04	0.14±0.04
0.15±0.07	0.13±0.05	0.13±0.02	0.14±0.06	0.13±0.05	0.16±0.11	0.11±0.02	0.15±0.06	0.13±0.05
BF#2								
South side			East side			North side		
0.16±0.06	0.15±0.04	0.16±0.08	0.12±0.04	0.16±0.06	0.19±0.08	0.18±0.12	0.16±0.07	0.11±0.02
0.11±0.02	0.15±0.04	0.14±0.08	0.12±0.04	0.13±0.08	0.15±0.05	0.11±0.02	0.16±0.06	0.13±0.04
0.15±0.05	0.12±0.04	0.15±0.06	0.13±0.06	0.17±0.05	0.16±0.07	0.10±0.00	0.13±0.04	0.16±0.06

An uneven distribution of woodchip moisture contents was also seen along both horizontal and vertical directions (Table 2-2). The average moisture content was 40.3% (±17.4%) for BF#1 and 44.7% (±17.2%) for BF#2. Both were within the optimal moisture range of 40-60% (Chen et al., 2008) but towards the lower side. Even though the average moisture content was acceptable, certain spots of BF#2 were exceptionally dry (e.g., Section 8 on the south side with 10.5% moisture, far beyond the optimal range). They were problematic from the biofilter operation standpoint. The air humidity and temperature data acquired from the Kestrel 5500 handheld meter correlated strongly with weather conditions. Thus, they were excluded from the discussion.

Table 2-2. Average woodchip moisture content (%) of each section over the entire monitoring period.

BF#1								
South side			East side			North side		
32.2±12.0	30.2±11.3	45.0±16.8	43.5±16.3	38.2±14.3	37.5±14.0	41.7±15.6	49.0±18.3	54.7±20.5
44.7±16.7	37.8±14.2	38.0±14.2	45.2±16.9	36.8±13.8	42.3±15.8	52.2±19.5	46.8±17.5	52.3±19.6
41.2±15.4	41.0±15.3	35.8±13.4	60.5±22.6	39.5±14.8	49.2±18.4	50.2±18.8	58.5±21.9	61.7±23.1
BF#2								
South side			East side			North side		
45.0±12.4	38.4±10.5	32.7±9.0	47.6±13.1	46.3±12.7	37.3±10.3	44.0±12.1	62.6±17.2	60.9±16.7
34.0±9.3	20.9±5.7	43.8±12.0	56.3±15.4	21.8±6.0	49.3±13.5	59.8±16.4	51.5±14.1	60.7±16.7
21.2±5.8	10.5±2.9	41.0±11.3	46.4±12.7	20.3±5.6	30.6±8.4	37.0±10.2	32.0±8.8	38.2±10.5

3.2. Side differences

The east outlet side that directly faced fan exhaust had an overall higher air velocity than the other two sides (Figure 2-3a). For BF#1, the average air velocity was 0.133 (±0.063) m/s on the south side, 0.154 (±0.080) m/s on the east side, and 0.137 (±0.056) m/s on the north side. For BF#2, the average air velocity was 0.143 (±0.054) m/s on the south side, 0.148 (±0.061) m/s on the east side, and 0.139 (±0.059) m/s on the north side. The higher air velocity on the east side is understandable because of the initial momentum of the exhaust airstream (Figure 2-2a). The air velocity difference was relatively minor for BF#2. This is likely because its greater length than BF#1 posed an additional volume and/or friction loss to the air exited through the east side. Therefore, for future vertical bed biofilter design, the inner plenum should be elongated along the incoming air direction to improve the uniformity of airflow distribution.
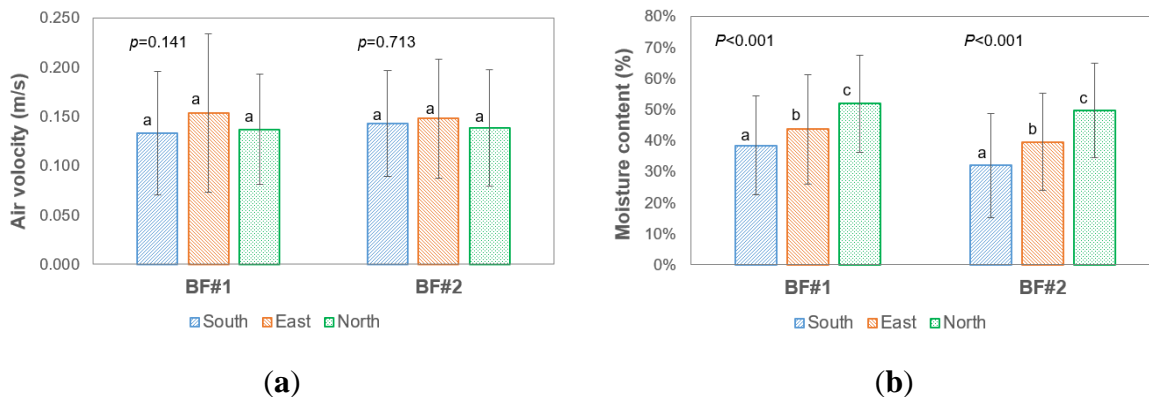
Figure 2-3. (a) Average air velocity and (b) average woodchip moisture content on the south, east, and north sides of each biofilter. Non-parametric ANOVA was performed for comparison. The sides annotated with the same letter were not significantly different.

The north outlet side had significantly higher moisture contents than the east side that, in turn, contained significantly more moisture than the south side. For BF#1, the average woodchip moisture contents were 51.9% ($\pm$15.6%), 43.6% ($\pm$17.5%), and 38.4% ($\pm$15.8%) on the north, east, and south sides, respectively. For BF#2, the moisture contents were 49.6% ($\pm$15.1%), 39.5% ($\pm$15.7%), and 31.9% ($\pm$16.8%), respectively. The average moisture content (31.9%) on the south side of BF#2 was considerably smaller than the lower limit (40%) of the optimal moisture range. A possible reason for the observed side difference is solar radiation. The farm is located in a relatively open area. The south side of the biofilters is believed to have received more sunlight and accordingly lost more water via evaporation than the east and then the north side. The woodchip moisture content is governed by a balance of water gain (e.g., rainfalls and watering) and loss (e.g., evaporation and leaching). With the same watering rate, elevated water evaporation would result in reduced moisture content. A solution to this problem is to increase the watering rate for the sun-facing side of a biofilter by placing a longer or larger soaker hose or increasing the watering time.

3.3. Row differences

Each biofilter was divided into three rows (top, middle, and bottom) along the vertical direction (Figure 2-2b). For each row, the average air velocity and the average moisture content were calculated (Figure 2-4). Although the top row had overall the highest air velocity, no significant difference was seen. This is a bit surprising – since both biofilters used filtration walls of uniform thickness, the bottom rows were expected to carry the smallest airflow because of woodchip settling and decay. The small particles produced from woodchip decay would settle and fill the pores between woodchips, causing the loss of porosity. The reason for the lack of significant vertical variability is uncertain. The biofilter operation started in July 2019 and, thus, the woodchips were relatively new. Also, cedar woodchips used in this study are known to be rot resistant. Only a minor degree of decay was noticed at the end of the monitoring campaign.

(a) **(b)**
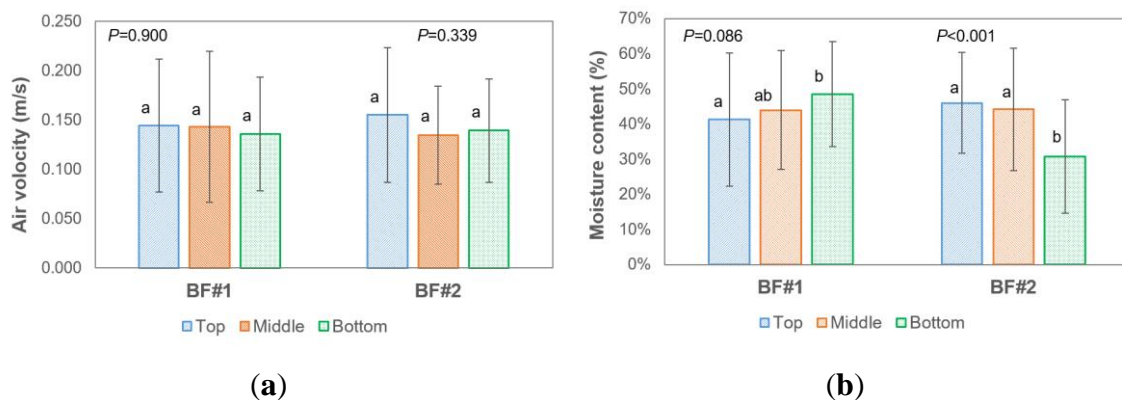
Figure 2-4. (a) Average air velocity and (b) average woodchip moisture content at the upper, middle, and lower rows of each biofilter. Non-parametric ANOVA was performed for comparison. The rows annotated with the same letter were not significantly different.

Regarding woodchip settling, although in theory it would cause reduced porosity in filtration media and accordingly a low air velocity, no agreement has been reached in the literature. Lefers (2006) compared vertical bed biofilters with three tapered angles (0°, 4.8°, and 9.6°) and reported the smallest raw difference in airflow at 9.6°. At 0° (non-

tapered), the lowest air velocity occurred near the bottom of a filtration wall. The author ascribed it to the settling of filtration media. However, Garlinski and Mann (2004) found that despite substantial woodchip settling, the pressure drop across non-tapered filtration walls was relatively uniform. In this study, after filling the biofilters, the woodchip packings were leveled off and lightly compressed with shovels from the top. It is uncertain whether and to what extent the exerted force could be transferred to the bottom. Furthermore, many factors other than woodchip settling can affect air restriction, e.g., dust buildup and moisture content. Thus, it is difficult to predict vertical airflow distribution in a biofilter. On the positive side, this study suggests that tapered wall design may not be necessary to address the uniformity issue, which simplifies the construction of vertical bed biofilters.

Regarding woodchip moisture contents, the two biofilters exhibited different vertical distribution patterns. For BF#1, the average moisture content increased from top to bottom, suggesting that the biofilter was overwatered; whereas, for BF#2, the average moisture content decreased from top to bottom, indicating the occurrence of under-watering. Again, the watering system of both biofilters was adjusted at the beginning of operation but uneven vertical distribution still occurred. This suggests the necessity of periodically (e.g., monthly or quarterly) adjusting the watering system since factors, such as temperature and rainfalls, could shift the water balance in a biofilter over time. In this study, the watering system of both biofilters shared the same waterline with pig waterers inside the barn, which resulted in fluctuated watering rates at the early stage of operation. To address this issue, the timer was set to water each biofilter twice per day (before sunrise and after sunset).

3.4. Uniformity of distribution

For BF#1, the uniformity of air velocity distribution increased with time, as indicated by a gradual decrease in CV; while for BF#2, no temporal trend in air velocity distribution was observed (Figure 2-5a). A significant correlation between outdoor temperature and the CV of air velocity in BF#1 was identified (r=0.726, p=0.017). However, it could be a pseudo-correlation because (1) no correlation occurred between outdoor temperature and the CV of air velocity in BF#2; and (2) no scientific evidence supports the effect of outdoor temperature on air velocity distribution. From the biofilter operation standpoint, the measurement data are encouraging, suggesting that a long-term operation may not reduce the uniformity of airflow.

(a)

(b)
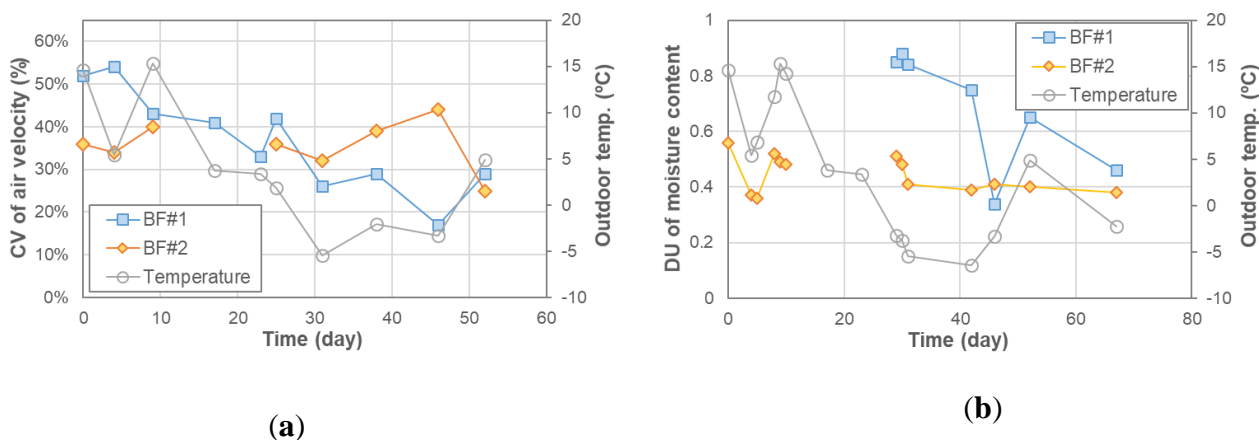
Figure 2-5. Temporal changes in the uniformity of (a) air velocity distribution and (b) woodchip moisture content. Note: A smaller CV value represents a more uniform distribution which a smaller DU value represents a less uniform distribution.

For BF#1, its watering system was fixed and re-adjusted on October 21, 2019. After that, the uniformity of woodchip moisture content distribution continued to decrease. For BF#2, the uniformity of moisture content distribution dropped at the beginning and became

stabilized after ~30 days of monitoring. Since the operation of BF#2 started in July 2019, BF#2 may have undergone a quick decrease in moisture content uniformity before the monitoring (day 0). In summary, the monitoring data suggest that the moisture content distribution is relatively uniform immediately after watering system adjustment, but the uniformity drops over time and finally stabilizes at a relatively low level. Thus, periodical adjustment of the watering system is needed.

DU is a prevalent measure for assessing the uniformity of irrigation. A DU of >0.90 (90%) can be achieved with, for example, dripping systems (Ella et al., 2013). However, it should be noted that for irrigation systems, DU characterizes the uniformity of 2D horizontal distribution. For vertical distribution, it is hard to achieve the same degree of uniformity because of the gravity flow; and no DU cutoff value for satisfactory watering performance has been established. Based on the experimental data, a tentative cutoff value of DU=0.7 is recommended. It is achievable once the side and row differences are addressed through watering system optimization.

3.5. Others

No freezing of woodchips was seen during the monitoring campaign. On the coldest day (-6ºC outdoor temperature), the treated air from the biofilters was still relatively warm (minimum of 6ºC for BF#1 and 4ºC for BF#2). However, our later visits in January 2020 (for another purpose) identified a few frozen spots. The watering system was disconnected on December 5, 2019 so the moisture of the frozen spots should have come from the exhaust air and/or precipitations.

A thorough inspection of both biofilters was done in May 2020. Two major issues were found: corrosion and cementing. First, even with vinyl coating, the poultry wires

(made of metal) were severely corroded, especially the wires netting the inner air plenum. This can be attributed to the high concentrations of hydrogen sulfide, ammonia, and dust in the untreated air. To solve the issue, heavy-duty plastic poultry wires were used for fixing the biofilters. Secondly, cementing occurred at the innermost layer of woodchips and it was caused by dust in the exhaust air. When mixed with water, the dust particles formed a paste-like mixture and caulked into air passages between woodchips. In reality, the cemented layer was so strong that it held the filtration wall even after the poultry wires corroded out; and chisels and shovels had to be used to breach the layer.

3.6. Reasons for non-uniformity and recommendations

The uneven distribution of air velocity and woodchip moisture content in the two vertical bed biofilters was ascribed to five possible reasons:

- Solar radiation. Solar-induced water evaporation can reduce the moisture level in a biofilter. For vertical bed biofilters, the amount of solar radiation received varies with side orientation, season, and weather.

- Poorly controlled and adjusted watering systems. Watering timers can only control the watering duration but not flowrates. The flowrate is affected by water pressure in the pipeline. Thus, a watering system is problematic when sharing the same waterline with other farm apparatus (e.g., waterers). Watering system adjustment in this study was done based on visual inspection of biofilter conditions (e.g., woodchip wetness and ground flooding). This could cause a large uncertainty in watering rates.

- Cementing. Cementing can substantially restrict airflow. No dust concentration measurement was done in this study. Assuming an average dust concentration of

1 mg/m^3 in the pit air (Yang et al., 2015), monthly dust loading would be 8.7 kg to BF#1 and 11.0 kg to BF#2 (estimated from the treated airflow rate). The inner air plenum in a vertical bed biofilter has a relatively small contact area to the exhaust air. As a result, the cementing issue could be more pronounced for vertical than horizontal biofilters (that usually have the same contact area on the inlet and outlet sides).

- Freezing. Freezing may initially develop on exceptionally cold days in winter. When it occurs, it restricts warm airflows from the barn exhaust. This in turn worsens the issue of freezing, leading to the further development of frozen spots.

- Netting attachment. The gravitational setting of woodchips is hindered by nets or meshes. It, along with the decay of woodchips, can result in void spaces and short airflows in a filtration wall after long-term operation. In this study, the issue was observed near the woodchip sampling points. After every sampling, mechanical tools were used to ensure the settling of woodchips.

The following recommendations are made for the future design and operation of vertical bed biofilters:

- For cubic biofilters, the air plenum should be elongated along the incoming air direction to improve the airflow uniformity. Use the same filtration bed thickness. No tapered filtration wall design is necessary.

- Use a circular vertical bed biofilter design to improve the uniformity of filtration bed thickness. The thicker filtration medium at the corner of cubic biofilters is unideal from the airflow distribution standpoint.

- Use a separate waterline for biofilters if possible. Apply a higher watering rate for biofilter sides or sections that receive significant sunshine – the suggestion also applies to horizontal biofilters.

- Clean the air plenum monthly to remove dust, thereby reducing the chance of cementing. Mechanically agitate the wires or nets monthly to facilitate the medium settling.

- Use a chisel to break the freezing spot to prevent the further development of freezing if winter operation is desired.

4. Conclusion

Two vertical bed biofilters with non-tapered filtration walls were examined for airflow and medium moisture content distribution over two months. Solar radiation was found to significantly affect the medium moisture content with the lowest value observed on the south side (wall). The initial momentum of exhaust air resulted in a higher air velocity on the east side (wall) that directly faced the exhaust airflow. Despite the careful adjustment of watering systems, one biofilter was overall under-watered and the other was overwatered during the monitoring campaign, and a significant variation in medium moisture content was found along the height of the two biofilters. Comparatively, no significant variation in air velocity was noted along the biofilters' height. This is different than the finding from a previous study (Lefers, 2006) in which medium settling was thought to cause a decreased air velocity at the bottom of a non-tapered filtration wall. The lack of significant variability in air velocity was ascribed to other factors (e.g., dust buildup) that could affect airflow restriction. Temporal changes in the distribution uniformity of airflow and medium moisture content were tracked. The uniformity of airflow distribution

remained relatively stable; whereas the uniformity of moisture content decreased after watering system adjustment, suggesting the necessity of periodic adjustment of watering systems. Several recommendations were made for the future design and operation of vertical bed biofilters. Efforts are needed to further study the impact of airflow and medium moisture content distribution on odor mitigation performance.

CHAPTER 3: Makeup Water Addition Affects The Growth Of Scenedesmus Dimorphus

in Photobioreactors

Authors: Augustina Osabutey, Noor Haleem, Seyit Uguz, Kaarle Albert, Gary Anderson, Kyungnan Min, and Xufei Yang

Status: Under review by the journal of *Environments*

Abstract

Makeup water constitutes a key component in water management of microalgal cultivation systems. However, the effect of makeup water addition on microalgal growth remains largely unexplored. This study compared two deionized water addition intervals (1 day and 4 days) for their effect on the growth of *Scenedesmus dimorphus* (*S. dimorphus* hereafter) in 2000-mL Pyrex bottles under controlled conditions. Cell counts and dry algal biomass (DAB) were measured to characterize the microalgal growth rate. Water addition intervals showed a large effect on algal cell counts but little effect on DAB. Adding makeup water every day resulted in a higher growth rate ($8.80\pm1.46\times10^5$ cells mL^{-1} day^{-1}) and an earlier occurrence of the peak cell count (day 9) than adding it every 4 days ($6.95\pm1.68\times10^5$ cells mL^{-1} day^{-1} and day 12, respectively). We speculate that water loss over an extended period and the following makeup water addition posed stress on *S. dimorphus*. Passing the peak cell count, *S. dimorphus* continued to grow in DAB, resulting in an increased cell weight as a response to nutrient starvation. Optical density at 670 nm (OD$_{670}$) was also measured. Its correlation with DAB was found to be affected by water addition intervals ($R^2=0.955$ for 1 day and 0.794 for 4 days), likely due to a water loss-induced change in

Chlorophyll *a* contents. This study is expected to facilitate the makeup water management of photobioreactor and open pond cultivation systems.

Keywords:

Makeup water, microalgae, optical density, *Scenedesmus dimorphus,* water loss

1. Introduction

Cultivation of microalgae as a renewable resource continues to receive intensive attention due to their fast growth, superior photosynthetic efficiency, low nutrient requirements, etc. (Brennan and Owende, 2010; Mascarelli, 2009). Microalgae have also been utilized for cleaning up contaminated water (Chen et al., 2020) and air (Uguz et al., 2022) and for fixing CO_2 from the atmosphere or flue gas (Zhao and Su). Water management is critical for microalgal cultivation – producing 1 kg of dry microalgal biomass requires approximately 5-10 kg of water (Murphy and Allen, 2011). Meanwhile, water is an invaluable resource, and water conservation represents an increasing challenge (Moglia et al., 2018). For water management, factors, including the volume of water needed for algal cultivation, water loss, and makeup water, must be properly assessed and controlled. Those factors are further related to target biomass productivity, cultivation system design, cultivation conditions, etc. Numerous efforts have been made to examine the water footprint of microalgal production systems, through experiments (Feng et al., 2016) and modeling (Clarens et al., 2010; Yang et al., 2011). Despite the importance of makeup water in overall water balance, the effect of makeup water on microalgal growth is largely unexplored.

Makeup water compensates for water loss from cultivation systems, and various processes can lead to substantial water loss. For photobioreactors (PBRs), the factors

affecting water loss include aeration, water circulation, temperature, relative humidity, light intensity, and surface-to-volume ratio. Many of them are related to evaporation, a primary cause of water loss in a PBR (Murphy and Allen, 2011). For open ponds (e.g., raceways), the additional factors affecting water loss include wind, mixing, solar radiation, and leakage (Quiroz et al., 2021). However, for cultivating microalgae in PBRs, many researchers assume evaporation water loss to be negligible and present their data without any correction (Martins et al., 2018). For open ponds, water loss is usually more pronounced and an evaporation rate can be estimated through modeling (Sander and Murthy, 2010; Yang et al., 2011) or a simple pan evaporation method (Murphy and Allen, 2011). To estimate the volume of makeup water required for open pond systems, precipitation must be considered and it is highly variable with time and location. Precipitation (e.g., rainfalls and snowfalls) contains mostly pure water relative to cultivation media. Thus, evaporation loss and precipitation (plus makeup water addition) would result in a fluctuation in parameters such as pH, salinity, nutrients, and microalgal concentrations in a pond. It remains poorly understood if and to what degree such water loss-gain cycles could affect microalgal cultivation.

To fill the knowledge gap, *S. dimorphus* was cultivated under lab conditions simulating the water loss-gain cycles in open ponds or PBRs. A hypothesis was that the time interval for makeup water addition affects microalgal growth. It is noteworthy that the time interval is generally proportional to the amount of water loss and accordingly the amplitude of parameter fluctuations. The specific research objectives were to (1) cultivate *S. dimorphus* in a medium for an extended period to make it well adapted to the medium and maintain stable growth; (2) compare *S. dimorphus* growth rates in cell counts and dry

algal biomass between different water addition time intervals; and (3) examine the optical density of the microalgal culture during the experiments and its correlation with *S. dimorphus* concentrations. Deionized water was selected as the makeup water due to its similar composition to precipitations. In reality, frequently refilling a PBR or open pond with cultivation media is difficult to manage. We think that a realistic way to maintain water levels is adding tap or other relatively pure water, in combination with less frequent addition of cultivation media.

2. Material and methods

2.1. Algal strain

S. dimorphus strain UTEX 1237 was obtained from UTEX Culture Collection of Algae at the University of Texas at Austin (Austin, TX, USA). The strain was selected due to its adaption to a wide pH range, efficient ammonia removal, and high growth rate (Kang et al., 2014; Xu et al., 2015). It had been cultured and maintained in four PBRs for six months before makeup water experiments. A Bold's Basal Medium (BBM) – widely used for freshwater green algae (Fábregas et al., 2000) – was selected for algal cultivation. The composition of the medium can be found in Uguz et al. (2022). The prepared BBM was adjusted for pH (to 6.4±0.5) and was autoclaved for 40 min at 121°C before use. The cultivation started from a 100-mL algal culture in a 500-mL glass flask. With the growth of *S. dimorphus*, the culture was periodically diluted and transferred to more or larger glass vessels. During cultivation, the culture was continuously aerated with air at an airflow rate of 0.5 LPM per liter of culture. Fluorescent lamps were placed near the vessels to offer a light intensity of 60-70 µmol m^{-2} s^{-2}. All glassware was autoclaved before use.

2.2. Algal cultivation with makeup water and growth medium

A 1200-mL healthy algal culture was evenly distributed into three 2000-mL Pyrex bottles. A 1600-mL autoclaved BBM was then added to each bottle. The 2000-mL algal culture in each bottle was continuously aerated at an airflow rate of 1 LPM. The same light source (fluorescent lamps) and intensity (60-70 μmol m^{-2} s^{-2}) were applied. The water levels in the bottles were daily measured and documented. Aeration and water evaporation led to a loss of water in the bottles. To study the effect of water makeup, two separate batches of experiments were conducted:

- Add makeup water every day (1D). Autoclaved deionized water was added to compensate for water loss and maintain a 2000-mL algal culture in each bottle. Before the addition of water, several parameters were measured, including temperature, pH, algal biomass, optical density, and cell counts. The tests consumed 26 mL of algal culture. This volume was also included in the water loss calculation. The entire experiment lasted for 14 days.

- Add makeup water every four days (4D). The experiment started from another 1200-mL healthy algal culture and, thus, was independent of the previous batch. Again, deionized water was added to maintain a 2000-mL algal culture in each bottle. Temperature, pH, algal biomass, optical density, and cell counts were measured every day; and on the day when water was added, the measurement was done right before water addition. The entire experiment lasted for 21 days.

2.3. Analytical methods

The pH of the algal cultures was monitored with an Oakton PC-450 pH meter and maintained at 6.0-7.0 using HCl or NaOH. However, pH adjustment (on the day of makeup

water addition) was rarely needed in reality. Temperature was measured with the same meter and was found to be relatively stable (21±4ºC) during the experiments.

Dry algal biomass (DAB; mg mL^{-1}) was determined gravimetrically, following a protocol described by Hu (2014). In brief, a 25-mL algal culture sample was taken and vacuum-filtered through a pre-weighed 70-mm glass fiber filter (Fisherbrand G4; Fisher Scientific International, Inc., Waltham, MA, USA). The algae-laden filter was dried in a lab oven at 105ºC for 1 hour and then cooled for 3 min in a desiccator before being weighed on an analytical balance (readability: 0.1 mg). For the pre-weighed filter, the same drying condition was followed before weight determination.

Algal cell counts (N; cell mL^{-1}) were measured using a Neubauer hemocytometer under an Olympus CX41 LEEDS optical microscope (Olympus Corp., Tokyo, Japan). Images were taken using the Infinity Analyze software that came along with the microscope. Algal cells on the acquired images were counted using ImageJ.

The optical density (absorbance) of algal culture at 670 nm (OD670) was measured using a DR3900 spectrophotometer (Hach Company, Loveland, CO, USA). The wavelength is characteristic of chlorophyll a, and OD670 is often selected as an indirect measure of algal biomass (Menegazzo et al., 2022). A BBM without algae was used as a lab blank for absorbance measurement.

2.4. Data analysis

DAB (mg mL^{-1}) was calculated as:

$$DAB = \frac{W_{f,t} - W_{f,0}}{V} \tag{1}$$

where, $W_{f,t}$ is the dry weight of an algae-laden filter (mg), $W_{f,0}$ is the dry weight of the filter without algae (mg), and V is the volume of an algal culture sample taken for DAB

measurement (25 mL). An average dry cell weight was calculated by dividing the DAB by

the cell count (N) of the same sample and presented in the unit of picogram per cell (pg

cell^{-1}). Because algae did not grow exponentially during the makeup water experiments, an

arithmetic average growth rate was calculated for algal biomass (μ_m; mg mL^{-1} day^{-1}) and

cell counts (μ_n; mg mL^{-1} day^{-1}):

$$\mu_n = \frac{N_t - N_0}{t - t_0} \tag{2}$$

$$\mu_m = \frac{DAB_t - \ln DAB_0}{t - t_0} \tag{3}$$

where N_t is the cell count on the day of measurement (t), N_0 is the initial cell count at day

0 (t_0), DAB_t is the DAB on the day of measurement (t), and DAB_0 is the initial DAB at day

0 (t_0),

A Shapiro-Wilk test was conducted to check the normality of measured and

calculated parameters. Results showed that most of these parameters did not follow the

normal distribution. As a result, a Kruskal-Wallis test (a non-parametric one-way ANOVA

method) was used to compare 1-day versus 3-day water makeup results and further

compare them with those acquired from the 6-month cultivation experiment. Linear

regression was done to assess a correlation between different algal concentration measures

(DAB, cell counts, and OD$_{670}$). Microsoft Excel and PAST (Hammer et al., 2001) were

used to perform the above analyses.

3. Results and Discussion

3.1. Algal cell counts

The time interval for makeup water addition had a large influence on algal cell

counts (Figure 3-1). For daily water addition (1D), the maximum cell counts occurred on

day 9 in all three Pyrex bottles (1.07×10^7, $1.06 \times 10^{7,}$ and 9.12×10^6 cells mL^{-1} in bottles A, B, and C, respectively). After that, the algal cell counts started to drop likely due to the depletion of nutrients. In comparison, for every four-day water addition (4D), the maximum cell counts occurred on day 12 in all three bottles (1.11×10^7, 1.01×10^7, and 7.94×10^6 cells mL^{-1} in bottles A, B, and C, respectively). Although no significant difference in the maximum cell counts was seen between 1D and 4D, 4D resulted in a more pronounced fluctuation in algal cell counts. In particular, on the following day after makeup water addition (e.g., days 5, 8, and 12), a dip in algal cell counts was observed in all the bottles. The dip was largely attributed to dilution by makeup water. Due to continuous aeration and lighting, the algal bottles lose 8-25% of water volume after four days. We speculate that this substantial water loss would have posed stress on *S. dimorphus*, resulting in a slower growth rate (μ_n) than 1D ($8.80 \pm 1.46 \times 10^5$ cells mL^{-1} day^{-1} for 1D versus $6.95 \pm 1.68 \times 10^5$ cells mL^{-1} day^{-1} for 4D) before the algae reached the maximum cell counts. Thus, the timely addition of makeup water is desirable for algal doubling.
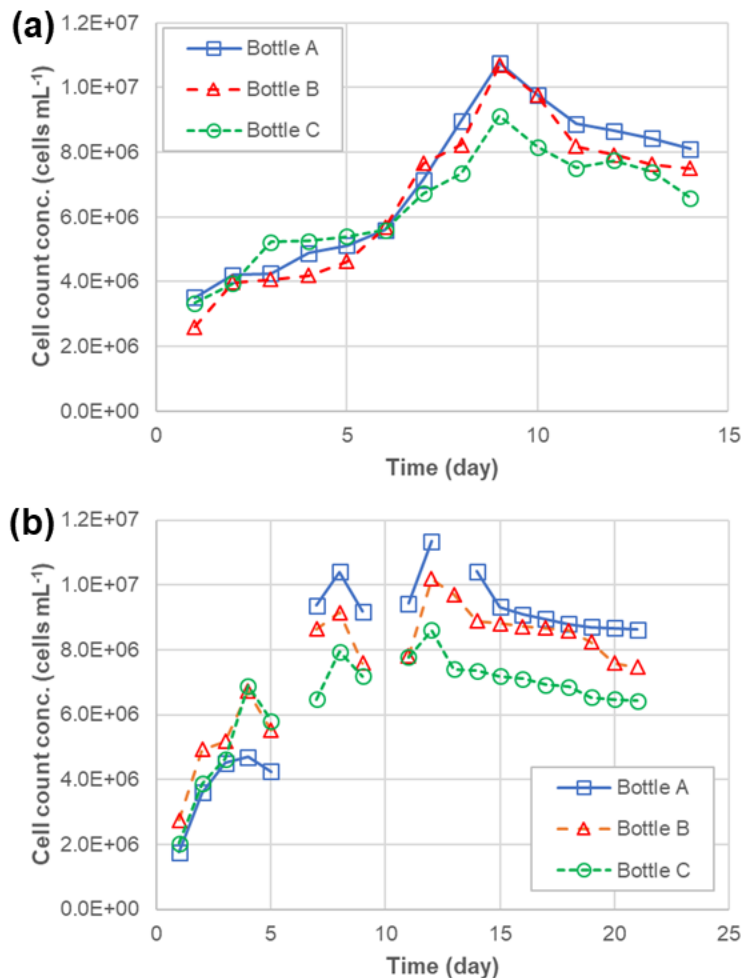
Figure 3-1. Cell count concentrations of S. dimorphus with different time interval of makeup water addition: (a) every day (1D) and (b) every four days (4D).

A control experiment was conducted with BBM added every four days. Algal cell counts continued to increase during the experiment and reached $1.97\pm0.23\times10^7$ cells mL^{-1} on day 21 in the three bottles. A time-average growth rate (μ_n) of $9.31\pm1.25\times10^5$ cells mL^{-1} day^{-1} was achieved, slightly greater than that of 1D but significantly greater than that of 4D. This again suggests that the frequent addition of makeup water would help sustain algal doubling before the doubling is constrained by nutrient deficits.

3.2. Dry algal biomass (DAB)

In contrast to cell counts, algal biomass continued to increase until the end of the experiments for both 1D and 4D (Figure 3-2). A linear increase pattern was seen and a time-average growth rate (μ_m) was calculated to be 0.054 ± 0.004 mg mL^{-1} day^{-1} for 1D (over 14 days) and 0.052 ± 0.003 mg mL^{-1} day^{-1} for 4D (over 21 days). Continual growth in algal biomass was also observed during the control experiment. A time-average growth rate of 0.078 ± 0.008 mg mL^{-1} day^{-1} was achieved (over 21 days), ~50% faster than that in 1D or 4D. Thus, keeping enough nutrients in the cultivation medium is critical for maintaining the fast growth of algal biomass. The time interval for makeup water addition showed little effect on the growth of algal biomass.
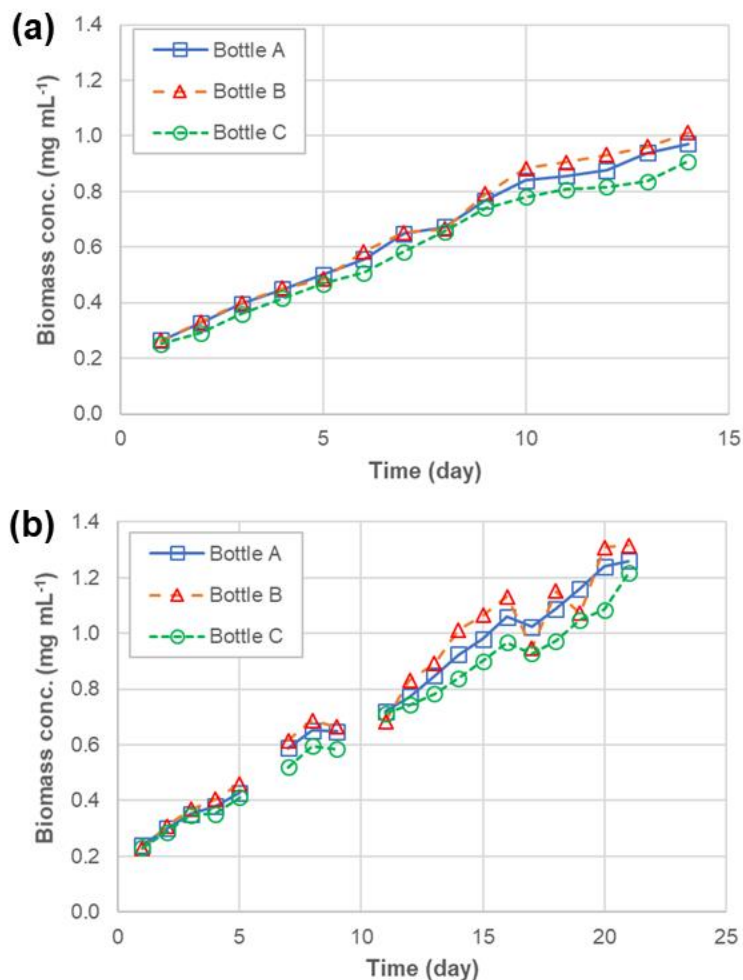
Figure 3-2. Dry biomass concentrations of S. dimorphus with different time interval of makeup water addition: (a) every day (1D) and (b) every four days (4D).

During both 1D and 4D experiments, the average cell weight decreased slightly at the beginning and then became relatively stable for days (Figure 3-3). However, it increased after day 9 in 1D and day 12 in 4D, the same days on which algal cell counts reached the maximum and started to decrease. It appears that part of *S. dimorphus* cells began to lyze with depleted nutrients. The remaining viable ones chose to grow in their cell size by possibly absorbing nutrients from lyzed algae. At the end of the experiments, the average cell weight reached 130.7 ± 9.6 pg cell^{-1} for 1D and 170.5 ± 22.0 pg cell^{-1} for 4D. As

a comparison, the average cell weight was 93.3 ± 19.5 pg cell^{-1} for the control experiment, similar to that during the "stable stage" of 1D and 4D.
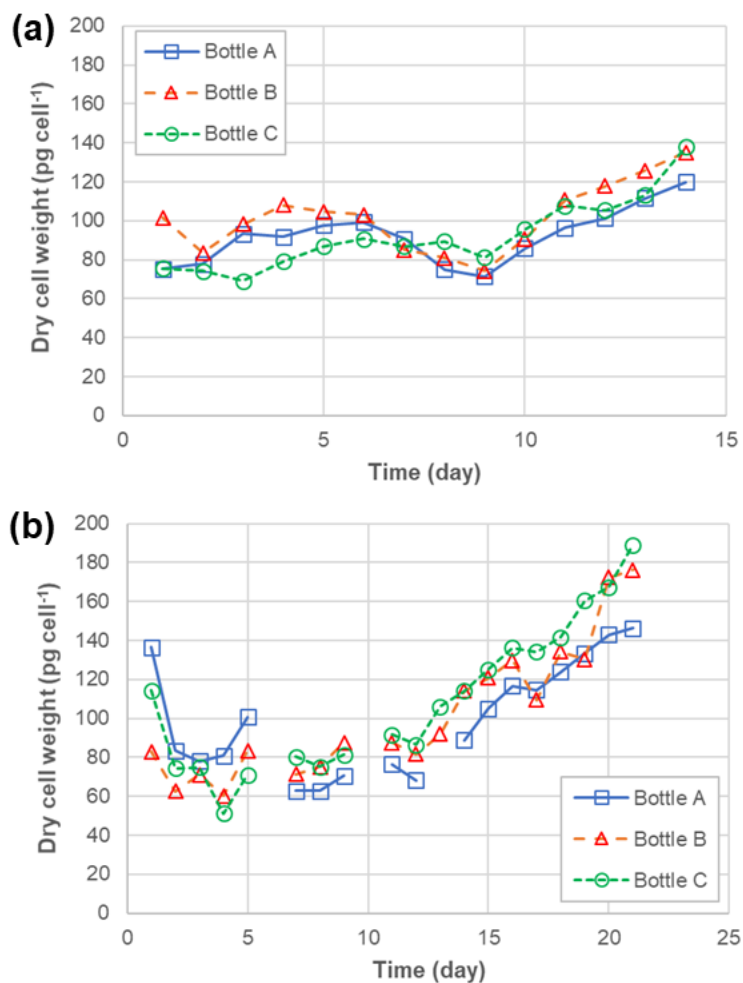
Figure 3-3. Average dry cell weight of S. dimorphus under with different time interval of makeup water addition: (a) every day (1D) and (b) every four days (4D).

3.3. OD$_{670}$ as a surrogate for algal biomass

The time interval for makeup water addition was found to affect the applicability of OD$_{670}$ as a surrogate measure for algal biomass. Here, a greater coefficient of determination (R^2) indicates a better prediction of algal biomass (DAB) from OD$_{670}$. As

shown in Figure 3-4, OD_{670} would better serve the purpose when makeup water was added every day (1D) than every four days (4D). The reason is uncertain but likely related to the chlorophyll *a* content in algal cells. Without timely adding makeup water, the water loss-induced stress on algal cells could lead to a change in their chlorophyll *a* content per DAB basis. It is noteworthy that for both 1D and 4D, high DAB concentrations occurred towards the end of the experiments when depleted nutrients could have resulted in enlarged algal cells and changes in the content of chlorophyll *a*.
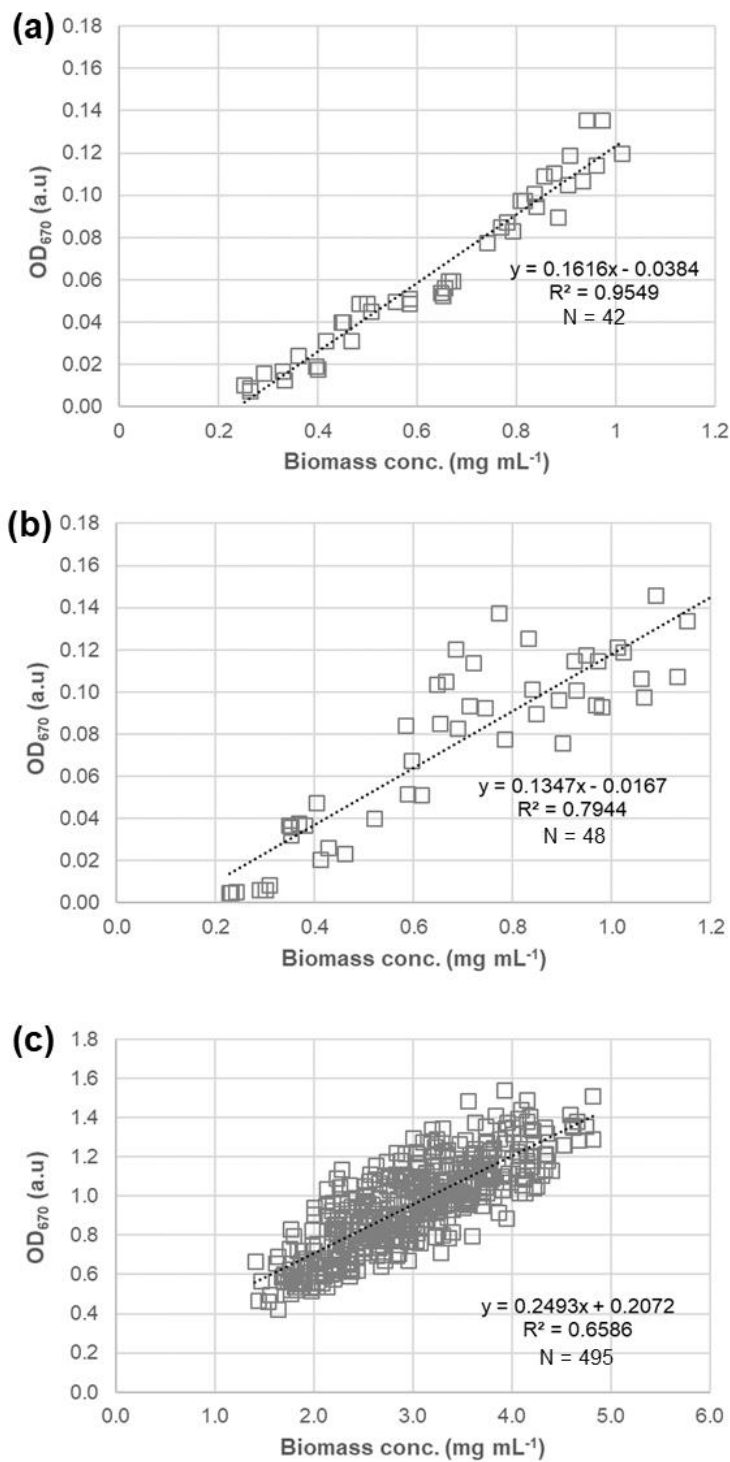
Figure 3-4. Correlation between OD670 and dry algal biomass concentration of S. dimorphus for: (a) makeup water addition every day; b) makeup water addition every four days; and (c) six-month algal cultivation with periodic nutrient addition.

To further examine the effect of nutrient constraints, the cell count and DAB data were retrieved from the six-month cultivation of *S. dimorphus*. During the cultivation, the algal culture was doubled every seven days and the BBM was periodically added to ensure sufficient nutrient supply to the microalgae. Only a moderate R^2 value (0.659) was obtained (Figure 3-4), indicating the relatively poor performance of OD_{670} as a surrogate measure for DAB during such long algal cultivation experiments. The regression coefficients (slope and intercept) acquired from the six-month cultivation were considerably different than those from 1D or 4D, suggesting a large effect of nutrients on the chlorophyll *a* content per DAB basis. Caution must be taken when using OD_{670} as a measure of algal biomass, and timely and case-specific calibration may be necessary.

A correlation analysis was also conducted between cell counts and OD_{670} readings. Only a moderate correlation was seen for the makeup water experiments (R^2=0.611 for 1D and 0.682 for 4D). The (relatively) highest R^2 value (0.715) was derived from the six-month cultivation. This could be attributed to changes in cell size – a larger variation in cell weight was seen during the 1D (95.2±23.0 pg cell^{-1}) and 4D experiments (103.7±33.6 pg cell^{-1}) than during the six-month cultivation (93.3±19.5 pg cell^{-1}).

3.4. Discussion

The DAB concentrations of *S. dimorphus* from 1D (0.96±0.05 mg mL^{-1} on day 14) and 4D (1.26±0.05 mg mL^{-1} on day 21) were lower than that (1.82±0.11 mg mL^{-1} on day 21) from the control experiment. They were similar to that (0.96 mg mL^{-1} on day 16) reported by Velichkova et al. (2013) in which *S. dimorphus* was also cultivated in a BBM but with no makeup water or BBM added during cultivation. In that study, a decrease in DAB concentrations was seen after day 16. Amending the BBM with nitrates raised the

maximum DAB concentration (up to 1.69 mg mL^{-1}) but, still, the concentration decreased after day 16. The addition of makeup water appears to benefit the continual growth of *S. dimorphus* biomass. A DAB concentration of 1.2 mg mL^{-1} was reported by Varsharani and Geeta (2011), which is also close to the concentrations derived from our makeup water experiments.

No exponential growth in cell counts or DAB concentrations was observed in this study. According to Padovan (1992), *S. dimorphus* ended exponential growth when its cell counts exceeded 1.2×10^5 cells mL^{-1}, substantially smaller than the cell count range in this study (Figure 3-1). This supports the use of arithmetic average growth rates in Eqs. 2 and 3. Padovan (1992) also reported an average dry cell weight of 194 pg cell^{-1}, larger than our observed values. The reason for different cell weights is uncertain but likely related to differences in algal strains, cultivation media [a strain isolated from rivers and cultivated in a WC medium in Padovan (1992)], and cell counts (1.2×10^4-2.9×10^5 cells mL^{-1} in Padovan (1992)].

For both 1D and 4D, algal cell counts declined after surpassing a peak value. We ascribed this to nutrient depletion. According to Narala et al. (2016), with limited nutrients, microalgal cells would stop dividing and start to accumulate triacylglycerides for survival. Nutrient starvation has been explored for enhanced lipid production from microalgae, including *S. dimorphus* (Latsos et al., 2020; Rugnini et al., 2020). During nutrient starvation, photosynthesis still occurs but towards the conversion to, and accumulation of lipids in a cell, resulting in a continuous increase in DAB concentrations (Narala et al., 2016; Velichkova et al., 2013). Frequent addition of makeup water appears to speed up the

coming of such a "flip point" (Figure 3-1). An analysis of lipid contents in *S. dimorphus* would be needed to further verify the enhancement of lipid production.

OD readings at various wavelengths have been measured as a surrogate for *S. dimorphus* concentrations. However, few studies included enough data to validate the adopted OD method. Velichkova et al. (2013) took OD_{550} readings but no correlation with DAB concentrations was attempted. Padovan (1992) measured OD_{438}, OD_{540}, OD_{678}, and OD_{750} and found a strong correlation of OD_{438} with *S. dimorphus* cell counts ($R^2=0.992$). But only five data points were used to establish the relationship. Perdana et al. (2021) reported a strong correlation of OD_{400}, OD_{500}, and OD_{680} with *S. dimorphus* cell counts ($R^2=0.883$, 0.916, and 0.994, respectively). But for each OD, only ten data points were available. Ferreira et al. (2016) used OD_{600} to measure *S. dimorphus* cell counts. A calibration curve ($R^2=0.999$) was built through the dilution of an agal culture to four dilution ratios (accordingly only four data points). Other adopted wavelengths include OD_{730} (Jiang et al., 2013) and OD_{690} (Cicci et al., 2013). The only study including a large data set was reported by Bohutskyi et al. (2016). A strong correlation of OD_{680} was found with UTEX B72 ($R^2=0.983$) and UTEX 1237 DAB concentrations ($R^2=0.986$). No calibration information was given and the number of data points was still fewer than that in our study. According to Ferreria et al. (2016), nitrogen starvation could change the chlorophyll content of *S. dirmophus*. This may explain the low R^2 values measured from the makeup water experiments.

High winds, elevated temperatures, low relative humidity, and strong aeration can lead to significant evaporation water loss from outdoor open ponds (e.g., raceways); while for PBRs, aeration and artificial lighting may result in great water loss (Murphy and Allen,

2011). The loss, if not timely compensated with makeup water or growth media (the latter being expensive), could cause a surge in salinity, toxic/inhibitory substances (e.g., metals), and algal count concentrations, thereby affecting microalgal growth. Our study suggests that the timely (frequent) addition of makeup water could buffer the changes in those parameters and benefit algal growth in PBRs. A similar benefit is expected for open pond systems. For an open pond, precipitation is an additional factor affecting the water balance and it contains relatively pure water. This makes our testing of deionized water addition also relevant to those systems.

4. Conclusion

Makeup water is needed to compensate for water loss from a microalgal cultivation system. This study compared two makeup water addition time intervals (1D and 4D) for their effects on *S. dimorphus* cell counts and dry biomass. Results showed that the timely addition of makeup water resulted in faster growth in algal cell counts but it had a negligible effect on the growth of algal biomass. Due to nutrient depletion, *S. dimorphus* cell counts decreased after surpassing a peak value, but the accumulation of algal biomass continued for days, leading to a greater cell weight. The time interval also affected the performance of the optical density (OD) method. OD_{670} offered a better prediction of dry algal biomass when makeup water was added more frequently. We ascribed this to the water loss-induced stress on *S. dimorphus* (due to fluctuations in salinity, pH, etc.) and associated changes in chlorophyll *a* contents in algal cells. For future use of the OD method, a timely and case-specific calibration is recommended. The findings from this study are expected to improve water management in both PBR and open pond algal cultivation systems.

CHAPTER 4: Growth Of *Scenedesmus Dimorphus* In Swine Wastewater With Versus Without Solid-Liquid Separation Pretreatment

Authors: Augustina Osabutey, Noor Haleem, Seyit Uguz, Kyungnan Min, Ryan Samuel, Karlee Albert, Gary Anderson, Xufei Yang

Abstract

Scenedesmus dimorphus was cultivated in raw and pretreated swine wastewater (SW) with 20-L photobioreactors (PBRs) to examine the effect of solid-liquid separation on algal growth. The same aerated PBRs containing no algae were used as control. Moderate COD and nitrogen removal from the SW was achieved with the algal PBRs. However, compared to the control reactors, they offered no consistent treatment boost. Improved algal growth occurred in the pretreated SW, as measured by maximum algal cell count ($3202\pm275\times10^6$ versus $2286\pm589\times10^6$ cells L^{-1}) and cell size. The enhanced algal growth in the pretreated SW resulted in relatively high nitrogen (5.7%) and organic matter contents in the solids harvested at the end of cultivation experiments, with ~25.6% of nitrogen in the SW retained in the solids and ~9.1% absorbed by algae. The pretreatment also resulted in elevated phosphorus removal. This study is anticipated to foster the development of microalgae-based SW treatment processes.

Keywords: Solid-liquid separation, swine wastewater, *Scenedesmus dimorphus,* microalgae, nutrient

1. Introduction

Swine production continues to go concentrated to meet the ever-increasing demand for affordable animal protein (Gomes et al., 2021). This however generates a large quantity

of SW. SW contains high concentrations of total suspended solids (TSS), nutrients (e.g., phosphorous, nitrogen, and organic matter), and bacteria (e.g., *E. coli*) (Bilotta et al., 2017) and, if not properly managed, can cause various environmental concerns including eutrophication of water bodies, coliform contamination, and odors (Lee and Chang, 2022). Traditionally, SW is land-applied as an organic fertilizer to enhance crop production. However, land application may not be a feasible solution for large concentrated swine operations due to the large volume of SW produced and land availability constraints (Wang et al., 2021). Treatment processes such as anaerobic digesters and lagoons have been in place at certain operations (Wang et al., 2015). However, they are difficult for average producers to use due to stringent requirements on temperature, pH, organic loading rate, hydraulic retention time, C/N ratio, etc. (Lv et al., 2018). As an alternative treatment method, microalgae cultivation has gained increasing attention because it offers multiple potential benefits such as high biomass productivity, nutrient recovery, carbon sequestration, and valorizability of harvested algae (Fongaro et al., 2014; Wu et al., 2020).

Despite its great potentials, cultivating microalgae in raw SW faces two major challenges: (1) limited light penetration, mixing, and aeration resulting from high concentrations of TSS and nutrients and (2) adverse effects on seeded microalgae by indigenous bacteria and protozoa, leading to poor microalgal growth and inefficient nutrient removal (Foladori et al., 2019). To address these challenges, many previous studies used diluted [e.g., Nam et al. (2017) and Wang et al. (2016)]) or sterilized SW [e.g., Park et al. (2010) and Zhu et al. (2013)] for microalgal cultivation. While dilution and sterilization resulted in improved algal growth, their applicability to large-scale farm operations is questionable.

An alternative to dilution is solid-liquid separation that also can reduce TSS and nutrient concentrations in SW. Three types of solid-liquid separation methods are commonly used for livestock wastewater management: gravitational (e.g., sediment basins), mechanical (e.g., screens and centrifuges), and chemical, the last of which involves the use of flocculants and/or coagulants. Flocculation-coagulation aims to agglomerate fine solid particles into large flocs so that they can be readily removed by gravitational and mechanical separation processes (Lee and Chang, 2022). Prevalent flocculants/coagulants for livestock wastewater management include aluminum sulfate, ferric chloride (or sulfate), and polyacrylamide (PAM) (González-Fernández et al., 2008). González-Fernández et al. (2008) found that 73% of TSS was removed from raw SW using PAM. Gabriel et al. (2019) reported a 68% turbidity reduction in SW using Tanfloc (a commercial coagulant) along with tannin (a natural flocculant). In addition to solids, nutrients can also be effectively removed through flocculation-coagulation. For example, using a combination of PAM and filtration, 61% of total Kjeldahl nitrogen (TKN), 72% of total phosphorus (TP), 83% of chemical oxygen demand (COD), and 97% of TSS was successfully removed from flushed swine manure (Vanotti et al., 2005). Additional relevant reports can be found in Table C-1. In short, chemical-assisted solid-liquid separation can effectively remove TSS and nutrients from raw SW (and the nutrient-rich solids can then be land applied). However, its effects on microalgal growth have yet to be studied.

Another question related to microalgal cultivation in SW is whether algae can enhance wastewater treatment effectiveness. Although a significant reduction in COD or nutrients was reported by previous studies (Abou-Shanab et al., 2013; Park et al., 2010;

Wang et al., 2016; Zhu et al., 2013), it remains uncertain whether the reduction was attributed to algae due to the lack of control groups. For example, aeration is adopted in many microalgal production systems to enhance mixing and CO_2 availability and it is known to facilitate the aerobic degradation of water-borne pollutants by bacteria (Cheng and Liu, 2001).

The goal of this study was to foster the further development of microalgae-based SW treatment processes by answering the two questions stated above. The specific objectives were to (1) remove TSS and nutrients from raw SW with a three-step pretreatment process; (2) compare microalgal growth in raw SW versus pretreated SW; and (3) compare COD and nutrient removal by algal PBRs versus control reactors (without algae). *Scenedesmus dimorphus* (*S. dimorphus*) was selected for its resilience to pH changes, efficient ammonia removal, and high growth rate (Kang et al., 2015). It has been researched in our lab for years, including a recent study of treating swine barn exhaust air with *S. dimorphus* PBRs (Uguz et al., 2022). The same species was used by González et al. (1997) for treating agricultural wastewater. Other microalgal species investigated for SW treatment include *Chlorella vulgaris* (Deng et al., 2018; Ji et al., 2013), *Scenedesmus obliquus* (Xu et al., 2015), and *Spirulina platensis* (Cheunbarn and Peerapornpisal, 2010). Different species may exhibit different degrees of adaptability to SW. Thus, the findings from this study should not be overgeneralized.

2. Methods and Materials

The study was conducted in two phases: microalgal cultivation in (1) raw SW and (2) pretreated SW. In neither phase, the SW was autoclaved or sterilized. The pretreatment,

which aimed to remove solids from the wastewater, consisted of three steps: initial sieving, coagulation-flocculation, and final sieving.

2.1. Swine wastewater

SW was acquired from the South Dakota State University (SDSU) off-site swine education and research facility in Flandreau, South Dakota, USA. The facility consists of two mechanically ventilated rooms with deep pits (2.4 m in depth) and houses ~1200 wean-to-finish pigs. Samples were collected in December 2020 and May 2021 during manure agitation and pumping and stored in airtight buckets at 4ºC in a lab refrigerator for later use. The SW sample collected from each manure pumping event was analyzed for pH (using an Apera PH700 pH meter), COD, TKN, ammonia (NH_3-N), nitrite (NO_2-N), nitrate (NO_3-N), TP, orthophosphate (PO_4-P) (using a Hach DR3900 spectrophotometer; Hach Company, Loveland, Colorado, USA), and TSS (through gravimetric analysis). A test sample was filtered with a Whatman 7-cm glass fiber filter to remove suspended solids before reacting with Hach reagents. Therefore, the measured COD and nutrient concentrations were for soluble parts (e.g., soluble COD [SCOD]) unless otherwise stated. A primary reason for measuring solubles was that microalgal cells also contributed to particulate COD, nitrogen, and phosphorus and they, along with other solids, would eventually be harvested. Thus, the soluble-part measurement data were anticipated to represent the condition of effluents from a microalgal treatment process. The same protocol (i.e., analyzing solubles) was adopted by Zhu et al. (2013) and Wang et al. (2015, 2017).

2.2. Algal culture

The *S. dimorphus* strain UTEX 1237 was purchased from the UTEX Culture Collection of Algae at the University of Texas at Austin (Austin, Texas, USA). The strain

was cultivated in an autoclaved bold basal medium (BBM) with pH=6.4±0.5 (Fábregas et al., 2000). The cultivation started from a 200-mL culture. Autoclaved BBM and deionized water were periodically added during a two-month cultivation period. A final culture volume of 16,000 mL was achieved. The culture was then transferred into rectangular PBRs made of plexiglass (wall thickness: 12 mm; inner dimensions: 508 mm $\times$ 102 mm $\times$ 356 mm). During the cultivation, the algal culture was continuously aerated with air at a rate of 0.5 L min^{-1} per liter of the culture volume. A light intensity of 60-70 µmol m^{-2} s^{-2} was maintained using white fluorescent lamps. *S. dimorphus* cell counts (as a measure of algal concentration) were determined using a Neubauer hemocytometer under an Olympus CX41 LEEDS optical microscope (Olympus Corp., Tokyo, Japan). An ImageJ software program was used to aid cell counting. The same method was also used to monitor algal growth in pretreated and untreated raw SW.

2.3. Flocculant/coagulant selection

To select the appropriate coagulant and flocculant, five coagulants/flocculants were compared through jar testing: ferric sulfate ($Fe_2(SO_4)_3$) (Fisher Scientific Inc., Hampton, New Hampshire, USA), polyacrylamide polymer (PAM) (Spectrum Chemical MFG Corp, Gardena, California, USA), Magnoflac (Solenis LLC, Wilmington, Delaware, USA), chitosan (Tidal Vision, Bellingham, Washington, USA), and cationic starch (with the degree of substitution [CS] = 0.86) prepared in our group (Haleem et al., 2022). The testing was done using a Phipps & Bird 7790 six-paddle stirrer (Phipps & Bird Company, Richmond, Virginia, USA) with the SW collected in December 2020. It involved 3-minute quick stirring at 300 rpm and 15-minute slow stirring at 60 rpm, followed by floc settling for 24 hours. $Fe_2(SO_4)_3$ and cation starch were selected for the pretreatment experiment.

2.4. Swine wastewater pretreatment

The pretreatment mimicked a solid-liquid separation system for dairy wastewater (rotary drums + coagulation/flocculation + a roller press). It was assumed that a similar system would be applied to SW management at large swine operations. In brief, the SW was first screened with a 35-mesh sieve (Fieldmaster, Yulee, Florida, USA) to remove coarse solid particles. The initially screened SW was then added with 2000 mg L^{-1} $Fe_2(SO_4)_3$ as a coagulant and 250 mg L^{-1} cationic starch as a flocculant, and was thoroughly mixed using an overhead mechanical stirrer (300 rpm for 3 minutes and then 60 rpm for 15 minutes). After being settled for 24 hours, the upper liquid faction of the treated SW was filtered with a 120-mesh sieve (Fieldmaster, Yulee, Florida, USA). The filtrates were then collected for the phase#2 experiment.

2.5. Algal cultivation in photobioreactors

Figure 4-1 shows the experimental setup in this study. Five rectangular PBRs were used. Three contained both SW and microalgae; while two contained SW only, serving as the control group. In the reactors with algae, the *S. dimorphus* culture and SW were mixed at a volumetric ratio of 3:1 (4.5 L versus 1.5 L). In the reactors without algae, the SW was diluted with sterile deionized water to ensure the same SW concentration as in the three algal PBRs. For both phases#1 and #2, algal cultivation was carried out under the illumination of white fluorescent lamps (75.6-83.7 $\mu mols^{-1}$ m^{-2} light intensity) for 30 days. No lighting was provided for the control group since no photosynthetic activity was expected. All the reactors (including the control and algal PBRs) were aerated with air (containing ~500-1000 ppm CO_2) at 0.5 L min^{-1} per liter of liquids. Environmental conditions, including pH (6-7), water level (adding deionized water to maintain the level),

aeration rate, and light intensity, were monitored and controlled throughout the experiments.
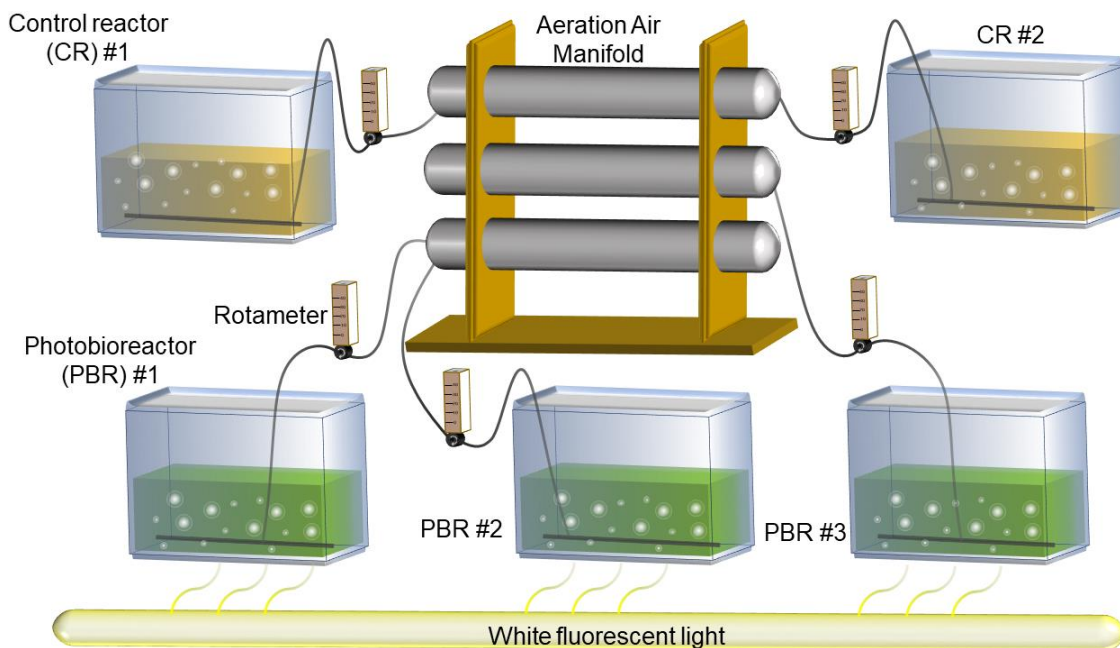
Figure 4-1. Setup of the experimental system. The system consisted of three replicate photobioreactors for microalgal cultivation in swine wastewater and two replicate reactors (without microalgae) serving as the control.

A 30-mL liquid sample was periodically collected from each PBR for the analysis of algal cell counts (not for the control group), pH, COD, TKN, NH_3-N, NO_3-N, TP, PO_4-P, and TSS. NO_2-N was also analyzed during the phase#1 experiment (i.e., algal cultivation in raw SW). Results showed that only trace amounts of NO_2-N occurred (0.14-2.25 mg L^{-1}; N=25). Thus, no NO_2-N analysis was conducted during the phase#2 experiment (i.e., algal cultivation in pretreated SW). Again, the measured COD and nutrient concentrations were for solubles (filtrates) only. To better understand the fate of nutrients, solid samples collected at the end of each experiment were analyzed for COD, total nitrogen (TN), and TP. The analysis involved the centrifugal separation of solids from the wastewater, vacuum

drying of separated solid samples (using a Cole-Parmer Stable Temp vacuum oven), and

microwave-assisted acid (HCl) digestion of dry solid samples, following the EPA Method

3015A. Thus, the solid samples would include algal biomass, bacterial biomass, and other

insoluble organics and inorganics. COD, TN, and TP contents in the acid digestates were

analyzed with Hach methods and the results were then translated into mass fractions of

COD, TN, and TP in the solid samples. Here, COD served as a measure of organic matter

in solids.

The initial cell counts in all the algal PBRs were set to be around 1500×10^6 cell L^- ^{1} to leave rooms for microalgae to grow while ensuring comparability between

experiments. This required ~20-fold dilution of the stock algal culture ($31,060 \times 10^6$ cell L^- ^{1}) maintained in the BBM. Due to the large dilution ratio, the soluble COD and nutrient

concentrations from the BBM (~2.7 mg L^{-1} PO_4-P, ~2.5 mg L^{-1} NO_3-N, and ~1.6 mg L^{-1}

COD) were negligible in the algal PBRs.

3. Results and discussion

3.1. Characteristics of raw swine wastewater

A substantial variation in wastewater characteristics was found between the SW

collected in December 2020 and that in May 2021 (Table 4-1). For TSS, total COD

(TCOD), and TP, the latter sample was around 2-4 times more concentrated. It also

contained ~1.5 times more TKN and PO_4-P than the December 2020 sample. The reason

is uncertain but likely related to collection season, flushing water usage, feed diet, and barn

conditions (Ra et al., 1997). "Outliers" included NH_3-N, NO_2-N, and NO_3-N, which may

be explained by differences in microbes moderating N conversions in manure and their

metabolic activities. Bulk parameters, such as temperature, pH, and TSS, can have a large impact on manure microbiomes (Lim et al., 2018).

Table 4-1. Characteristics of raw swine wastewater. [a]

Parameters	December 2020 sample	May 2021 sample
pH (unitless)	8.3±0.1	7.4±0.1
TSS (mg L^{-1})	24,890±3,358	73,950±3,598
TCOD [b] (mg L^{-1})	24,700±9,030	84,417±116
SCOD (mg L^{-1})	4,538±452	n/a [c]
TKN (mg L^{-1})	4,457±1,249	6,433±5
NH_3-N (mg L^{-1})	3,085±393	2,996±1
NO_2-N (mg L^{-1})	0.5±0.0	200±0.1
NO_3-N (mg L^{-1})	9.7±0.6	0.7±0.1
TP (mg L^{-1})	371±2	1,034±14
PO_4-P (mg L^{-1})	288±30	410±0.1

Note: [a] Measurement values were presented in average (range). For certain parameters, replicate samples gave the same value. [b] TCOD – total COD, the sum of particulate COD and soluble COD. [c] The SCOD concentration was unavailable for the May 2021 sample due to the loss of testing records.

3.2. Flocculant/coagulant selection

PAM and cation starch were the best two performers in solid removal from raw SW (Figure C-1). Without pH adjustment (pH=8.0), PAM delivered the highest TSS removal (93%), followed by cationic starch (78%) and Magnoflac (72%). As the only coagulant tested, $Fe_2(SO_4)_3$ showed only a moderate TSS removal rate (61%). Its performance improved with a decrease in pH (67% at pH=6.5 and 75% at pH=5) (Table C-2). However, slow floc formation was observed under low pH conditions (30% TSS removal at pH=5 after 30 minutes). For PAM, the effect of its dosage level was further studied, with 193 mg L^{-1} found to be the optimal level. The performance of PAM is similar to that (95% TSS removal at 140 mg L^{-1}) reported by Vanotti et al. (2002).

A combination of cation starch and $Fe_2(SO_4)_3$ was selected for raw SW pretreatment, considering factors (besides performance) such as environmental impacts,

product availability, and cost-effectiveness. Although effective in TSS removal (Wong et al., 2006), the use of PAM, especially cationic PAM, raises environmental concerns due to its slow degradation in soil and sludge (Hennecke et al., 2018) and ecotoxicity (Buczek et al., 2017). The cationic starch in this study was made from potato peel waste and, thus, is attractive from cost and sustainability standpoints. The combined use of coagulant and flocculant is known for enhanced solid-liquid separation in wastewater (Teh et al., 2016; Wang et al., 2019). With 2000 mg L^{-1} $Fe_2(SO_4)_3$ and 250 mg L^{-1} cationic starch, 83% TSS was removed from the December 2020 SW. The efficiency was achieved without pH adjustment.

3.3. Solid and nutrient removal upon pretreatment

A total of 50.8% TSS and 52.7% of PO_4-P were removed from the May 2021 SW through the three-step pretreatment (Figure 4-2). The relatively low TSS removal efficiency was ascribed to differences in SW characteristics (Table 4-2), especially TSS concentrations. Lee et al. (2004) reported a 90-95% TSS reduction in SW using aluminum sulfate ($Al_2(SO_4)_3$), a prevalent chemical coagulant; however, the initial TSS concentration (7,300-9,500 mg L^{-1}) was substantially lower than that in this study. For every different SW sample, a separate jar testing experiment may be needed to determine the appropriate flocculants/coagulants and their optimal dosage levels. Unfortunately, due to material (SW and chemical reagents) availability issues, no such experiment was conducted in this study.
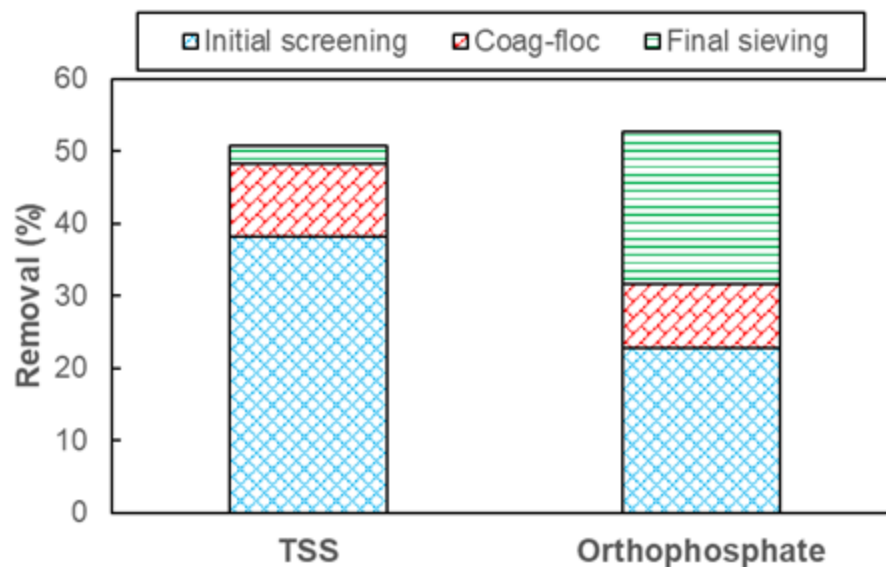
Figure 4-2. TSS and orthophosphate removal after each step of pretreatment.

Table 4-2. Characteristics of pretreated/diluted swine wastewater used for algal cultivation experiments.

Parameters	After pretreatment & dilution
pH (unitless)	8.5±0.0
TSS (mg L^{-1})	5,033±401
TCOD (mg L^{-1})	13,100±16
SCOD (mg L^{-1})	2,788±13
TKN (mg L^{-1})	1,381±1
NH$_3$-N (mg L^{-1})	609±0.5
NO$_2$-N (mg L^{-1})	0.23±0.0
NO$_3$-N (mg L^{-1})	40±0.0
TP (mg L^{-1})	200±1.1
PO$_4$-P (mg L^{-1})	41±0.1

The initial sieving with 35-mesh sieves contributed the majority of TSS removal (38.2% out of 50.8%; equivalent to 29,250 mg L^{-1} TSS removed), suggesting the occurrence of a large fraction of coarse particles in the May 2021 SW. The coagulation-flocculation step resulted in 10.2% of TSS removal (7,543 mg L^{-1}) and the removal was driven by the gravitational settling of formed flocs. The final polishing with 120-mesh sieves only removed 2.4% of TSS. The remaining TSS was small enough (≤146 μm) to be

handled by many irrigation systems – which is encouraging from the manure land application standpoint – but still too concentrated (36,383 mg L^{-1}) for microalgal cultivation. In contrast, 22.9%, 8.9%, and 21% of PO_4-P were removed during the initial sieving, coagulation-flocculation, and final sieving steps, respectively. In SW, PO_4-P exists in both soluble and insoluble forms, depending on co-existing cations. During the flocculation-coagulation step, Fe^{3+} ions released from $Fe_2(SO_4)_3$ can react with dissolved inorganic phosphate to form particulate phosphate (Park et al., 2016). The particles can then agglomerate or attach to large solids and, thus, be removed during the final sieving step.

A change in pH value was noted during the pretreatment process: pH=7.4 in the raw SW, pH=8.9 after initial sieving, pH=8.8 after flocculation-coagulation, and pH=8.7 after the final sieving. This is possibly caused by the removal of solids rich in fatty acids (produced from the anaerobic degradation of organic matter). Only 22.4% of TCOD was removed after the pretreatment.

3.4. Algal growth in swine wastewater

Given the low TSS removal resulting from the pretreatment, certain changes in the initial experimental plan were implemented to ensure a reasonable comparison between the two phases of algal cultivation experiments. A challenge was that only the May 2021 SW was available for the phase#2 experiment and it contained a high TSS concentration even after pretreatment. To address the challenge, we assumed that 80% of TSS would be removed from the December 2020 SW with the proposed pretreatment (Note: The 80% efficiency was achievable based on the jar testing experiment) and accordingly diluted the pretreated May 2021 SW with deionized water to the calculated TSS level (5,033 mg L^{-1})

(Table 4-1). It is noteworthy that after the pretreatment and dilution, the acquired SW showed differences (e.g., [NO_3-N]/[TKN]) than the raw SW from December 2020 or May 2021, which was likely caused by sieving and flocculation-coagulation processes.

S. dimorphus grew better in the pretreated than the raw SW (Figure 4-3), as measured by maximum algal cell counts: $3,202\pm275\times10^6$ versus $2,286\pm589\times10^6$ cells L^{-1} (Note: Average $\pm$ standard deviation derived from replicate PBRs). In the raw SW, the initial algal growth appeared to be inhibited by high TSS concentrations at the beginning of the experiment. *S. dimorphus* cell counts started to increase after day 19 when the continual aeration decreased the TSS concentration from $6,448\pm210$ to $2,308\pm381$ mg L^{-1}. High TSS concentrations in SW were believed to suppress algal growth because of limited light penetration (Cheng et al., 2019). High nutrient concentrations were also thought inhibitive (Cheng et al., 2019). In addition, because SW was not sterilized, a possible competition between *S. dimorphus* and bacteria could have occurred (Abou-Shanab et al., 2013; Amini et al., 2016; Li et al., 2020). After day 19, the TSS concentration in the raw SW continued to decrease ($2,077\pm240\times10^6$ cells L^{-1} on day 26), and the maximum cell count occurred on day 29 – the end of the experiment. Comparatively, the lag phase of algal growth in the treated SW was considerably shorter. *S. dimorphus* cell counts started to grow (but slowly) on day 1 and entered an exponential growth phase on day 11. A stationary phase and a death/lysis phase were noted between days 17-21 and days 21-29, respectively, suggesting the occurrence of nutrient constraints as cultivation proceeded (95 mg L^{-1} NH$_3$-N on day 20 and 48 mg L^{-1} on day 27). TSS concentrations were relatively stable in the pretreated SW over the entire experimental period ($1,574\pm196$ mg L^{-1}).
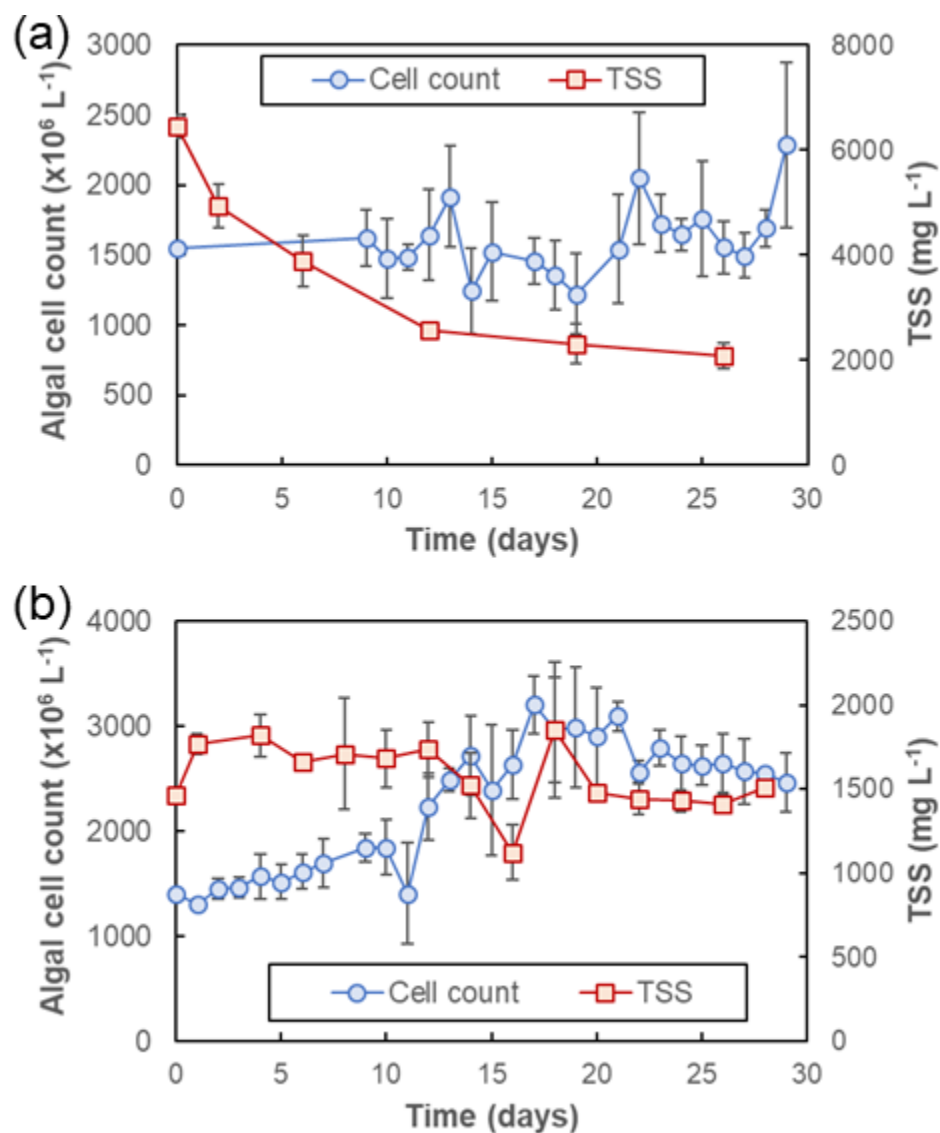
Figure 4-3. Algal growth under different conditions: (a) raw swine wastewater; and (b) pretreated swine wastewater. Error bars (standard deviations) were calculated from replicate reactors.

High TSS concentrations in the raw SW raised a major challenge to microalgal growth measurement. No algal cell counting was successfully done from day 1 to 9 (Figure 4-3a) due to the interference of numerous black particles – as part of TSS – under the microscope (Figure C-2a). It also made the optical density (OD) method unsuitable for

tracking algal growth because black particles have strong light absorption of nearly all wavelengths. Due to the occurrence of a large number of non-algae solid particles, using TSS as a surrogate for algal biomass was inappropriate. Algal cell counts were selected as the sole measure of algal growth in this study.

The microscopic images (Figure C-2) also supported the finding that decreased TSS concentrations after the pretreatment/dilution were beneficial for *S. dimorphus* cultivation. On day 7 (exemplifying the early stage of algal cultivation), *S. dimorphus* cells in the pretreated SW were overall larger and greener (Figure C-2b) than those in the raw SW (Figure C-2a). On day 21, a similar trend was observed. The number of non-algae black particles decreased substantially in both SW on day 21. Particularly, in the pretreated SW, algal cells appeared to be a dominant contributor to solids (Figure C-2d). Assuming that the dry cell weight of *S. dimorphus* was 194 pg cell^{-1} (Padovan, 1992), the mass contribution of *S. dimorphus* to TSS in the pretreated SW would be ~18.7% at the beginning and ~32.7% toward the end of the cultivation experiment. Thus, the TSS loss due to the degradation of non-algae particles could be offset by algal growth-induced TSS gains, resulting in a relatively stable TSS concentration in the pretreated SW PBRs. Comparatively, in the raw SW, the contribution of *S. dimorphus* to TSS increased from ~4.6% on day 0 to ~21.3% on day 26, largely due to a substantial reduction in TSS. The effect of TSS concentrations on algal growth can also be seen from visual inspection of PBRs (Figure C-3). With the pretreatment, the algal culture in the PBRs was greener.

No consistent conclusion was drawn from the previous studies of microalgal cultivation in diluted or pretreated SW. Ji et al. (2013) found that *Chlorella vulgaris* (*C. vulgaris*) YSW-04 grew faster in terms of dry algal biomass in 20% SW than in 50%, 80%,

and undiluted SW. Franchino et al. (2016) reported a better growth performance of *C. vulgaris* in 20% and 40% than 10% SW digestates. Wen et al. (2017) isolated an indigenous *C. vulgaris* strain (MBFJNU-1) from SW and found that it grew better in undiluted SW, while a freshwater *C. vulgaris* strain (FACHB-8) grew poorly in SW>40%. It is noteworthy that none of the studies measured TSS, and the raw SW in Ji et al. (2013) and Wen et al. (2017) had much lower COD and nutrient (N and P) concentrations than that in this study. Thus, the optimal dilution ratio(s) derived from one study can hardly be applied to others. In addition to SW characteristics, microalgal strains can also have a large effect on algal growth. Compared to *C. vulgaris*, *S. dimorphus* is less commonly selected for SW treatment partly due to a discouraging finding from Hasan et al. (2014) that "*S. dimorphus* was unable to grow on the swine wastewater." Despite being freshwater microalgae, *S. dimorphus* has been successfully cultivated in various types of wastewaters (Gentili, 2014; Hu et al., 2021; Lutzu et al., 2016), including SW-containing agroindustrial wastewater (González et al., 1997). Our experiments showed that *S. dimorphus* could grow in both raw and pretreated SW and it grew better with reduced TSS. Since cell count was selected as the sole measure of algal concentration in this study, a direct comparison with previous similar studies (which instead measured dry algal biomass) is difficult. (Again) Assuming the dry cell weight of *S. dimorphus* was 194 pg cell^{-1}, the maximum algal biomass growth rate would be 49.8 mg L^{-1} d^{-1} from day 11 to 17 in the pretreated SW. This is lower than the maximum growth rate of *C. vulgaris* in raw SW, e.g., 160 mg L^{-1} d^{-1} (Amini et al., 2016) and 244.8 mg L^{-1} d^{-1} (Deng et al., 2018). However, both references used SW far less concentrated than that in this study. Thus, a higher growth rate of *S. dimorphus* in SW (than 49.8 mg L^{-1} d^{-1}) may be achievable upon further experiments.

3.5. COD and nutrients in wastewater and algae

Aeration has been tested as a treatment technology for SW management for years. It is often required during algal cultivation as it provides essential mixing and CO_2 for algal growth. A key question is – Will cultivating microalgae in aerated SW provide any additional treatment benefits? Our results showed no overall or consistent treatment improvement. Rather, a potential benefit came from the N-rich solids harvested from PBR operation.

During the phase#1 experiment, algal PBRs removed more SCOD but a similar amount of TKN from the raw SW than the control (Figure 4-4). On day 20, 89% and 88% of TKN were removed by the algal and control reactors, respectively. On the same day, 46% SCOD was removed by the algal PBRs and 33% by the control reactors. In the latter reactors, SCOD concentrations slightly increased from day 0 to day 13, which may be explained by the dissolution of particulate COD to SCOD due to aeration. Both the algal and control reactors offered no net TP reduction on day 13. After an initial decrease, the TP concentrations increased after day 7. This could be ascribed to the mineralization of organic P or the conversion of attached P in SW to soluble phosphates. No SCOD, TKN, or TP analysis was conducted between days 20 and 30. Thus, the final reduction efficiencies were uncertain. During the phase#2 experiment, algal PBRs removed more TKN but lesser SCOD from the pretreated SW than the control. After 27 days of operation, 46% of SCOD, 55% of TKN, and 26% of TP were removed by algal PRBs; while in the control reactors, the corresponding removal efficiencies were 64%, 40%, and 55%, respectively. Similarly, the TP concentration in the control reactors increased after day 7, likely due to the conversion of organic P and attached P to solubles.

Figure 4-4. Changes in COD, TKN, and TP concentrations during the experiments: (a), (b) and (c) for phase#1 (raw swine wastewater); and (d), (e), and (f) for phase#2 (pretreated swine wastewater). Error bars (standard deviations) were calculated from replicate reactors.

To further study the transformation of nutrients, NH_3-N, NO_3-N, and PO_4-P were also analyzed during the experiments (Figure 4-5). NH_3-N can be produced from the mineralization of organic N (which is rich in livestock wastewater), NO_3-N can be formed through nitrification, and PO_4-P can be converted from organic P or polyphosphate. For NH_3-N, an overall higher reduction efficiency was found in the raw SW. On day 20, 82% and 86% of NH_3-N were removed from the raw SW by the algal and control reactors, respectively. In contrast, on day 27, 68% and 61% of NH_3-N were removed from the pretreated SW by the algal and control reactors, respectively. The initial concentration of organic N, calculated as TKN minus NH_3-N, was 343 mg L^{-1} for phase#1 and 193 mg L^{-1} for phase#2. During the phase#1 experiment, nearly all organic N was converted on day 13; while during the phase#2 experiment, the organic N concentration first decreased and gradually increased after day 13. The reason is unknown but likely related to the lysis of algal or bacterial cells. The initial concentrations of NO_3-N were low in both the phase#1

and #2 reactors, which is understandable given the exceptionally high COD concentrations in the SW. Aeration promoted nitrification by adding oxygen into the wastewater, thereby resulting in elevated NO_3-N concentrations. But in general, the NO_3-N concentrations remained relatively low during the experiment, as compared to TKN or NH_3-N. For PO_4-P, no well-defined data trends were seen during the phase#1 experiment. During the phase#2 experiment, PO_4-P concentrations first increased and then gradually decreased and were significantly higher in algal PBRs than in the control reactors.
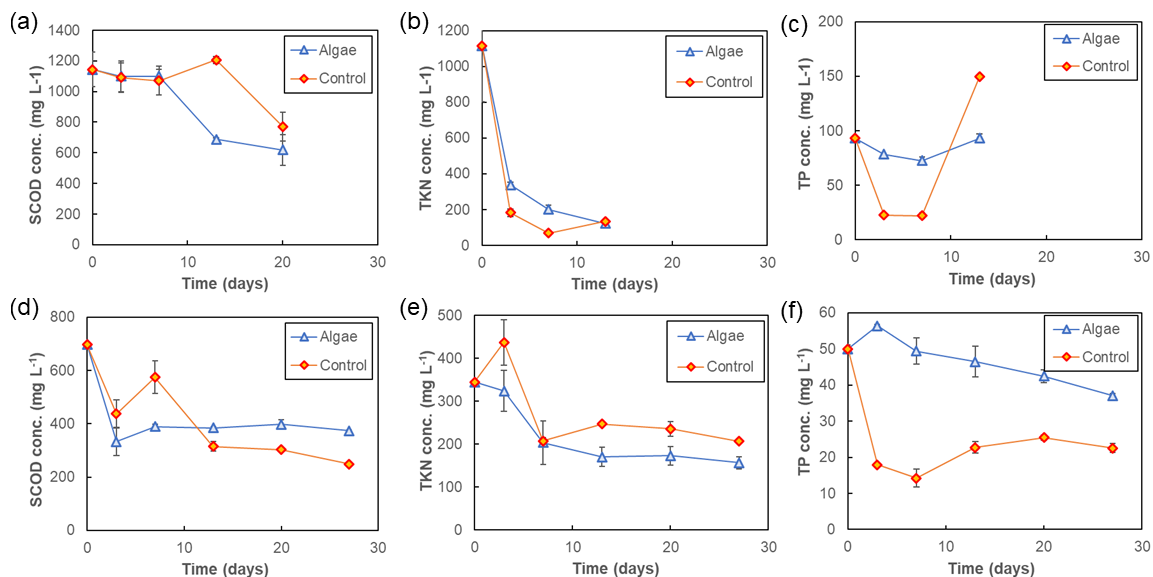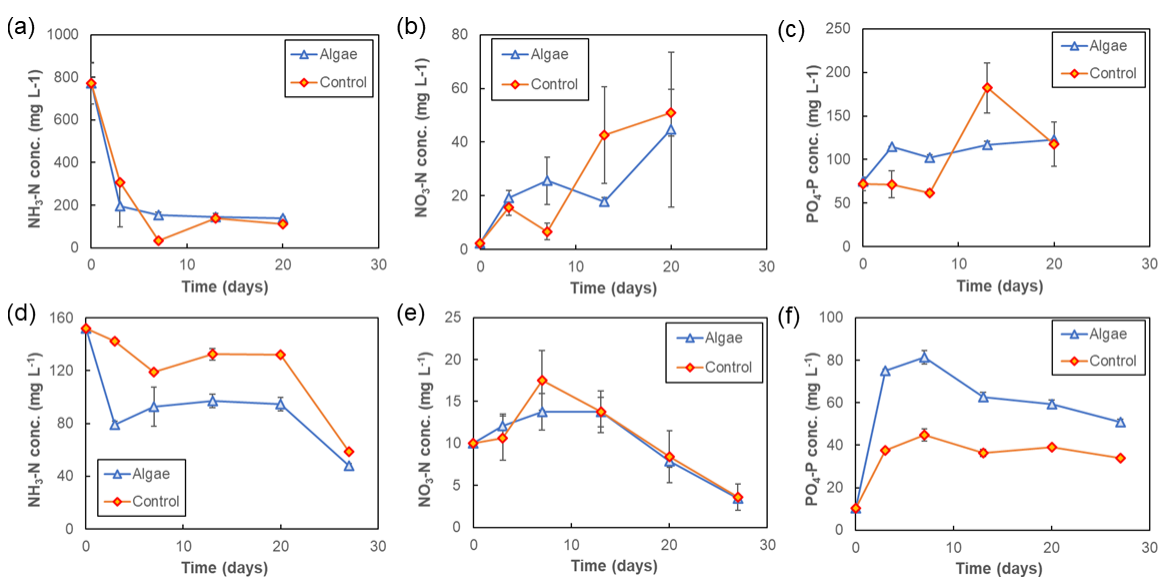

Figure 4-5. Changes in NH_3-N, NO_3-N, and PO4-P concentrations during the experiments: (a), (b) and (c) for phase#1 (raw swine wastewater); and (d), (e), and (f) for phase#2 (pretreated swine wastewater). Error bars (standard deviations) were calculated from replicate reactors.

Again, compared to simple aeration, cultivating *S. dimorphus* in SW offered no consistent improvement in pollutant removal. However, the solids harvested from the pretreated SW algal PBRs were rich in N and could potentially be used as fertilizers or animal feed. Table 4-3 listed the COD, TN, and TP contents of solids separated at the end of algal cultivation experiments. The solids from the phase#2 experiment contained ~5.7% of TN on a dry basis, which is lower than that in pure *S. dimorphus* (~8.75%) (Bordoloi et

al., 2016) but higher than that in raw swine manure (2.8%) (Xiu et al., 2010). The high TN

content is clearly related to algal growth in PBRs – algal cells were estimated to account

for 32.7% of dry weight in the harvested solids. *S. dimorphu* is known for its superior

capability of absorbing NH_3-N from wastewater (González et al., 1997). To further

illustrate the N absorption by the cultivated algae, we compared solid samples from the

algal PBRs versus the control reactors and defined an enrichment factor as the ratio of the

solids' COD, TN, or TP contents (Note: PRB to control) (Table 4-3). In general, the solids

from the algal PBRs contained more organic matter but lesser TP. The improved microalgal

growth in the pretreated/diluted SW (phase#2) further increased the solids' organic matter

and TN contents.

Table 4-3. COD, TN, and TP contents (mg g^{-1}) and their enrichment factors in solids collected at the end of swine wastewater algal cultivation experiments. [a]

	COD	TN	TP
Phase#1	555±47 (1.15)	1.37±1.12 (0.14)	0.17±0.04 (0.38)
Phase#2	1868±206 (3.57)	57.8±0.1 (1.72)	0.06±0.01 (0.31)

Note: [a] An enrichment factor (in the parenthesis under a content value) was calculated as a ratio of the COD, TN, or TP content in the solids from the algal PBRs versus those from the control reactors.

3.6. Discussions and recommendations

The COD and nutrient removal by aeration in the control reactors were largely

attributed to aerobic degradation of these substances by indigenous bacteria in SW (Cheng

and Liu, 2001). A similar process occurs in aerobic lagoons, a proven treatment technology

for SW management (Liu et al., 2013). Inoculating SW with *S. dimorphus* enabled additional removal mechanisms.

NH$_3$-N was possibly removed through assimilation to algal biomass (Cai et al., 2013), assimilation to bacterial biomass, nitrification, and NH$_3$ stripping (González et al., 1997). In this study, the NH$_3$-N assimilation was affirmed by an increase in algal cell counts and the N-rich solids harvested from the phase#2 algal cultivation experiment. Bacterial oxidation of NH$_3$-N to nitrite and nitrate, i.e., nitrification was affirmed by the accumulation of NO$_3$-N in the algal PBRs (Figure 4-5). NH$_3$ stripping was anticipated due to continuous aeration and relatively high pH and alkaline levels in the SW. A characteristic NH$_3$ odor was smelled especially during the first few days of aeration. It is hard to accurately assess the relative contribution of each possible removal mechanism. For algal cultivation in the pretreated SW, 25.6% of TN in the SW was estimated to be retained in the solids and 9.1% absorbed into *S. dimorphus* at the end of the experiment. A detailed estimation procedure can be found in the supplementary material. The majority of TN could be stripped out as gases or stay in the wastewater.

In principle, P can be removed by algal/bacterial uptake and chemical precipitation. However, no improved P removal was found in the algal PRBs, compared to the control reactors (Figure 4-4). This is consistent with the TP analysis result of solid samples (Table 4-2) – with algae, the final solids contained even lesser TP. Thus, *S. dimorphus* is unlikely a suitable algal species for P recovery. A different observation was reported by Cristóvão et al. (2016) and González et al. (1997). However, neither of the studies had control reactors and the concentrations of TP were lower than those in this study. It is unclear whether and to what degree bacteria and aeration played a role in TP removal or transformation. During

the phase#2 experiment, the concentrations of PO_4-P, the most utilizable P form for microalgae (Nagarajan et al., 2019), increased after day 0, which may be ascribed to bacterial activity or aeration-induced changes in water chemistry.

Organic matter (measured as COD) in wastewater can serve as a precursor of carbonates to support microalgae growth. In this study, only moderate SCOD removal efficiencies were found with the raw SW (phase#1) and the pretreated SW (phase#2), lower than those (66-80%) reported by Zhu et al. (2013) with *Chlorella zofingiensis*. It is noteworthy that the SW in Zhu et al. (2013) was autoclaved and, thus, the SCOD reduction was solely attributed to algal growth. Without sterilization, bacteria present in the wastewater can contribute significantly to COD degradation (Heredia-Arroyo et al., 2011). On the other hand, sterilization may increase the availability of nutrients (e.g., released from lysed cells) to microalgae. A further study is still needed to examine COD reduction mechanisms in algae-bacteria treatment systems.

A limitation of this study lies in the substantial difference in SW characteristics between the phase#1 and #2 experiments. Considering both SW samples were taken from the same farm, the difference was beyond our anticipation. The flocculant/coagulant selected with the phase#1 SW did not perform as well as anticipated when pretreating the phase#2 SW. Additional dilution was made to adjust the TSS concentration in the pretreated SW. As a result, this study offered a likely YES but yet no direct answer to whether solid-liquid separation is beneficial for microalgal cultivation. For future similar studies, the same raw SW sample should be used for all phases of experiments. If different SW samples must be used (e.g., due to the long time duration of algal cultivation), they should be diluted to the same TSS or COD level before subsequent experiments. If the

experiments involve flocculation-coagulation, a jar test is needed for every different SW to identify the best-performing reagents and/or optimal dosage levels.

Another limitation is the lack of accurate methods for determining dry algal biomass in SW or similar wastewaters. Previous studies showed that the cell size/weight of *S. dimorphus* varies with growth stages and nutrient conditions (Narala et al., 2016). Thus, the assumption of 194 pg cell^{-1} dry cell weight and the calculations based on it carry large uncertainties. Using cell counts as the only algal concentration measure has multiple constraints. In addition to the uncertainty associated with microscopic counting, it fails to depict a complete picture of algal growth, e.g., the larger algal cell size in the pretreated/diluted SW than in the raw SW (Note: The maximum cell count was only 40% higher in the former SW. Without further information, this could make readers underestimate algal growth improvement.). TSS was selected as a surrogate of dry algal biomass in several previous studies, e.g., Wang et al. (2017; 2019). However, its applicability to SW algal cultivation is questionable given the abundance of non-algae suspended solids. A possible solution is to develop an AI-based image analysis program to automatically identify algal cells from other solids and measure the cells' counts, size, agglomeration status, and other useful parameters.

4. Conclusion

Treating SW with microalgae is regarded an ecofriendly technology for SW management. However, microalgal growth can be inhibited by high TSS and nutrient concentrations in raw SW. Solid-liquid separation pretreatment can effectively remove TSS and nutrients from raw SW but its effects on microalgal growth remained understudied. This study adopted a three-step pretreatment process (initial sieving,

flocculation-coagulation, and final sieving) and compared *S. dimorphus* growth and pollutant/nutrient removal in raw versus pretreated SW. An improved growth performance was observed in the pretreated SW, as measured by algal cell counts and cell size. Control reactors (the same PBRs and SW but without algae seeded) were used as reference to benchmark the pollutant/nutrient removal in algal PBRs. Moderate reductions in SCOD, TKN, NH_3-N were seen in both types of reactors. However, no consistent reduction efficiency gain (or loss) was seen between the algal PBRs and control reactors. *S. dimorphus* was unlikely a suitable microalgal species for phosphorus recovery, as indicated by lesser TP removal and higher PO_4-P concentrations in the algal PBRs than the control reactors. The analysis of algae-containing solids harvested at the end of the experiment also supported the observation. The solids harvested from algal cultivation in the pretreated SW contained substantially higher nitrogen (5.7% TN) and organic matter contents than those from the raw SW. They may potentially be used as an organic fertilizer or animal feed. Nitrogen balance estimation showed that ~25.6% of TN in the pretreated SW was captured in the solids and ~9.1% absorbed into *S. dimorphus* biomass. Efforts are needed to further study the carbon, nitrogen and phosphorus balances in algal PBRs and clarify the benefits and limitations of microalgae-based SW treatment processes.

REFERENCES

1. Anderson, M. A., Cudero, A. L., & Palma, J. (2010). Capacitive deionization as an electrochemical means of saving energy and delivering clean water. Comparison to present desalination practices: Will it compete? Electrochimica Acta, 55(12), 3845–3856. https://doi.org/10.1016/j.electacta.2010.02.012

2. Asimov, I. (1974). Asimov on Chemistry. Doubleday & Company.

3. Avraham, E., Bouhadana, Y., Soffer, A., & Aurbach, D. (2009). Limitation of Charge efficiency in capacitive deionization: I. on the behavior of single activated carbon. Journal of the Electrochemical Society, 156, P95–P99. https://doi.org/10.1149/1.3115463

4. Avraham, E., Noked, M., Cohen, I., Soffer, A., & Aurbach, D. (2011). The Dependence of the Desalination Performance in Capacitive Deionization Processes on the Electrodes PZC. Journal of The Electrochemical Society, 158, P168. https://doi.org/10.1149/2.078112jes

5. Banu, J. R., Do, K.-U., & Yeom, I.-T. (2008). Effect of ferrous sulphate on nitrification during simultaneous phosphorus removal from domestic wastewater using a laboratory scale anoxic/oxic reactor. World Journal of Microbiology and Biotechnology, 24(12), 2981–2986. https://doi.org/10.1007/s11274-008-9841-0

6. Bazant, M. Z., Thornton, K., & Ajdari, A. (2004). Diffuse-Charge Dynamics in Electrochemical Systems. Physical Review E, 70(2), 021506. https://doi.org/10.1103/PhysRevE.70.021506

7. Bharath, G., Alhseinat, E., Ponpandian, N., Khan, M. A., Siddiqui, M. R., Ahmed, F., & Alsharaeh, E. H. (2017). Development of adsorption and electrosorption

techniques for removal of organic and inorganic pollutants from wastewater using novel magnetite/porous graphene-based nanocomposites. Separation and Purification Technology, 188, 206–218. https://doi.org/10.1016/j.seppur.2017.07.024

8. Bian, Y., Chen, X., Lu, L., Liang, P., & Ren, Z. J. (2019). Concurrent Nitrogen and Phosphorus Recovery Using Flow-Electrode Capacitive Deionization. ACS Sustainable Chemistry & Engineering, 7(8), 7844–7850. https://doi.org/10.1021/acssuschemeng.9b00065

9. Bian, Y., Chen, X., & Ren, Z. J. (2020). PH Dependence of Phosphorus Speciation and Transport in Flow-Electrode Capacitive Deionization. Environmental Science & Technology, 54(14), 9116–9123. https://doi.org/10.1021/acs.est.0c01836

10. Bian, Y., Liang, P., Yang, X., Jiang, Y., Zhang, C., & Huang, X. (2016). Using activated carbon fiber separators to enhance the desalination rate of membrane capacitive deionization. Desalination, 381, 95–99. https://doi.org/10.1016/j.desal.2015.11.016

11. Biesheuvel, M., & Wal, A. (2010). Membrane capacitive deionization. Journal of Membrane Science, 346, 256–262. https://doi.org/10.1016/j.memsci.2009.09.043

12. Biesheuvel, P. M., Bazant, M. Z., Cusick, R. D., Hatton, T. A., Hatzell, K. B., Hatzell, M. C., Liang, P., Lin, S., Porada, S., Santiago, J. G., Smith, K. C., Stadermann, M., Su, X., Sun, X., Waite, T. D., van der Wal, A., Yoon, J., Zhao, R., Zou, L., & Suss, M. E. (2017). Capacitive Deionization—Defining a class of desalination technologies. ArXiv:1709.05925 [Physics]. http://arxiv.org/abs/1709.05925

13. Biesheuvel, P. M., van Limpt, B., & van der Wal, A. (2009). Dynamic Adsorption/Desorption Process Model for Capacitive Deionization. The Journal of Physical Chemistry C, 113(14), 5636–5640. https://doi.org/10.1021/jp809644s

14. Biesheuvel, P. M., Zhao, R., Porada, S., & van der Wal, A. (2011). Theory of membrane capacitive deionization including the effect of the electrode pore space. Journal of Colloid and Interface Science, 360(1), 239–248. https://doi.org/10.1016/j.jcis.2011.04.049

15. BLAIR, J. W., & MURPHY, G. W. (1960). Electrochemical Demineralization of Water with Porous Electrodes of Large Surface Area. In SALINE WATER CONVERSION (Vol. 27, pp. 206–223). American Chemical Society. https://doi.org/10.1021/ba-1960-0027.ch020

16. Bond, P. L., Hugenholtz, P., Keller, J., & Blackall, L. L. (1995). Bacterial community structures of phosphate-removing and non-phosphate-removing activated sludges from sequencing batch reactors. Applied and Environmental Microbiology, 61(5), 1910–1916. https://doi.org/10.1128/AEM.61.5.1910-1916.1995

17. Bouhadana, Y., Avraham, E., Soffer, A., & Aurbach, D. (2010). Several basic and practical aspects related to electrochemical deionization of water. AIChE Journal, 56(3), 779–789. https://doi.org/10.1002/aic.12005

18. Bradford-Hartke, Z., Lane, J., Lant, P., & Leslie, G. (2015). Environmental Benefits and Burdens of Phosphorus Recovery from Municipal Wastewater. Environmental Science & Technology, 49(14), 8611–8622. https://doi.org/10.1021/es505102v

19. Carrillo, V., Fuentes, B., Gómez, G., & Vidal, G. (2020). Characterization and recovery of phosphorus from wastewater by combined technologies. Reviews in Environmental Science and Bio/Technology, 19(2), 389–418. https://doi.org/10.1007/s11157-020-09533-1

20. Chen, F.-F., Li, H.-F., Jia, X.-R., Wang, Z.-Y., Qin, Y.-Y., Liang, X., Chen, W.-Q., & Ao, T.-Q. (2020). A quantitative prediction model for the phosphate adsorption capacity of carbon materials based on pore size distribution. Electrochimica Acta, 331, 135377. https://doi.org/10.1016/j.electacta.2019.135377

21. Chrispim, M. C., Scholz, M., & Nolasco, M. A. (2019). Phosphorus recovery from municipal wastewater treatment: Critical review of challenges and opportunities for developing countries. Journal of Environmental Management, 248, 109268. https://doi.org/10.1016/j.jenvman.2019.109268

22. Committee Report. (1970). CHEMISTRY OF NITROGEN AND PHOSPHORUS IN WATER. Wiley, 15.

23. Dabkowski, B. (2015). Understanding the different phosphorus tests. HACH.

24. Desmidt, E., Ghyselbrecht, K., Zhang, Y., Pinoy, L., Van der Bruggen, B., Verstraete, W., Rabaey, K., & Meesschaert, B. (2015). Global Phosphorus Scarcity and Full-Scale P-Recovery Techniques: A Review. Critical Reviews in Environmental Science and Technology, 45(4), 336–384. https://doi.org/10.1080/10643389.2013.866531

25. Folaranmi, G., Bechelany, M., Sistat, P., Cretin, M., & Zaviska, F. (2020). Towards Electrochemical Water Desalination Techniques: A Review on Capacitive Deionization, Membrane Capacitive Deionization and Flow Capacitive

Deionization. Membranes, 10(5), Article 5. https://doi.org/10.3390/membranes10050096

26. Forrestal, C., Xu, P., & Ren, Z. (2012). Sustainable desalination using a microbial capacitive desalination cell. Energy & Environmental Science, 5(5), 7161–7167. https://doi.org/10.1039/C2EE21121A

27. Gabelich, C. J., Tran, T. D., & Suffet, I. H. "Mel." (2002). Electrosorption of Inorganic Salts from Aqueous Solution Using Carbon Aerogels. Environmental Science & Technology, 36(13), 3010–3019. https://doi.org/10.1021/es0112745

28. Gao, F., Li, X., Shi, W., & Wang, Z. (2022). Highly Selective Recovery of Phosphorus from Wastewater via Capacitive Deionization Enabled by Ferrocene-polyaniline-Functionalized Carbon Nanotube Electrodes. ACS Applied Materials & Interfaces, 14(28), 31962–31972. https://doi.org/10.1021/acsami.2c06248

29. Gao, F., Shi, W., Dai, R., & Wang, Z. (2022). Effective and Selective Removal of Phosphate from Wastewater Using Guanidinium-Functionalized Polyelectrolyte-Modified Electrodes in Capacitive Deionization. ACS ES&T Water, 2(1), 237–246. https://doi.org/10.1021/acsestwater.1c00393

30. Ge, Z., Chen, X., Huang, X., & Ren, Z. J. (2018). Capacitive deionization for nutrient recovery from wastewater with disinfection capability. Environmental Science: Water Research & Technology, 4(1), 33–39. https://doi.org/10.1039/C7EW00350A

31. Guisasola, A., Chan, C., Larriba, O., Lippo, D., Suárez-Ojeda, M. E., & Baeza, J. A. (2019). Long-term stability of an enhanced biological phosphorus removal

system in a phosphorus recovery scenario. Journal of Cleaner Production, 214, 308–318. https://doi.org/10.1016/j.jclepro.2018.12.220

32. Hach. (2013). Water Analysis Handbook (8th ed.).

33. He, Y., Zhang, X., Zuo, K., Yang, F., Gao, T., & Liang, P. (2022). Highly efficient and selective extraction of phosphorous from wastewater as vivianite in a strategically operated four-chamber flow electrode capacitive deionization. Desalination, 544, 116089. https://doi.org/10.1016/j.desal.2022.116089

34. Hong, S. P., Yoon, H., Lee, J., Kim, C., Kim, S., Lee, J., Lee, C., & Yoon, J. (2020). Selective phosphate removal using layered double hydroxide/reduced graphene oxide (LDH/rGO) composite electrode in capacitive deionization. Journal of Colloid and Interface Science, 564, 1–7. https://doi.org/10.1016/j.jcis.2019.12.068

35. Huang, G.-H., Chen, T.-C., Hsu, S.-F., Huang, Y.-H., & Chuang, S.-H. (2013). Capacitive deionization (CDI) for removal of phosphate from aqueous solution. Desalination and Water Treatment, 52(4–6), 759–765. https://doi.org/10.1080/19443994.2013.826331

36. Huang, X., He, D., Tang, W., Kovalsky, P., & Waite, T. D. (2017). Investigation of pH-dependent phosphate removal from wastewaters by membrane capacitive deionization (MCDI). Environ. Sci.: Water Res. Technol., 3(5), 875–882. https://doi.org/10.1039/C7EW00138J

37. Huang, Z., Lu, L., Cai, Z., & Ren, Z. J. (2016). Individual and competitive removal of heavy metals using capacitive deionization. Journal of Hazardous Materials, 302, 323–331. https://doi.org/10.1016/j.jhazmat.2015.09.064

38. Jande, Y. A. C., & Kim, W. S. (2013). Desalination using capacitive deionization at constant current. Desalination, 329, 29–34. https://doi.org/10.1016/j.desal.2013.08.023

39. Jeon, S., Park, H., Yeo, J., Yang, S., Cho, C. H., Han, M. H., & Kim, D. K. (2013). Desalination via a new membrane capacitive deionization process utilizing flow-electrodes. Energy & Environmental Science, 6(5), 1471–1475. https://doi.org/10.1039/C3EE24443A

40. Jiang, J., Kim, D. I., Dorji, P., Phuntsho, S., Hong, S., & Shon, H. K. (2019). Phosphorus removal mechanisms from domestic wastewater by membrane capacitive deionization and system optimization for enhanced phosphate removal. Process Safety and Environmental Protection, 126, 44–52. https://doi.org/10.1016/j.psep.2019.04.005

41. Johir, M. A. H., George, J., Vigneswaran, S., Kandasamy, J., & Grasmick, A. (2011). Removal and recovery of nutrients by ion exchange from high rate membrane bio-reactor (MBR) effluent. Desalination, 275(1–3), 197–202. https://doi.org/10.1016/j.desal.2011.02.054

42. Koh, K. Y., Zhang, S., & Chen, J. P. (2020). Improvement of Ultrafiltration for Treatment of Phosphorus-Containing Water by a Lanthanum-Modified Aminated Polyacrylonitrile Membrane. ACS Omega, 5(13), 7170–7181. https://doi.org/10.1021/acsomega.9b03573

43. Le, D., Pham Quoc, N., & Le, K. (2016). Capacitive deionization (CDI) for desalisation using carbon aerogel electrodes. Science and Technology Development Journal, 19, 155–164. https://doi.org/10.32508/stdj.v19i3.570

44. Lee, D.-J., & Park, J.-S. (2014). Mesoporous Carbon Electrodes for Capacitive Deionization. Journal of the Korean Electrochemical Society, 17. https://doi.org/10.5229/JKES.2013.17.1.57

45. Lee, J.-B., Park, K.-K., Eum, H.-M., & Lee, C.-W. (2006). Desalination of a thermal power plant wastewater by membrane capacitive deionization. Desalination, 196(1), 125–134. https://doi.org/10.1016/j.desal.2006.01.011

46. Lee, J.-Y., Seo, S.-J., Yun, S.-H., & Moon, S.-H. (2011). Preparation of ion exchanger layered electrodes for advanced membrane capacitive deionization (MCDI). Water Research, 45(17), 5375–5380. https://doi.org/10.1016/j.watres.2011.06.028

47. Liang, P., Yuan, L., Yang, X., Zhou, S., & Huang, X. (2013). Coupling ion-exchangers with inexpensive activated carbon fiber electrodes to enhance the performance of capacitive deionization cells for domestic wastewater desalination. Water Research, 47(7), 2523–2530. https://doi.org/10.1016/j.watres.2013.02.037

48. Machnicka, A., Grűbel, K., & Suschka, J. (2008). Enhanced Biological Phosphorus Removal and Recovery. Water Environment Research, 80(7), 617–623. https://doi.org/10.2175/106143008X268461

49. Mayer, B. K., Baker, L. A., Boyer, T. H., Drechsel, P., Gifford, M., Hanjra, M. A., Parameswaran, P., Stoltzfus, J., Westerhoff, P., & Rittmann, B. E. (2016). Total Value of Phosphorus Recovery. Environmental Science & Technology, 50(13), 6606–6620. https://doi.org/10.1021/acs.est.6b01239

50. Mehta, C. M., Khunjar, W. O., Nguyen, V., Tait, S., & Batstone, D. J. (2015). Technologies to Recover Nutrients from Waste Streams: A Critical Review.

Critical Reviews in Environmental Science and Technology, 45(4), 385–427. https://doi.org/10.1080/10643389.2013.866621

51. Melcer, H. (2003). Methods for Wastewater Characterization in Activated Sludge Modelling. IWA Publishing.

52. Miao, L., Deng, W., Chen, X., Gao, M., Chen, W., & Ao, T. (2021). Selective adsorption of phosphate by carboxyl-modified activated carbon electrodes for capacitive deionization. Water Science and Technology, 84(7), 1757–1773. https://doi.org/10.2166/wst.2021.358

53. Miladinovic, N., & Weatherley, L. R. (2008). Intensification of ammonia removal in a combined ion-exchange and nitrification column. Chemical Engineering Journal, 135(1–2), 15–24. https://doi.org/10.1016/j.cej.2007.02.030

54. Morgens, H. (2008). 3-Wastewater Characterization Biological Wastewater Treatment: Principles. Modelling and Design IWA Publishing.

55. Nakayama, Y., Imamura, E., & Noda, S. (2021). Capacitive deionization characteristics of compressed granular activated carbon. Separation and Purification Technology, 277, 119454. https://doi.org/10.1016/j.seppur.2021.119454

56. Oehmen, A., Lemos, P. C., Carvalho, G., Yuan, Z., Keller, J., Blackall, L. L., & Reis, M. A. M. (2007). Advances in enhanced biological phosphorus removal: From micro to macro scale. Water Research, 41(11), 2271–2300. https://doi.org/10.1016/j.watres.2007.02.030

57. Ong, Y. H., Chua, A. S. M., Huang, Y. T., Ngoh, G. C., & You, S. J. (2016). The microbial community in a high-temperature enhanced biological phosphorus

removal (EBPR) process. Sustainable Environment Research, 26(1), 14–19. https://doi.org/10.1016/j.serj.2016.04.001

58. Oren, Y. (1978). Electrochemical Parametric Pumping. Journal of The Electrochemical Society, 125(6), 869. https://doi.org/10.1149/1.2131570

59. Oren, Y., & Soffer, A. (1983). Water desalting by means of electrochemical parametric pumping. Journal of Applied Electrochemistry, 13(4), 473–487. https://doi.org/10.1007/BF00617522

60. Porada, S., Zhao, R., van der Wal, A., Presser, V., & Biesheuvel, P. M. (2013). Review on the science and technology of water desalination by capacitive deionization. Progress in Materials Science, 58(8), 1388–1442. https://doi.org/10.1016/j.pmatsci.2013.03.005

61. Puchongkawarin, C., Gomez-Mont, C., Stuckey, D. C., & Chachuat, B. (2015). Optimization-based methodology for the development of wastewater facilities for energy and nutrient recovery. Chemosphere, 140, 150–158. https://doi.org/10.1016/j.chemosphere.2014.08.061

62. Raj, S. E., Banu, J. R., Kaliappan, S., Yeom, I.-T., & Adish Kumar, S. (2013). Effects of side-stream, low temperature phosphorus recovery on the performance of anaerobic/anoxic/oxic systems integrated with sludge pretreatment. Bioresource Technology, 140, 376–384. https://doi.org/10.1016/j.biortech.2013.04.061

63. Raj, S., Kaliappan, S., Kumar, S., & Banu, R. (2012). Combinative treatment (thermal-anaerobic) of EBPR sludge for the enhanced release and recovery of phosphorous. Int. J. of Environmental Engineering, 4, 92–104. https://doi.org/10.1504/IJEE.2012.048097

64. Rajesh Banu, J., Uan, D. K., & Yeom, I.-T. (2009). Nutrient removal in an A2O-MBR reactor with sludge reduction. Selected Papers from the International Conference on Technologies and Strategic Management of Sustainable Biosystems, 100(16), 3820–3824. https://doi.org/10.1016/j.biortech.2008.12.054

65. Remillard, E. M., Shocron, A. N., Rahill, J., Suss, M. E., & Vecitis, C. D. (2018). A direct comparison of flow-by and flow-through capacitive deionization. Desalination, 444, 169–177. https://doi.org/10.1016/j.desal.2018.01.018

66. Rittmann, B. E., Mayer, B., Westerhoff, P., & Edwards, M. (2011). Capturing the lost phosphorus. The Phosphorus Cycle, 84(6), 846–853. https://doi.org/10.1016/j.chemosphere.2011.02.001

67. Salari, K., Zarafshan, P., Khashehchi, M., Chegini, G., Etezadi, H., Karami, H., Szulżyk-Cieplak, J., & Łagód, G. (2022). Knowledge and Technology Used in Capacitive Deionization of Water. Membranes, 12(5), 459. https://doi.org/10.3390/membranes12050459

68. Santiago, J. G., & Qu, Y. (n.d.). Flow-through CDI cells: A new architecture. Retrieved May 27, 2020, from https://microfluidics.stanford.edu/Projects/Current/ftCDI.html

69. Schönborn, C., Bauer, H., & Röske, I. (2001a). Stability of enhanced biological phosphorus removal and composition of polyphosphate granules. Water Research, 35, 3190–3196. https://doi.org/10.1016/S0043-1354(01)00025-2

70. Schönborn, C., Bauer, H.-D., & Röske, I. (2001b). Stability of enhanced biological phosphorus removal and composition of polyphosphate granules. Water Research, 35(13), 3190–3196. https://doi.org/10.1016/S0043-1354(01)00025-2

71. Stevens, D. P., McLaughlin, M. J., & Smart, M. K. (2003). Effects of long-term irrigation with reclaimed water on soils of the Northern Adelaide Plains, South Australia. Soil Research, 41(5), 933–948.

72. Suss, M. E., Porada, S., Sun, X., Biesheuvel, P. M., Yoon, J., & Presser, V. (2015). Water desalination via capacitive deionization: What is it and what can we expect from it? Energy & Environmental Science, 8(8), 2296–2319.

73. Tang, W., Liang, J., He, D., Gong, J., Tang, L., Liu, Z., Wang, D., & Zeng, G. (2019). Various cell architectures of capacitive deionization: Recent advances and future trends. Water Research, 150, 225–251. https://doi.org/10.1016/j.watres.2018.11.064

74. Tonini, D., Saveyn, H. G. M., & Huygens, D. (2019). Environmental and health co-benefits for advanced phosphorus recovery. Nature Sustainability, 2(11), 1051–1061. https://doi.org/10.1038/s41893-019-0416-x

75. US EPA, O. (2013, March 12). Sources and Solutions [Collections and Lists]. US EPA. https://www.epa.gov/nutrientpollution/sources-and-solutions

76. Venkatesan, A. K., Hamdan, A.-H. M., Chavez, V. M., Brown, J. D., & Halden, R. U. (2016). Mass Balance Model for Sustainable Phosphorus Recovery in a US Wastewater Treatment Plant. Journal of Environmental Quality, 45(1), 84–89. https://doi.org/10.2134/jeq2014.11.0504

77. Vera, I., Araya, F., Andrés, E., Sáez, K., & Vidal, G. (2014). Enhanced phosphorus removal from sewage in mesocosm-scale constructed wetland using zeolite as medium and artificial aeration. Environmental Technology, 35(13), 1639–1649. https://doi.org/10.1080/09593330.2013.877984

78. Wimalasiri, Y., Mossad, M., & Zou, L. (2015). Thermodynamics and kinetics of adsorption of ammonium ions by graphene laminate electrodes in capacitive deionization. Desalination, 357, 178–188. https://doi.org/10.1016/j.desal.2014.11.015

79. Wong, M.-T., Mino, T., Seviour, R. J., Onuki, M., & Liu, W.-T. (2005). In situ identification and characterization of the microbial community structure of full-scale enhanced biological phosphorous removal plants in Japan. Water Research, 39(13), 2901–2914. https://doi.org/10.1016/j.watres.2005.05.015

80. Xu, L., Yu, C., Tian, S., Mao, Y., Zong, Y., Zhang, X., Zhang, B., Zhang, C., & Wu, D. (2021). Selective Recovery of Phosphorus from Synthetic Urine Using Flow-Electrode Capacitive Deionization (FCDI)-Based Technology. ACS ES&T Water, 1(1), 175–184. https://doi.org/10.1021/acsestwater.0c00065

81. Xuan, T. B., Chart, C., Takahiro, F., & Sunita, V. (2019). Water and Wastewater Treatment Technologies. Springer.

82. Yin, Q., Liu, M., & Ren, H. (2019). Biochar produced from the co-pyrolysis of sewage sludge and walnut shell for ammonium and phosphate adsorption from water. Journal of Environmental Management, 249, 109410. https://doi.org/10.1016/j.jenvman.2019.109410

83. Ying, T.-Y., Yang, K.-L., Yiacoumi, S., & Tsouris, C. (2002). Electrosorption of Ions from Aqueous Solutions by Nanostructured Carbon Aerogel. Journal of Colloid and Interface Science, 250(1), 18–27. https://doi.org/10.1006/jcis.2002.8314

84. Zhang, C., Cheng, X., Wang, M., Ma, J., Collins, R., Kinsela, A., Zhang, Y., & Waite, T. D. (2021). Phosphate recovery as vivianite using a flow-electrode capacitive desalination (FCDI) and fluidized bed crystallization (FBC) coupled system. Water Research, 194, 116939. https://doi.org/10.1016/j.watres.2021.116939

85. Zhang, C., Wang, M., Xiao, W., Ma, J., Sun, J., Mo, H., & Waite, T. D. (2021). Phosphate selective recovery by magnetic iron oxide impregnated carbon flow-electrode capacitive deionization (FCDI). Water Research, 189, 116653. https://doi.org/10.1016/j.watres.2020.116653

86. Zhang, H., Wang, Q., Zhang, J., Chen, G., Wang, Z., & Wu, Z. (2022). Development of novel ZnZr-COOH/CNT composite electrode for selectively removing phosphate by capacitive deionization. Chemical Engineering Journal, 439, 135527. https://doi.org/10.1016/j.cej.2022.135527

87. Zhang, Y., Desmidt, E., Van Looveren, A., Pinoy, L., Meesschaert, B., & Van der Bruggen, B. (2013). Phosphate Separation and Recovery from Wastewater by Novel Electrodialysis. Environmental Science & Technology, 47(11), 5888–5895. https://doi.org/10.1021/es4004476

88. Zhao, R., Biesheuvel, P. M., & van der Wal, A. (2012). Energy consumption and constant current operation in membrane capacitive deionization. Energy & Environmental Science, 5(11), 9520–9527. https://doi.org/10.1039/C2EE21737F

89. Zou, H., & Wang, Y. (2016). Phosphorus removal and recovery from domestic wastewater in a novel process of enhanced biological phosphorus removal coupled

with crystallization. Bioresource Technology, 211, 87–92. https://doi.org/10.1016/j.biortech.2016.03.073

90. Abou-Shanab, R. A. I., Ji, M.-K., Kim, H.-C., Paeng, K.-J., & Jeon, B.-H. (2013). Microalgal species growing on piggery wastewater as a valuable candidate for nutrient removal and biodiesel production. Journal of Environmental Management, 115, 257–264.

91. Amini, H., Wang, L., & Shahbazi, A. (2016). Effects of harvesting cell density, medium depth and environmental factors on biomass and lipid productivities of Chlorella vulgaris grown in swine wastewater. Chemical Engineering Science, 152, 403–412.

92. Barbusinski, K., Kalemba, K., Kasperczyk, D., Urbaniec, K., & Kozik, V. (2017). Biological methods for odor treatment–A review. *Journal of Cleaner Production*, *152*, 223-241.

93. Bilotta, P., Steinmetz, R. L. R., Kunz, A., & Mores, R. (2017). Swine effluent post-treatment by alkaline control and UV radiation combined for water reuse. Journal of Cleaner Production, 140, 1247–1254.

94. Bohutskyi, P., Kligerman, D. C., Byers, N., Nasr, L. K., Cua, C., Chow, S., Su, C., Tang, Y., Betenbaugh, M.J. & Bouwer, E. J. (2016). Effects of inoculum size, light intensity, and dose of anaerobic digestion centrate on growth and productivity of Chlorella and Scenedesmus microalgae and their poly-culture in primary and secondary wastewater. Algal Research, 19, 278-290.

95. Bordoloi, N., Narzari, R., Sut, D., Saikia, R., Chutia, R. S., & Kataki, R. (2016). Characterization of bio-oil and its sub-fractions from pyrolysis of Scenedesmus dimorphus. Renewable Energy, 98, 245-253.

96. Brennan, L., & Owende, P. (2010). Biofuels from microalgae—a review of technologies for production, processing, and extractions of biofuels and co-products. Renewable and Sustainable Energy Reviews, 14(2), 557-577.

97. Buczek, S. B., Cope, W. G., McLaughlin, R. A., & Kwak, T. J. (2017). Acute toxicity of polyacrylamide flocculants to early life stages of freshwater mussels. Environmental Toxicology and Chemistry, 36(10), 2715-2721.

98. Cai, T., Park, S. Y., & Li, Y. (2013). Nutrient recovery from wastewater streams by microalgae: Status and prospects. Renewable and Sustainable Energy Reviews, 19, 360–369.

99. Chelme-Ayala, P., El-Din, M.G., Smith, R., Code, K.R., Leonard, J. 2011. Advanced treatment of liquid swine manure using physico-chemical treatment. Journal of Hazardous Materials, 186(2), 1632-1638.

100. Chen, C.-Y., Kuo, E.-W., Nagarajan, D., Ho, S.-H., Dong, C.-D., Lee, D.-J., & Chang, J.-S. (2020). Cultivating Chlorella sorokiniana AK-1 with swine wastewater for simultaneous wastewater treatment and algal biomass production. Bioresource Technology, 302, 122814. https://doi.org/10.1016/j.biortech.2020.122814

101. Chen, L., & Hoff, S. J. (2009). Mitigating odors from agricultural facilities: a review of literature concerning biofilters. *Applied Engineering in Agriculture*, *25*(5), 751-766.

102. Chen, L., Hoff, S. J., Koziel, J. A., Cai, L., Zelle, B., & Sun, G. (2008). Performance evaluation of a wood-chip based biofilter using solid-phase microextraction and gas chromatography–mass spectroscopy–olfactometry. *Bioresource Technology*, *99*(16), 7767-7780.

103. Cheng, D. L., Ngo, H. H., Guo, W. S., Chang, S. W., Nguyen, D. D., & Kumar, S. M. (2019). Microalgae biomass from swine wastewater and its conversion to bioenergy. Bioresource Technology, 275, 109–122.

104. Cheng, J., & Liu, B. (2001). Nitrification/denitrification in intermittent aeration process for swine wastewater treatment. Journal of Environmental Engineering, 127(8), 705-711.

105. Cheunbarn, S., & Peerapornpisal, Y. (2010). Cultivation of Spirulina platensis using Anaerobically Swine Wastewater Treatment Effluent. International Journal of Agriculture and Biology, 12, 1560–853012.

106. Choi, J. H., Kim, Y. H., Joo, D. J., Choi, S. J., Ha, T. W., Lee, D. H., Park, I. H., & Jeong, Y. S. (2003). Removal of ammonia by biofilters: A study with flow-modified system and kinetics. *Journal of the Air & Waste Management Association*, *53*(1), 92-101.

107. Cicci, A., Stoller, M., & Bravi, M. (2013). Microalgal biomass production by using ultra-and nanofiltration membrane fractions of olive mill wastewater. Water Research, 47(13), 4710-4718.

108. Clarens, A. F., Resurreccion, E. P., White, M. A., & Colosi, L. M. (2010). Environmental Life Cycle Comparison of Algae to Other Bioenergy Feedstocks.

Environmental Science & Technology, 44(5), 1813–1819. https://doi.org/10.1021/es902838n

109. Cooper, C. D., & Alley, F. C. (2010). *Air Pollution Control: A Design Approach (Fourth Edition)*. Waveland Press, Long Grove, IL.

110. Cristóvão, M. B. (2016). Microalgae treatment of piggery wastewater. Instituto Superior Técnico. Accessed https://fenix.tecnico.ulisboa.pt/downloadFile/1689244997257241/Resumo%20ala rgado%20microalgae%20treatment%20of%20piggery%20wastewater%20Beatriz %20C.pdf

111. Deng, X., Gao, K., Addy, M., Chen, P., Li, D., Zhang, R., Lu, Q., Ma, Y., Cheng, Y., Liu, Y., & Ruan, R. (2018). Growing Chlorella vulgaris on mixed wastewaters for biodiesel feedstock production and nutrient removal. Journal of Chemical Technology and Biotechnology, 93(9).

112. Devinny, J. S., Deshusses, M. A., & Webster, T. S. (2017). *Biofiltration for air pollution control*. CRC press, Washington DC.

113. Ella, V. B., Keller, J., Reyes, M. R., & Yoder, R. (2013). A low-cost pressure regulator for improving the water distribution uniformity of a microtube-type drip irrigation system. *Applied Engineering in Agriculture*, *29*(3), 343-349.

114. Fábregas, J., Domínguez, A., Regueiro, M., Maseda, A., & Otero, A. (2000). Optimization of culture medium for the continuous cultivation of the microalga Haematococcus pluvialis. Applied Microbiology and Biotechnology, 53(5), 530– 535. https://doi.org/10.1007/s002530051652

115. Feng, P.-Z., Zhu, L.-D., Qin, X.-X., & Li, Z.-H. (2016). Water Footprint of Biodiesel Production from Microalgae Cultivated in Photobioreactors. Journal of Environmental Engineering, 142(12), 04016067. https://doi.org/10.1061/(ASCE)EE.1943-7870.0001150

116. Ferreira, V. S., Pinto, R. F., & Sant'Anna, C. (2016). Low light intensity and nitrogen starvation modulate the chlorophyll content of Scenedesmus dimorphus. Journal of Applied Microbiology, 120(3), 661-670.

117. Foladori, P., Petrini, S., & Andreottola, G. (2019). How suspended solids concentration affects nitrification rate in microalgal-bacterial photobioreactors without external aeration. Heliyon, 6(1), e03088.

118. Fongaro, G., Viancelli, A., Magri, M. E., Elmahdy, E. M., Biesus, L. L., Kich, J. D., Kunz, A., & Barardi, C. R. M. (2014). Utility of specific biomarkers to assess safety of swine manure for biofertilizing purposes. Science of the Total Environment, 479–480, 277–283.

119. Franchino, M., Tigini, V., Varese, G. C., Mussat Sartor, R., & Bona, F. (2016). Microalgae treatment removes nutrients and reduces ecotoxicity of diluted piggery digestate. Science of the Total Environment, 569–570, 40–45.

120. Gabriel, M., Rosa, G. M., Wastowski, A. D., Costa, J. A., & Volpatto, F. (2019). Use of organic coagulant/flocculant for treatment of effluents generated in intensive rearing of swine. Environmental Quality Management, 29(2), 149–154.

121. Gabriel, M., Rosa, G. M., Wastowski, A. D., Costa, J. A., & Volpatto, F. (2019). Use of organic coagulant/flocculant for treatment of effluents generated in intensive rearing of swine. Environmental Quality Management, 29(2), 149–154.

122. Garlinski, E. M., & Mann, D. D. (2004). Airflow Characteristics through a Horizontal-Airflow Biofilter. In *2004 ASAE Annual Meeting* (Paper No. 044055). American Society of Agricultural and Biological Engineers, St. Joseph, MI.

123. Gentili, F. G. (2014). Microalgal biomass and lipid production in mixed municipal, dairy, pulp and paper wastewater together with added flue gases. Bioresource Technology, 169, 27-32.

124. Goldstein, N. (1999). Longer life for biofilters. *BioCycle*, *40*(7), 62.

125. Gomes, J., Domingues, E., Fernandes, E., Castro, L., Martins, R. C., & Quinta-Ferreira, R. M. (2021). Coagulation and biofiltration by Corbicula fluminea for COD and toxicity reduction of swine wastewater. Journal of Water Process Engineering, 42, 102145.

126. Gomes, J., Domingues, E., Fernandes, E., Castro, L., Martins, R. C., & Quinta-Ferreira, R. M. (2021). Coagulation and biofiltration by Corbicula fluminea for COD and toxicity reduction of swine wastewater. Journal of Water Process Engineering, 42, 102145.

127. González, L. E., Cañizares, R. O., & Baena, S. (1997). Efficiency of ammonia and phosphorus removal from a Colombian agroindustrial wastewater by the microalgae Chlorella vulgaris and Scenedesmus dimorphus. Bioresource Technology, 60(3), 259–262.

128. González-Fernández, C., Nieto-Diez, P. P., León-Cofreces, C., & García-Encina, P. A. (2008). Solids and nutrients removals from the liquid fraction of swine slurry through screening and flocculation treatment and influence of these processes on anaerobic biodegradability. Bioresource Technology, 99(14), 6233–6239.

129. González-Fernández, C., Nieto-Diez, P. P., León-Cofreces, C., & García-Encina, P. A. (2008). Solids and nutrients removals from the liquid fraction of swine slurry through screening and flocculation treatment and influence of these processes on anaerobic biodegradability. Biores1ource Technology, 99(14), 6233–6239.

130. Haleem, N., Osabutey, A., Albert, K., Zhang, C., Min, K., Anderson, G., Yang, X. (2022). Flocculation of livestock wastewater using cationic starch prepared from potato peels. Under review.

131. Hammer, Ø., Harper, D. A., & Ryan, P. D. (2001). PAST: Paleontological statistics software package for education and data analysis. *Palaeontologia Electronica*, *4*(1), 9.

132. Hammer, Ø., Harper, D. A., & Ryan, P. D. (2001). PAST: Paleontological statistics software package for education and data analysis. Palaeontologia electronica, 4(1), 1-9.

133. Hasan, R., Zhang, B., Wang, L., & Shahbazi, G. (2014). Bioremediation of Swine Wastewater and Biofuel Potential by using Chlorella vulgaris, Chlamydomonas reinhardtii, and Chlamydomonas debaryana. Journal of Petroleum & Environmental Biotechnology, 5, 175-180.

134. Hennecke, D., Bauer, A., Herrchen, M., Wischerhoff, E., & Gores, F. (2018). Cationic polyacrylamide copolymers (PAMs): Environmental half life determination in sludge-treated soil. Environmental Sciences Europe, 30(1), 1-13.

135. Heredia-Arroyo, T., Wei, W., Ruan, R., & Hu, B. (2011). Mixotrophic cultivation of Chlorella vulgaris and its potential application for the oil accumulation from non-sugar materials. Biomass and Bioenergy, 35(5), 2245–2253.

136. Hu, D., Zhang, J., Chu, R., Yin, Z., Hu, J., Nugroho, Y. K., ... & Zhu, L. (2021). Microalgae Chlorella vulgaris and Scenedesmus dimorphus co-cultivation with landfill leachate for pollutant removal and lipid production. Bioresource Technology, 342, 126003.

137. Hu, W. (2014). Dry Weight and Cell Density of Individual Algal and Cyanobacterial Cells for Algae Research and Development. MS Thesis. University of Missouri-Columbia, Columbia, MO, USA.

138. Huang, H., & Miller, G. Y. (2006). Citizen complaints, regulatory violations, and their implications for swine operations in Illinois. *Review of Agricultural Economics*, *28*(1), 89-110.

139. Huang, Z., Wang, T., Shen, M., Huang, Z., Chong, Y., & Cui, L. (2019). Coagulation treatment of swine wastewater by the method of in-situ forming layered double hydroxides and sludge recycling for preparation of biochar composite catalyst. Chemical Engineering Journal, 369.

140. Iranpour, R., Cox, H. H., Deshusses, M. A., & Schroeder, E. D. (2005). Literature review of air pollution control biofilters and biotrickling filters for odor and volatile organic compound removal. *Environmental Progress*, *24*(3), 254-267.

141. Ji, M.-K., Kim, H.-C., Sapireddy, V. R., Yun, H.-S., Abou-Shanab, R. A. I., Choi, J., Lee, W., Timmes, T. C., Inamuddin, & Jeon, B.-H. (2013). Simultaneous nutrient removal and lipid production from pretreated piggery wastewater by Chlorella vulgaris YSW-04. Applied Microbiology and Biotechnology, 97(6), 2701–2710.

142. Jiang, Y., Zhang, W., Wang, J., Chen, Y., Shen, S., & Liu, T. (2013). Utilization of simulated flue gas for cultivation of Scenedesmus dimorphus. Bioresource Technology, 128, 359–364. https://doi.org/10.1016/j.biortech.2012.10.119

143. Kang, J., & Wen, Z. (2015). Use of microalgae for mitigating ammonia and CO2 emissions from animal production operations—Evaluation of gas removal efficiency and algal biomass composition. Algal Research, 11, 204-210.

144. Kang, J., Wang, T., Xin, H., & Wen, Z. (2014). A laboratory study of microalgae-based ammonia gas mitigation with potential application for improving air quality in animal production operations. Journal of the Air & Waste Management Association, 64(3), 330–339. https://doi.org/10.1080/10962247.2013.859185

145. Latsos, C., van Houcke, J., & Timmermans, K. R. (2020). The Effect of Nitrogen Starvation on Biomass Yield and Biochemical Constituents of Rhodomonas sp. Frontiers in Marine Science, 7. https://doi.org/10.3389/fmars.2020.563333

146. Lee, S., Lamchaturapatr, J., Polprasert, C., & Ahn, K. (2004). Application of chemical precipitation for piggery wastewater treatment. Water Science & Technology, 49, 5–6.

147. Lee, W.-C., & Chang, C.-C. (2022). Effectively Recycling Swine Wastewater by Coagulation–Flocculation of Nonionic Polyacrylamide. Sustainability, 14, 1742.

148. Lee, W.-C., & Chang, C.-C. (2022). Effectively Recycling Swine Wastewater by Coagulation–Flocculation of Nonionic Polyacrylamide. Sustainability, 14, 1742.

149. Lefers, R. M. (2006). A design of analysis for a vertical bed biofilter and biofilter moisture control system. MS thesis, South Dakota State University, Brookings, SD.

150. Li, X., Yang, C., Zeng, G., Wu, S., Lin, Y., Zhou, Q., Lou, W., Du, C., Nie, L., & Zhong, Y. (2020). Nutrient removal from swine wastewater with growing microalgae at various zinc concentrations. Algal Research, 46, 101804.

151. Lim, J. S., Yang, S. H., Kim, B. S., & Lee, E. Y. (2018). Comparison of microbial communities in swine manure at various temperatures and storage times. Asian-Australasian Journal of Animal Sciences, 31(8), 1373.

152. Liu, J., Ge, Y., Cheng, H., Wu, L., & Tian, G. (2013). Aerated swine lagoon wastewater: a promising alternative medium for Botryococcus braunii cultivation in open system. Bioresource technology, 139, 190-194.

153. Lutzu, G. A., Zhang, W., & Liu, T. (2016). Feasibility of using brewery wastewater for biodiesel production and nutrient removal by Scenedesmus dimorphus. Environmental Technology, 37(12), 1568-1581.

154. Lv, J., Liu, Y., Feng, J., Liu, Q., Nan, F., & Xie, S. (2018). Nutrients removal from undiluted cattle farm wastewater by the two-stage process of microalgae-based wastewater treatment. Bioresource Technology, 264, 311–318.

155. Mackie, R. I., Stroot, P. G., & Varel, V. H. (1998). Biochemical identification and biological origin of key odor components in livestock waste. *Journal of Animal Science*, *76*(5), 1331-1342.

156. Mann, D. D. & Garlinski, E. M. (2002). Design of a horizontal airflow biofilter. In *AIC 2002 Meeting* (Paper No. 034051). Canadian Society of Agricultural Engineers, Mansonville, Quebec, Canada.

157. Martins, A. A., Marques, F., Cameira, M., Santos, E., Badenes, S., Costa, L., Vieira, V. V., Caetano, N. S., & Mata, T. M. (2018). Water footprint of microalgae

cultivation in photobioreactor. 5th International Conference on Energy and Environment Research, ICEER 2018, 23-27 July 2018, Prague, Czech Republic, 153, 426–431. https://doi.org/10.1016/j.egypro.2018.10.031

158. Mascarelli, A. L. (2009). Algae: Fuel of the future? Environmental Science & Technology, 43(19), 7160–7161. https://doi.org/10.1021/es902509d

159. Menegazzo, M. L., Ribeiro, D. M., De Oliveira, N. N., Marques, O. G. B., & Fonseca, G. G. (2022). Evaluation of Chlorella sorokiniana Biomass Recovery by Using Different Chemical-based Flocculants. Journal of Applied Biotechnology Reports, 9(1), 477-483.

160. Moglia, M., Cook, S., & Tapsuwan, S. (2018). Promoting water conservation: where to from here?. Water, 10(11), 1510.Murphy, C. F., & Allen, D. T. (2011a).

161. Energy-Water Nexus for Mass Cultivation of Algae. Environmental Science & Technology, 45(13), 5861–5868. https://doi.org/10.1021/es200109z

162. Nagarajan, D., Kusmayadi, A., Yen, H.-W., Dong, C.-D., Lee, D.-J., & Chang, J.-S. (2019). Current advances in biological swine wastewater treatment using microalgae-based processes. Bioresource Technology, 289, 121718.

163. Nam, K., Lee, H., Heo, S. W., Chang, Y. K., & Han, J. I. (2017). Cultivation of Chlorella vulgaris with swine wastewater and potential for algal biodiesel production. Journal of Applied Phycology, 29(3), 1171-1178.

164. Narala, R. R., Garg, S., Sharma, K. K., Thomas-Hall, S. R., Deme, M., Li, Y., & Schenk, P. M. (2016a). Comparison of Microalgae Cultivation in Photobioreactor, Open Raceway Pond, and a Two-Stage Hybrid System. Frontiers in Energy Research, 4. https://doi.org/10.3389/fenrg.2016.00029

165. Narala, R. R., Garg, S., Sharma, K. K., Thomas-Hall, S. R., Deme, M., Li, Y., & Schenk, P. M. (2016). Comparison of microalgae cultivation in photobioreactor, open raceway pond, and a two-stage hybrid system. Frontiers in Energy Research, 4, 29.

166. Ni, J. Q., Robarge, W. P., Xiao, C., & Heber, A. J. (2012). Volatile organic compounds at swine facilities: A critical review. *Chemosphere*, *89*(7), 769-788

167. Nicolai, R. E., & Lefers, R. M. (2006). Biofilters used to reduce emissions from livestock housing: A literature review. In *Workshop on Agricultural Air Quality* (pp. 952-960), North Carolina State University, Raleigh, NC.

168. Nicolai, R. E., & Thaler, R. (2007). Vertical biofilter construction and performance. In *International Symposium on Air Quality and Waste Management for Agriculture,* (pp. 35-41). American Society of Agricultural and Biological Engineers, St. Joseph, MI.

169. Nicolai, R. E., Lefers, R., & Pohl, S. H. (2005). Configuration of a vertical biofilter. In *Livestock Environment VII* (pp. 358-363). American Society of Agricultural and Biological Engineers, St. Joseph, MI.

170. Noren, O. (1986). Design and use of biofilters for livestock buildings. In V.C. Nielsen, J. H. Voorburg & P. L'Hermite (Eds.) *Odour Prevention and Control of Organic Sludge and Livestock Farming* (pp. 234-237), Taylor & Francis, Abingon, UK.

171. Padovan, A. (1992). Isolation and culture of five species of freshwater algae from the alligator rivers region, northern territory. Australian Government Publishing Service, Canberra, Australia. Access at https://www.awe.gov.au/science-

research/supervising-scientist/publications/technical-memoranda/isolation-and-culture-five-species-freshwater-algae-alligator-rivers-region

172. Padovan, A. (1992). Isolation and culture of five species of freshwater algae from the alligator rivers region, northern territory. Australian Government Publishing Service, Canberra, Australia. Access at https://www.awe.gov.au/science-research/supervising-scientist/publications/technical-memoranda/isolation-and-culture-five-species-freshwater-algae-alligator-rivers-region

173. Park, J., Jin, H.-F., Lim, B.-R., Park, K.-Y., & Lee, K. (2010). Ammonia removal from anaerobic digestion effluent of livestock waste using green alga Scenedesmus sp. Bioresource Technology, 101(22), 8649–8657. Park, T., Ampunan, V., Lee, S., & Chung, E. (2016). Chemical behavior of different species of phosphorus in coagulation. Chemosphere, 144, 2264–2269.

174. Park, T., Ampunan, V., Lee, S., & Chung, E. (2016). Chemical behavior of different species of phosphorus in coagulation. Chemosphere, 144, 2264–2269.

175. Perdana, B. A., Dharma, A., Zakaria, I. J., & Syafrizayanti, S. (2021). Freshwater pond microalgae for biofuel: Strain isolation, identification, cultivation and fatty acid content. Biodiversitas Journal of Biological Diversity, 22(2), 505-511. https://doi.org/10.13057/biodiv/d220201

176. Quiroz, D., Greene, J. M., McGowen, J., & Quinn, J. C. (2021). Geographical assessment of open pond algal productivity and evaporation losses across the United States. Algal Research, 60, 102483. https://doi.org/10.1016/j.algal.2021.102483

177. Ra, C. S., Lo, K. V., & Mavinic, D. S. (1997). Swine Wastewater Treatment by a Batch-Mode 4-Stage Process: Loading Rate Control Using Orp. Environmental Technology, 18(6), 615–621.

178. Ra, C. S., Lo, K. V., & Mavinic, D. S. (1997). Swine Wastewater Treatment by a Batch-Mode 4-Stage Process: Loading Rate Control Using Orp. Environmental Technology, 18(6), 615–621.

179. Rugnini, L., Rossi, C., Antonaroli, S., Rakaj, A., & Bruno, L. (2020). The Influence of Light and Nutrient Starvation on Morphology, Biomass and Lipid Content in Seven Strains of Green Microalgae as a Source of Biodiesel. Microorganisms, 8(8), 1254. PubMed. https://doi.org/10.3390/microorganisms8081254

180. Sander, K., & Murthy, G. S. (2010). Life cycle analysis of algae biodiesel. The International Journal of Life Cycle Assessment, 15(7), 704–714. https://doi.org/10.1007/s11367-010-0194-1

181. Teh, C. Y., Budiman, P. M., Shak, K. P. Y., & Wu, T. Y. (2016). Recent advancement of coagulation–flocculation and its application in wastewater treatment. Industrial & Engineering Chemistry Research, 55(16), 4363-4389.

182. Teh, C. Y., Budiman, P. M., Shak, K. P. Y., & Wu, T. Y. (2016). Recent advancement of coagulation–flocculation and its application in wastewater treatment. Industrial & Engineering Chemistry Research, 55(16), 4363-4389.

183. Uguz, S., Anderson, G., Yang, X., Simsek, E., & Osabutey, A. (2022). Cultivation of Scenedesmus dimorphus with air contaminants from a pig confinement building. Journal of Environmental Management, 314, 115129.

184. Uguz, S., Anderson, G., Yang, X., Simsek, E., & Osabutey, A. (2022). Cultivation of Scenedesmus dimorphus with air contaminants from a pig confinement building. Journal of Environmental Management, 314, 115129.

185. Vanotti, M. B., Rashash, D. M. C., & Hunt, P. G. (2002). Solid–liquid separation of flushed swine manure with pam: effect of wastewater strength. Transactions of the ASAE, 45(6), 1959-1569.

186. Vanotti, M. B., Rashash, D. M. C., & Hunt, P. G. (2002). Solid–liquid separation of flushed swine manure with PAM: effect of wastewater strength. Transactions of the ASAE, 45(6), 1959-1969.

187. Vanotti, M. B., Rice, J. M., Ellison, A. Q., Hunt, P. G., Humenik, F. J., & Baird, C. L. (2005). Solid-liquid separation of swine manure with polymer treatment and sand filtration. Transactions of the ASAE, 48(4), 1567–1574.

188. Varsharani, H., & Geeta, G. (2011). Isolation of microalgae with limitation on fatty acid and lipid content of marine microalgae. Biodiesel productivity prospects. 24(4), 585–588.

189. Velichkova, K., Sirakov, I., & Georgiev, G. (2013). Cultivation of Scenedesmus dimorphus strain for biofuel production. Agricultural Science & Technology (1313-8820), 5(2), 181–185. Academic Search Premier.

190. Walker, P., Kelley, T. 2003. Solids, organic load and nutrient concentration reductions in swine waste slurry using a polyacrylamide (PAM)-aided solids flocculation treatment. Bioresource Technology, 90(2), 151-158.

191. Wang, H. F., Hu, H., Wang, H. J., & Zeng, R. J. (2019). Combined use of inorganic coagulants and cationic polyacrylamide for enhancing dewaterability of sewage sludge. Journal of Cleaner Production, 211, 387-395.

192. Wang, H. F., Hu, H., Wang, H. J., & Zeng, R. J. (2019). Combined use of inorganic coagulants and cationic polyacrylamide for enhancing dewaterability of sewage sludge. Journal of Cleaner Production, 211, 387-395.

193. Wang, M., Yang, Y., Chen, Z., Chen, Y., Wen, Y., & Chen, B. (2016). Removal of nutrients from undiluted anaerobically treated piggery wastewater by improved microalgae. Bioresource Technology, 222, 130–138.

194. Wang, M., Yang, Y., Chen, Z., Chen, Y., Wen, Y., & Chen, B. (2016). Removal of nutrients from undiluted anaerobically treated piggery wastewater by improved microalgae. Bioresource Technology, 222, 130–138.

195. Wang, M., Yang, Y., Chen, Z., Chen, Y., Wen, Y., & Chen, B. (2016). Removal of nutrients from undiluted anaerobically treated piggery wastewater by improved microalgae. Bioresource Technology, 222, 130–138.

196. Wang, Q., Hyman, M., & Higgins, B. T. (2021). Factors impacting the effectiveness of biological pretreatment for the alleviation of algal growth inhibition on anaerobic digestate. Algal Research, 53, 102129.

197. Wang, Y. C., Han, M. F., Jia, T. P., Hu, X. R., Zhu, H. Q., Tong, Z., Lin, Y.T., Wang, C., Liu, D.Z., Peng, Y.Z., Wang, G., Meng, J., Zhai, Z. X., Zhang, Y., Deng, J. G., & Hsi, H. C. (2021). Emissions, measurement, and control of odor in livestock farms: A review. *Science of the Total Environment*, 145735.

198. Wang, Y., Guo, W., Yen, H.-W., Ho, S.-H., Lo, Y.-C., Cheng, C.-L., Ren, N., & Chang, J.-S. (2015). Cultivation of Chlorella vulgaris JSC-6 with swine wastewater for simultaneous nutrient/COD removal and carbohydrate production. Bioresource Technology, 198, 619–625.

199. Wang, Y., Ho, S.-H., Cheng, C.-L., Nagarajan, D., Guo, W.-Q., Lin, C., Li, S., Ren, N., & Chang, J.-S. (2017). Nutrients and COD removal of swine wastewater with an isolated microalgal strain Neochloris aquatica CL-M1 accumulating high carbohydrate content used for biobutanol production. Special Issue on International Conference on Current Trends in Biotechnology & Post ICCB-2016 Conference on Strategies for Environmental Protection and Management (ICSEPM-2016), 242, 7–14.

200. Warrick, A. W. (1983). Interrelationships of irrigation uniformity terms. *Journal of Irrigation and Drainage Engineering*, *109*(3), 317-332.

201. Wen, Y., He, Y., Ji, X., Li, S., Chen, L., Zhou, Y., Wang, M., & Chen, B. (2017). Isolation of an indigenous Chlorella vulgaris from swine wastewater and characterization of its nutrient removal ability in undiluted sewage. Bioresource Technology, 243, 247–253.

202. Wing, S., Horton, R. A., Marshall, S. W., Thu, K., Tajik, M., Schinasi, L., & Schiffman, S. S. (2008). Air pollution and odor in communities near industrial swine operations. *Environmental Health Perspectives*, *116*(10), 1362-1368.

203. Wong, S. S., Teng, T. T., Ahmad, A. L., Zuhairi, A., & Najafpour, G. (2006). Treatment of pulp and paper mill wastewater by polyacrylamide (PAM) in polymer induced flocculation. Journal of Hazardous Materials, 135(1), 378–388.

204. Wu, W., Cheng, L.-C., & Chang, J.-S. (2020). Environmental life cycle comparisons of pig farming integrated with anaerobic digestion and algae-based wastewater treatment. Journal of Environmental Management, 264, 110512.

205. Xiu, S., Shahbazi, A., Shirley, V., & Cheng, D. (2010). Hydrothermal pyrolysis of swine manure to bio-oil: Effects of operating parameters on products yield and characterization of bio-oil. Journal of Analytical and Applied Pyrolysis, 88(1), 73-79.

206. Xu, J., Zhao, Y., Zhao, G., & Zhang, H. (2015). Nutrient removal and biogas upgrading by integrating freshwater algae cultivation with piggery anaerobic digestate liquid treatment. Applied Microbiology and Biotechnology, 99(15), 6493–6501.

207. Xu, X., Shen, Y., & Chen, J. (2015). Cultivation of Scenedesmus dimorphus for C/N/P removal and lipid production. Electronic Journal of Biotechnology, 18(1), 46–50. https://doi.org/10.1016/j.ejbt.2014.12.003

208. Yang, J., Xu, M., Zhang, X., Hu, Q., Sommerfeld, M., & Chen, Y. (2011). Life-cycle analysis on biodiesel production from microalgae: Water footprint and nutrients balance. Bioresource Technology, 102(1), 159–165. https://doi.org/10.1016/j.biortech.2010.07.017

209. Yang, X., Lee, J., Zhang, Y., Wang, X., & Yang, L. (2015). Concentration, size, and density of total suspended particulates at the air exhaust of concentrated animal feeding operations. *Journal of the Air & Waste Management Association*, *65*(8), 903-911.

210. Zhao, B., & Su, Y. (2014). Process effect of microalgal-carbon dioxide fixation and biomass production: A review. Renewable and Sustainable Energy Reviews, 31, 121–132. https://doi.org/10.1016/j.rser.2013.11.054

211. Zhu, L., Wang, Z., Shu, Q., Takala, J., Hiltunen, E., Feng, P., & Yuan, Z. (2013). Nutrient removal and biodiesel production by integration of freshwater algae cultivation with piggery wastewater treatment. Water Research, 47(13), 4294–4302.

APPENDIX

Appendix A: Protocol of Experiments of the Manuscripts (chapter 3 & 4)

I.   5 L Bold Basal Medium Preparation Protocol

1. Add (2500 mL) 2.5 L DI water in beaker on hot plate with stirring bar.

    (Temperature: 80 ºC and Speed: 5-6)

2. Measure the chemicals below on the scale and add them to the water in the beaker

    on the hot plate.

Table A-1. Chemicals and their corresponding weight used in preparing 5 L bold basal medium.

Chemicals used	Weight (g)
KH_2PO_4	0.875
$CaCl_2*2H_2O$	0.125
$MgSO_4*7H_2O$	0.375
$NaNO_3$	1.25
K_2HPO_4	0.375
MoO_3	0.0071
NaCl	0.125
EDTA $C_{10}H_{16}N_2O_8$	0.25
KOH	0.155
$FeSO_4*7H_2O$	0.0249
H_3BO_3	0.0571
H_2SO_4	100
Trace Metal Solution	5 mL

3. Prepare trace metal solution following the procedure below.

    a. Get a 1 L bottle then add 400 mL DI water.

    b. Put it over the hot plate then turn on the heating and stir.

    c. Measure and add the four chemicals on the list in the table below.

Table A-2. Chemicals and their corresponding weight used in preparing 5 L bold basal medium.

Trace Metal Solution (1 mL/L)	
$ZnSO_4*7H_2O$	8.82 g
$MnCl_2*4H_2O$	1.44 g
$CuSO_4*5H_2O$	1.57 g
$Co(NO3)_2*6H_2O$	0.49 g

    d.   The amounts will be like on the first column (8,82 g, 1,44 g)

    e.   Allow all chemicals melt in the DI water.

4. Add 2.245 L (2245 mL) DI water to the beaker and continue stirring.

5. Let it sit for 10 minutes.

6. Measure and record pH.

7. Adjust or increase pH to 6.40 (make sure it is between 6.36 to 6.40) with NaOH

8. Record final pH.

9. Put BBM medium into 2000 mL Pyrex bottles, cover bottle lid with aluminum film.

10. Autoclave BBM. Choose "Liquid 40" on Autoclave for the cycle.

II.   ***Scenesdesmus Dimorphous* Seed Cultivation**

1. Autoclave all glassware and BBM.

2. Put 200 mL autoclaved BBM each in 3 autoclaved 500 mL flat bottom flask.

3. Put each S. dimorphous Alga seed obtained from UTEX in the flat bottom flask containing BBM and connect the air pumps for aeration and mixing.

4. Monitor and record data on cell count, temperature, pH, and Alga solution volume in each flask for the next four days.

5. Add autoclaved DI water to replace water lost through evaporation to attain original volume of alga solution.

6. Add BBM to double the original volume (200 mL) of Alga solution in flask. In this case 200 mL of autoclaved BBM.

7. Monitor and record data on cell count, temperature, pH, and Alga solution volume in each flask for the next seven days. Repeat point number 5 and 6 after every seven days till the needed volume of algae solution is achieved. Replace glassware as needed considering volume of algae solution.

III. **Swine Wastewater Pretreatment**

1. Initial sieving: Screen the swine wastewater with 35 -mesh sieve to remove coarse solid particles.

2. Coagulation - Flocculation (Jar test): Add 2000 mg L-1 $Fe_2(SO_4)_3$ as a coagulant and 250 mg L-1 cationic starch as a flocculant to the initially screened SW while stirring thoroughly to mix using an overhead mechanical stirrer at 300 rpm for 3 minutes and then 60 rpm for 15 minutes.

3. Final Sieving: Sieve the upper liquid fraction of the treated swine wastewater and store in the refrigerator at 4 degrees Celsius until use.

IV. **TSS Analysis**

1. Dry clean filter in the oven for 1 hour at 105 ºC.

2. Cool the clean filter down in a desiccator.

3. Measure the clean filter weight with a balance and record.

4. Place filter on vacuum filtering hurt and add sample to filter. Write down volume of sample filtered.

5. Dry filter in oven for 2 hours after filtration.

6. Cool filter in desiccator and measure weight

7. Calculate the TSS using the formular below.

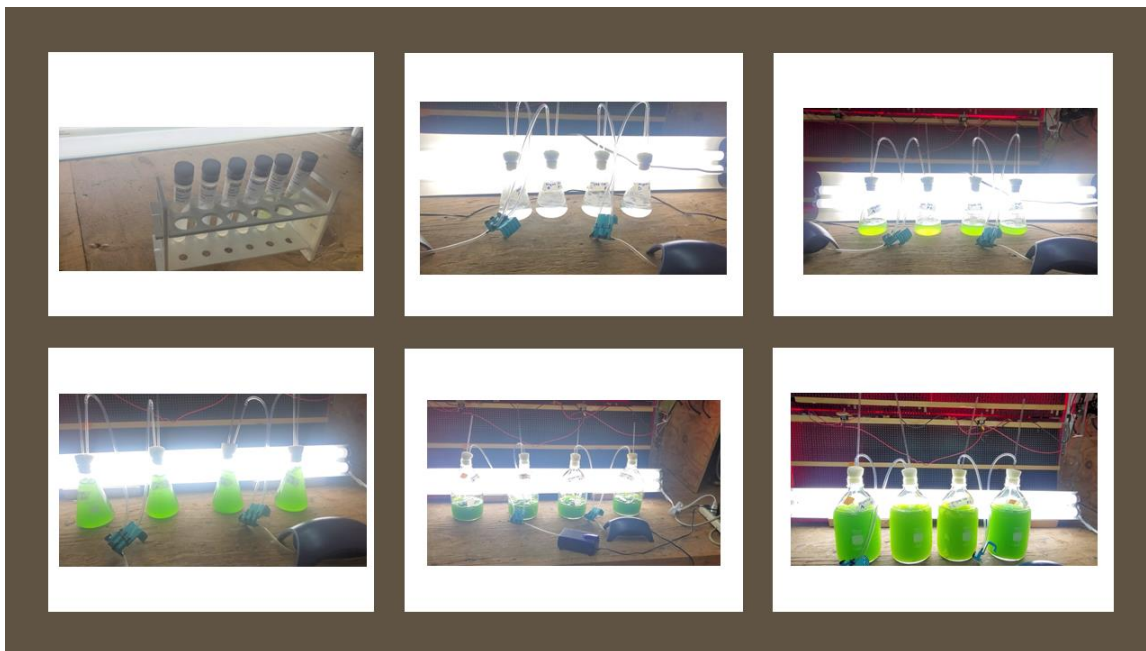$$\frac{Weight\ difference\ (mg)}{Sample\ volume\ (L)} = \_mg/L$$

Appendix B: Experimental Setup Pictures of the Manuscripts (chapter 3 & 4)

Figure B-1. Early stages of *S. dimorphus* cultivation.

Figure B-2. Setup of S. dimorphus cultivation in PBR.

Figure B-3. Pictorial view of data collection methods applied in *S. dimorphus* cultivation.

Figure B-4. Pictorial view of solid separation by sieving.

Figure B-5. Pictorial view of Jar test experiment for solid separation.
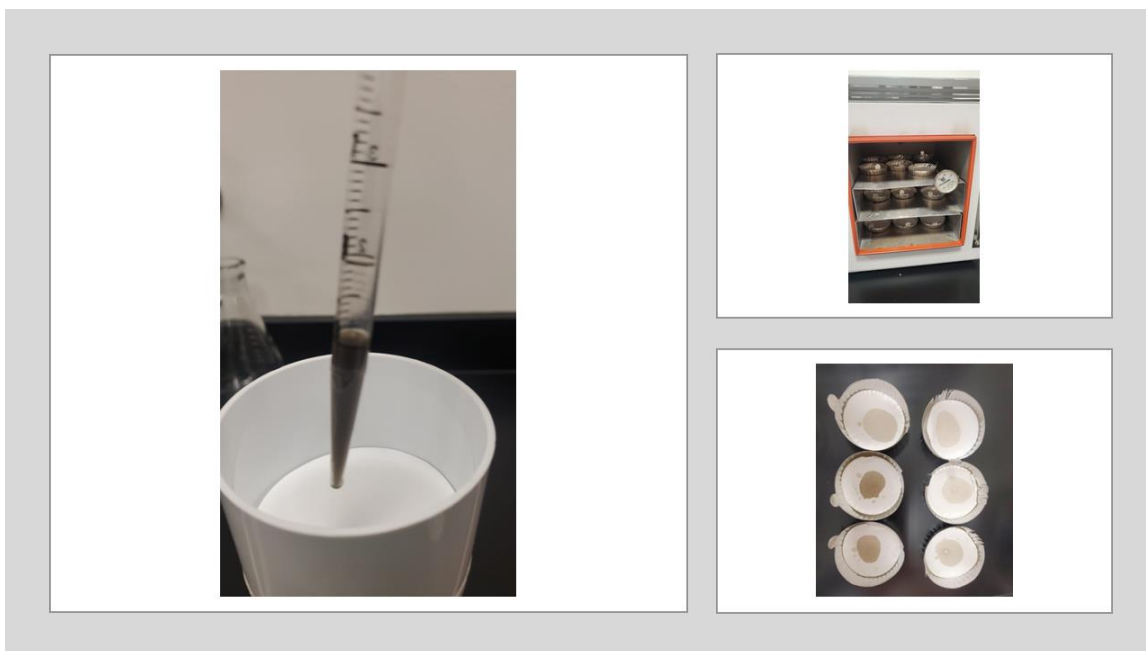
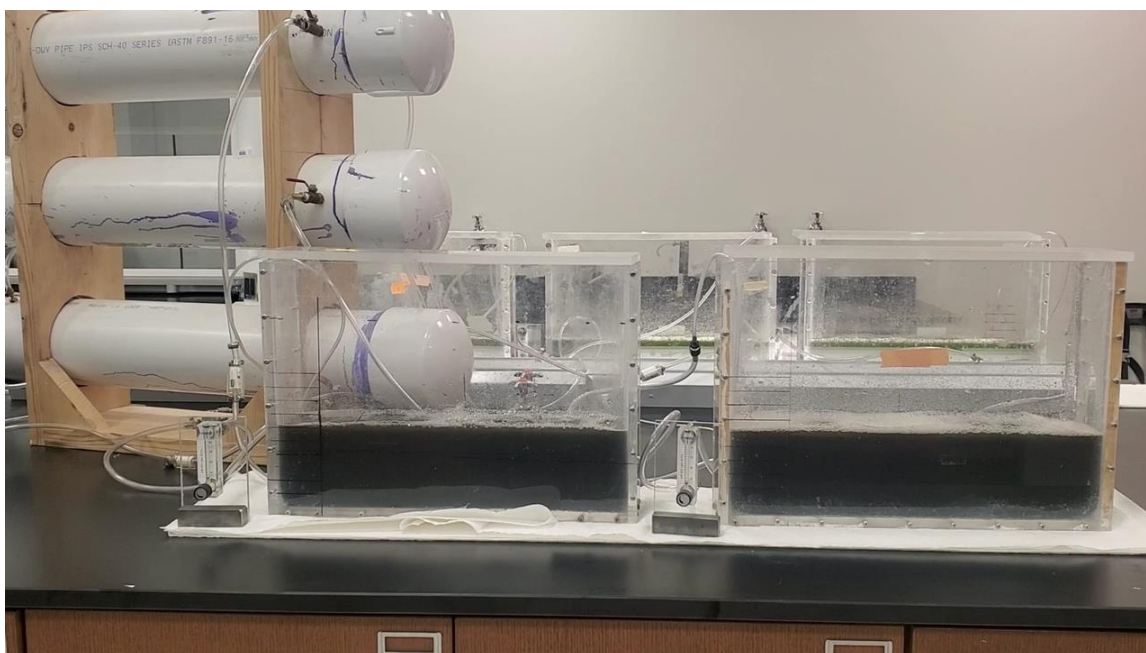**Figure B-6.** Pictorial view of TSS analysis (Filtration, oven drying)

Figure B-7. Pictorial view of PBR setup in the laboratory at SDSU

Appendix C: Supplementary Materials of the Manuscript (chapter 4)

Growth of *Scenedesmus dimorphus* in swine wastewater with versus without solid-liquid separation pretreatment.

S1. Estimation of TN retained in solids and algae

For the phase#2 experiment, the TN concentration in the pretreated SW before algal cultivation: $[TN] = [TKN] + [NO_2\text{-}N] + [NO_3\text{-}N] = (1381 + 0.23 + 40)$ mg $L^{-1} = 1421$ mg L^{-1}. In each algal PRB, 1.5 L of the pretreated SW was mixed with 4.5 L algal culture. Thus, totally $(1421$ mg $L^{-1} \times 1.5$ L$) = 2138$ mg of TN in each algal PBR was from the pretreated SW. At the end of algal cultivation, the TN concentration was calculated as: $[TN] = [TKN] + [NO_2\text{-}N] + [NO_3\text{-}N] = (156.8 + 0 + 3.4)$ mg $L^{-1} = 160.2$ mg L^{-1} and the total amount of TN in the wastewater was $(160.2$ mg $L^{-1} \times 6$ L$) = 961$ mg. Thus, a total of $(2138 - 961) = 1177$ mg of TN in the wastewater was either gone to the air or absorbed by algae and bacteria as solids.

Before the algal cultivation, the solids (TSS) from the pretreated SW contained 1258 mg $L^{-1} \times 6$ L $\times 2.8\%$N $= 211.3$ mg TN. At the end of algal cultivation, the solids collected contained 1914 mg $L^{-1} \times 6$ L $\times 5.7\%$N $= 654.6$ mg TN. The net TN accumulation in the solids was $(654.6\text{-}211.3) = 443.3$ mg TN. Thus, approximately $(443.3/1177) = 37.6\%$ of TN in the wastewater was retained in the solids harvested.

Meanwhile, a net increase in algal cell counts was $(2462\text{-}1408) \times 10^6 = 1054 \times 10^6$ cells L^{-1}. Assuming the cells remained constant in size (194 pg cell^{-1}) and composition (8.75%N) during the algal cultivation experiment, the total mass gain of the algal biomass was $(1054 \times 10^6$ cells $L^{-1}) \times 6$ L $\times (194 \times 10^{-12}$ g cell$^{-1}) = 1.227$ g $= 1227$ mg. It contained

1227 mg × 8.75% = 107 mg of TN. Thus, approximately (107/1177) = 9.6% of TN in the
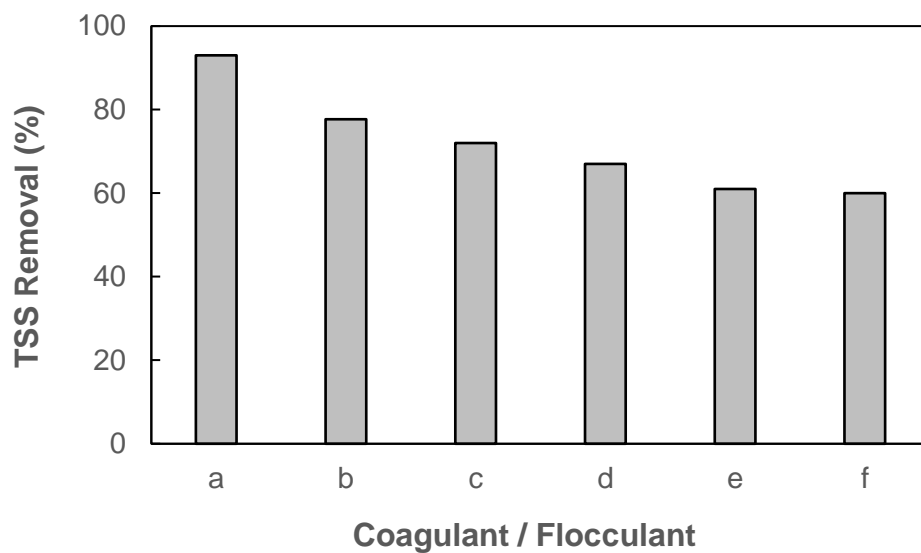
wastewater was absorbed by the algae.

Figure C-1. Comparison of coagulants/flocculants in TSS removal from raw swine
wastewater after 24-hour settling: (a) 193 mg L^{-1} PAM, (b) 250 mg L^{-1} cationic starch, (c)
258 mg L^{-1} Magnofloc LT-7995, (d) 2.5 g L^{-1} Fe$_2$(SO$_4$)$_3$ at pH=6.5, (e) 2.5 g L^{-1}
Fe$_2$(SO$_4$)$_3$ at pH=8, and (f) 500 mg L^{-1} chitosan. The experiments were conducted without
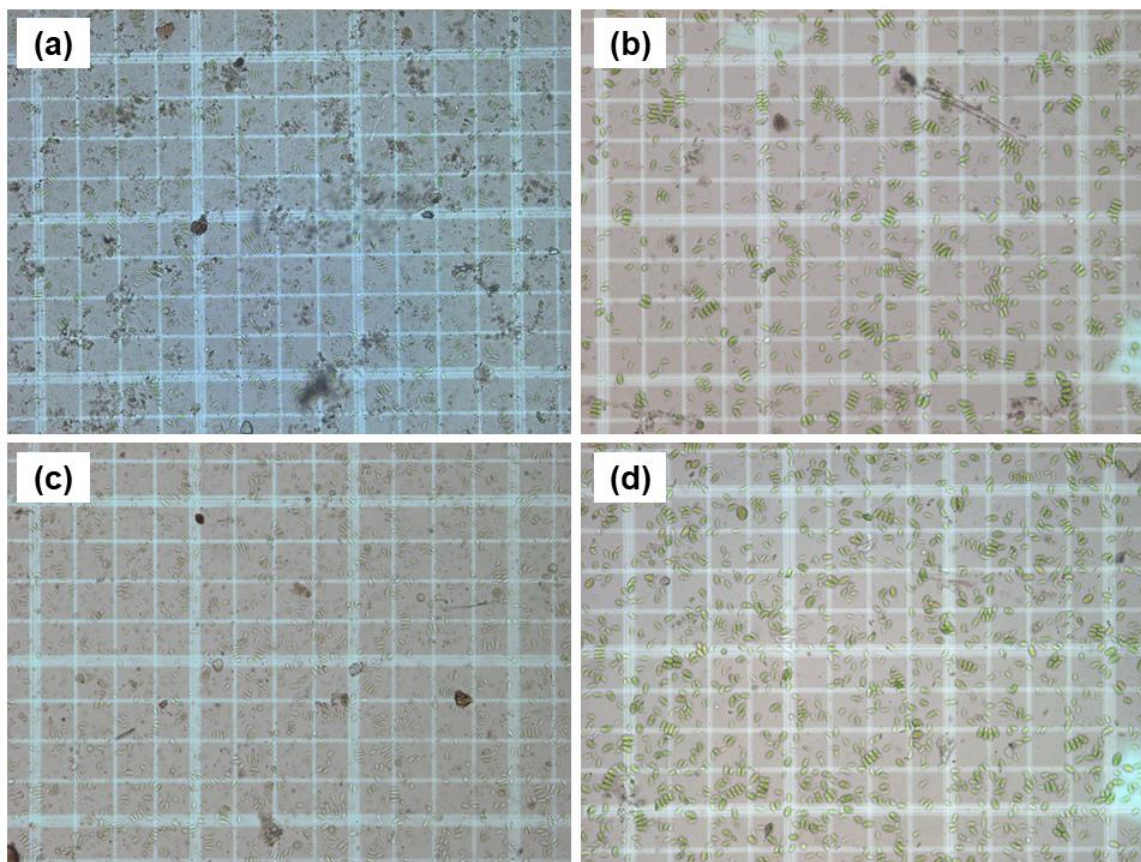pH readjustment (pH=8) of raw swine wastewater unless otherwise noted.

Figure C-2. Microscopic images of S. dimorphus grown in raw and pretreated swine wastewater: (a) day 7 in raw swine wastewater, (b) day 7 in pretreated swine wastewater, (c) day 21 in raw swine wastewater, and (d) day 21 in pretreated swine wastewater.
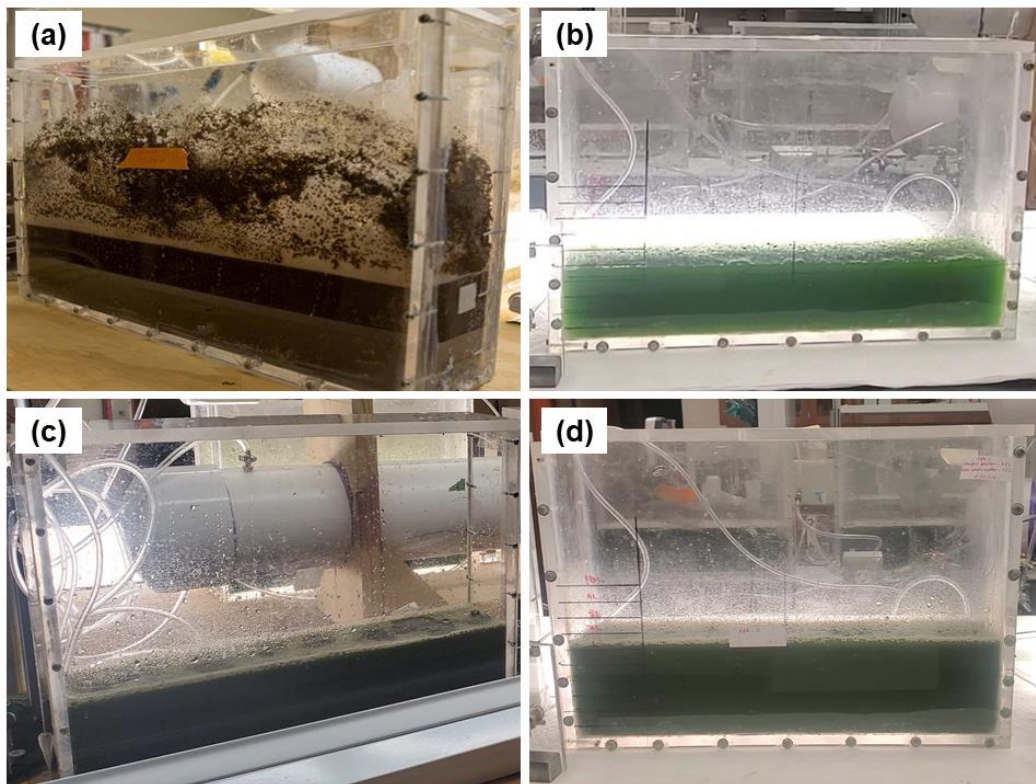
Figure C-3. Photos of photobioreactors with (a) raw swine wastewater, (b) pure microalgae culture, (c) microalgae grown in untreated swine wastewater, and (d) microalgae grown in pretreated swine wastewater.

Table C-1. Testing of flocculants/coagulants with raw swine wastewater collected in Dec 2020.

Flocculant/coagulants	Dosage (mg L^{-1})	Ph	TSS removal (%) after 30 min	TSS removal (%) after 24 hrs
Polyacrylamide (PAM)	258	8.0	90	93
	193	8.0	95	96
	129	8.0	73	79
	77	8.0	52	74
	39	8.0	62	72
Ferric sulfate	2500	8.0	n/a	61
	2500	7.0	62	68
	2500	6.5	64	67
	2500	6.0	52	71
	2500	5.0	30	75
Chitosan	500	8.0	n/a	60
	1000	8.0	n/a	56
Cationic starch	250	8.0	n/a	78
Magnoloc LT-7995	258	8.0	n/a	72

Table C-2. Flocculation-coagulation removal of pollutants/nutrients from swine wastewater: Examples of previous studies.

Coagulant/ Flocculant [1]	Dosage (mg L^{-1})	TSS (%)	COD (%)	TN (%)	P (%)	NH$_3$ (%)	Reference
PAM	140	95	69	85	92	-	Vanotti et al. (2002)
PAM	350	95.6	-	-	-	-	Walker and Kelley (2003)
PAM	80-200	37-64	71	-	34	-	González-Fernández et al. (2008)
SAP	1250	28	-	-	-	-	Cheme-Ayahla et al. (2011)
Tanfloc SG® coagulant + tannin flocculant	n/a	68	-	-	-	48.1	Gabriel et al. (2019)
FeCl$_3$ and MgCl$_2$	60	-	98.5	-	82.6	-	Huang et al. (2019)
PolyDADMAC	40		51	-	-	-	Gomes et al. (2021)
NPAM	n/a	-	-	99.1	94.9	-	Lee and Chang (2022)

[1] PAM – polyacrylamide; SAP – superabsorbent polymer; PolyDADMAC – polydiallyldimethylammonium chloride; NPAM – non-ionic polyacrylamide.